NASA Technical Paper 1124

Wind-Tunnel Investigation at Mach Numbers From 1.90 to 2.86 of a Canard-Controlled Missile With Ram-Air-Jet Spoiler Roll Control

A. B. Blair, Jr.

MARCH 1978

NASA

NASA Technical Paper 1124

Wind-Tunnel Investigation at Mach Numbers From 1.90 to 2.86 of a Canard-Controlled Missile With Ram-Air-Jet Spoiler Roll Control

A. B. Blair, Jr.
Langley Research Center
Hampton, Virginia

National Aeronautics
and Space Administration

**Scientific and Technical
Information Office**

1978

SUMMARY

A wind-tunnel investigation was made at free-stream Mach numbers from 1.90 to 2.86 to determine the efficacy of using a ram-air-jet spoiler roll control device on a typical canard-controlled missile configuration. For roll control comparisons, conventional aileron controls on the tail fins were also tested.

The results indicate that the roll control of the ram-air-jet spoiler tail fins at the highest free-stream Mach number compared favorably with that of the conventional 11-percent area-ratio tail fin ailerons, each deflected 10°. The roll control of the tail fin ailerons decreased while that of the ram-air-jet spoiler increased with free-stream Mach number. The addition of the ram-air-jet spoiler tail fins or flow-through tip chord nacelles on the tail fins resulted in only small changes in basic missile longitudinal stability. The axial-force coefficient of the operating ram-air-jet spoiler is significantly larger than that of conventional ailerons and results primarily from the total pressure behind a normal shock in front of the nacelle inlets.

INTRODUCTION

From 1955 to 1960 the NACA/NASA investigated at the Langley pilotless aircraft research station at Wallops Island, Virginia, a number of roll control devices with potentially low actuating force (torque) requirements. One of the most effective of these was a jet flap or jet-free-stream interaction device which used ram-air pressure for the jet working fluid. An excellent account of the ram-air-jet spoiler research can be found in references 1 to 4. More recently, interest has been renewed in the ram-air-jet spoiler as a roll control device to reduce or compensate for unwanted induced rolling moments that characterize forward controlled missile configurations. Current cursory experimental investigations have demonstrated the potential of these devices for roll control of maneuvering cruciform missiles. In addition, the feasibility of interfacing a ram-air-jet spoiler system with an all fluidic-logic roll control system has been investigated. (See refs. 5 and 6.)

In view of the need to negate undesirable induced rolling moments of canard-controlled missile configurations, an experimental investigation has been conducted to determine the efficacy of using a ram-air-jet spoiler roll control device on a typical canard-controlled missile configuration. The present study included model configurations which represented the ram-air-jet spoiler devices operating at zero and maximum roll control as well as a comparison with conventional aileron controls, all at various missile maneuvering attitudes.

The tests were conducted in the Langley Unitary Plan wind tunnel at free-stream Mach numbers from 1.90 to 2.86. The nominal angle-of-attack range was -4° to 28° at model roll angles from -90° to 180° for a Reynolds number of 6.6×10^6 per m (2.0×10^6 per ft).

SYMBOLS

The aerodynamic coefficient data are referred to the body-axis system except for lift and drag which are referred to the stability-axis system. The moment reference was located at 46.8 percent of the reference body length aft of the model nose.

Measurements and calculations were made in U.S. Customary Units. Measurements are presented in the International System of Units (SI) with the equivalent values given parenthetically in U.S. Customary Units. (See ref. 7.)

A maximum cross-sectional area of body, 0.004560 m^2 (0.049087 ft^2)

A_e jet-exit slot area, cm^2 (in^2)

A_i cross-sectional area of inlet, 1.29 cm^2 (0.20 in^2)

C_A axial-force coefficient, $\dfrac{\text{Axial force}}{q_\infty A}$

$C_{A,b}$ base axial-force coefficient, $\dfrac{\text{Base axial force}}{q_\infty A}$

C_D drag coefficient, $\dfrac{\text{Drag}}{q_\infty A}$

$C_{D,b}$ base drag coefficient, $\dfrac{\text{Base drag}}{q_\infty A}$

C_L lift coefficient, $\dfrac{\text{Lift}}{q_\infty A}$

C_l rolling-moment coefficient, $\dfrac{\text{Rolling moment}}{q_\infty A d}$

C_m pitching-moment coefficient, $\dfrac{\text{Pitching moment}}{q_\infty A_l}$

C_N normal-force coefficient, $\dfrac{\text{Normal force}}{q_\infty A}$

C_n yawing-moment coefficient, $\dfrac{\text{Yawing moment}}{q_\infty A d}$

C_Y side-force coefficient, $\frac{\text{Side force}}{q_\infty A}$

d reference diameter, 7.62 cm (3.00 in.)

l reference body length, 107.493 cm (42.320 in.)

M_∞ free-stream Mach number

$p_{t,2}$ total pressure behind normal shock, Pa (psfa)

p_∞ free-stream static pressure, Pa (psfa)

q_∞ free-stream dynamic pressure, Pa (psfa)

S_a/S_{exp} ratio of tail fin aileron area to total exposed tail fin area for one tail fin surface

α angle of attack, deg

ΔC_l incremental rolling-moment coefficient due to controls

δ_{roll} roll-control deflection of four tail fin ailerons, positive to provide clockwise rotation as viewed from rear, deg

ϕ model roll angle (for $\phi = 0^o$, canards and tails are in vertical and horizontal planes), deg

APPARATUS AND TESTS

Wind Tunnel

The investigation was conducted in the low Mach number test section of the Langley Unitary Plan wind tunnel, which is a variable pressure, continuous flow facility. The test section is approximately 2.13 m (7 ft) long and 1.22 m (4 ft) square. The asymmetric sliding-block nozzle leading to the test section permits a continuous variation in free-stream Mach number from about 1.5 to 2.9.

Model Concept

To simulate the concept of an operating control system, the ram-air-jet spoiler tail fin operated in the following manner. Free-stream air is directed into each tail fin plenum by a tip-mounted normal-shock inlet and is expelled through slots on one side only near the trailing edge of the fin in a direction normal to the surface. The expelling air produces a jet force (thrust) which is magnified several times at supersonic speeds; a total control force (reaction) results. The aerodynamic jet interaction is physically similar to a ramp-wedge or step-induced boundary-layer separation on a flat plate at super-

sonic speeds. For the present investigation the ram-air-jet spoiler tail fins were used only to produce positive rolling moments.

In order to evaluate the ram-air-jet spoiler as a roll control, a general research missile model was chosen as the basic airframe. (See fig. 1(a) for the dimensional details.) The airframe is a cruciform missile configuration consisting of a cylindrical body with a modified ogive nose, a set of canards, and aft tail fins mounted in-line. The canards and plain tail fins have trapezoidal planforms with beveled leading- and trailing-edge airfoil sections. For the major portion of these tests, the airframe had ram-air-jet spoiler tail fins with the same planform geometry and slab thickness as the plain tail fins. (See fig. 1(b).) Each ram-air-jet spoiler fin had tip-mounted normal-shock inlets of one-sixth body diameter d. For the operating ram-air-jet spoilers, several ratios of exit area to inlet area were investigated for each ram-air-jet spoiler tail fin to produce positive rolling moments. (See table I.) These ratios were obtained from an arbitrary selection of different exit areas (using interchangeable slotted cover plates) combined with a constant inlet cross-sectional area. In addition, a closed plenum exit configuration was tested.

The tests were conducted in the following sequence. Four ram-air-jet spoiler tail fins were investigated (fig. 2(a)) that used the most effective roll control area ratios from unpublished single ram-air-jet spoiler fin data. For roll control comparisons, plain tail fins (fig. 2(b)) were tested with conventional trailing-edge ailerons ($S_a/S_{exp} \approx 11$ percent) having arbitrary deflection angles of 0^o and 10^o. Finally, in an attempt to simulate the concept of a nonoperating ram-air-jet spoiler control with an open control valve, four tail fins with flow-through tip chord nacelles were tested. (See fig. 2(c).)

There were small planform geometry differences between the operating and nonoperating (flow-through) ram-air-jet spoiler configurations. For example, the operating ram-air-jet spoiler has a nacelle boattail, whereas the flow-through nacelle configuration does not. The flow-through nacelle due to its inlet-exit taper geometry has a slightly smaller inlet diameter than the operating ram-air-jet spoiler inlet. (See fig. 1(b).) The two test configurations are believed to be adequate for illustrating general trends in longitudinal and lateral aerodynamic characteristics.

Test Conditions

Tests were performed at the following tunnel conditions:

Free-stream Mach number	Stagnation temperature		Stagnation pressure		Reynolds number	
	K	^oF	kPa	psfa	per meter	per foot
1.90	339	150	60.9	1271	6.6×10^6	2.0×10^6
2.16	339	150	68.5	1430	6.6	2.0
2.40	339	150	77.2	1612	6.6	2.0
2.86	339	150	98.4	2056	6.6	2.0

The dewpoint temperature measured at stagnation pressure was maintained below 239 K (-30° F) to assure negligible condensation effects. All tests were performed with boundary-layer transition strips on the body 3.05 cm (1.20 in.) aft of the nose and 1.02 cm (0.40 in.) aft of the leading edges measured streamwise on both sides of the canard and tail fin surfaces. The transition strips were approximately 0.157 cm (0.062 in.) wide and were composed of No. 50 sand grains sprinkled in acrylic plastic.

Measurements and Corrections

Aerodynamic forces and moments on the model were measured by means of a six-component electrical strain-gage balance which was housed within the model. The balance was attached to a sting which, in turn, was rigidly fastened to the tunnel support system. Balance-chamber pressure (base pressure) was measured by means of a single static-pressure orifice located in the vicinity of the balance. No internal pressure measurements were made in the ram-air-jet spoiler tail fin inlet-duct-plenum system. The model balance rolling-moment coefficient accuracy varied from ±0.014 to ±0.017.

The angles of attack have been corrected for deflection of the balance and sting due to aerodynamic loads and tunnel-flow misalinement. The drag and axial-force coefficient data have been adjusted to free-stream conditions acting over the model base. Typical values of base axial-force and base drag coefficients are presented in figure 3.

PRESENTATION OF RESULTS

The results of the investigation are presented in the following figures:

DISCUSSION

A comparison of roll control for the four ram-air-jet spoiler tail fins and the four plain tail fins with trailing-edge ailerons is presented in figure 4. The ram-air-jet spoilers were tested with the most effective roll-producing exit area to inlet area ratios (e.g., $A_e/A_i = 0.75$ and 1.00) obtained from unpublished data of a single ram-air-jet spoiler tail fin. Each of the four plain tail fins had an arbitrary aileron deflection of 10° to represent a typical conventional roll control on a canard-controlled missile. Incremental roll values ΔC_l were obtained by subtracting the rolling-moment coefficients of the respective baseline configuration from the total rolling-moment coefficients of each configuration. (Typical baseline configurations: 0° aileron deflected data for the plain fin and the closed plenum exit data for the ram-air-jet spoiler.) Even though an effort was made to make the plenum entrance (see fig. 1(b)) as large as possible for the ram-air-jet spoiler, while staying within the structural limits of the fin, some flow restriction might have occurred. As a result, the magnitudes of ΔC_l for exit area to inlet area ratios of 0.75 and 1.00 may not be at their maximum potential values. Nevertheless, for the test angle of attack and model ϕ angles, the data indicate that the ram-air-jet spoilers are effective roll-producing devices with exit area to inlet area ratios of 0.75 and 1.00. At $M_\infty = 1.90$, the ram-air-jet spoiler roll control ($A_e/A_i = 0.75$) is about half of that developed by the plain fin configuration throughout the α range. Increasing the free-stream Mach number to 2.86 leads to a greater roll control for the ram-air-jet spoiler ($A_e/A_i = 0.75$) than for the plain fin configuration up to moderate angles of attack, with about the same control as the plain fin configuration at the higher angles of attack. Figure 5 presents a summary comparison of zero-lift roll control ΔC_l between the ram-air-jet spoiler and tail fin aileron configurations. In general, the roll control of the 11-percent area-ratio tail fin ailerons, each deflected 10°, decreases while the ram-air-jet spoiler roll control increases with free-stream Mach number.

The effect of closed plenum exit and flow-through nacelle configurations on the longitudinal aerodynamic characteristics of the model is presented in figures 6 to 8 for roll angles of 0°, 22.5°, and 45°, respectively. The flow-through tip chord tail fin nacelle configuration simulated the concept of a

nonoperating ram-air-jet spoiler control with an open control valve. Schlieren photographs of the closed plenum exit and the flow-through nacelle configurations are presented in figure 19. In general, with the addition of either the closed plenum exit or the flow-through nacelle tail fins, only small changes resulted in the basic missile longitudinal stability ($\alpha \approx 0^{\circ}$). The pitching-moment coefficients were more negative at the higher angles of attack for both configurations, with the flow-through nacelle generally having the most negative values. There was about a 7-percent increase in the axial-force coefficient at $M_{\infty} = 1.90$ with the addition of the flow-through nacelles. This increase was reduced to 4 percent at the higher free-stream Mach numbers. The closed plenum exit configuration has a significant increase in the axial-force coefficient over that of the plain tail configuration. This increase varied from about 21 percent at $M_{\infty} = 1.90$ to 28 percent at $M_{\infty} = 2.86$.

The effect of exit area to inlet area ratios for roll control on the longitudinal aerodynamic characteristics of the model with ram-air-jet spoiler tail fins is presented in figures 9 to 11 for roll angles of 0°, 22.5°, and 45°, respectively. The exit area to inlet area ratio had little effect on the model longitudinal aerodynamic characteristics. The configuration for $A_e/A_i = 1.00$ had the largest axial-force coefficients at the higher angles of attack.

The effect of closed plenum exit and flow-through nacelle configurations on the lateral aerodynamic characteristics of the model is presented in figures 12 to 14 for roll angles of 0°, 22.5°, and 45°, respectively. These data indicate that the addition of either closed plenum exit or flow-through nacelle tail fins generally produces a more negative rolling-moment coefficient with angle of attack. Both configurations produce their most negative rolling-moment coefficients with angle of attack at a model roll angle of 22.5° where the model rolling-moment coefficients have their largest magnitudes and nonlinearities due to asymmetric roll-induced effects.

The effect of exit area to inlet area ratios for roll control on the lateral aerodynamic characteristics of the model with ram-air-jet spoiler tail fins is presented in figures 15 to 17 for roll angles of 0°, 22.5°, and 45°, respectively. In general, the roll control of the model configuration for $A_e/A_i = 0.75$ was accompanied by a small amount of proverse yaw (except at $\phi = 45^{\circ}$ for the lower free-stream Mach numbers) at the higher angles of attack, whereas the configuration for $A_e/A_i = 1.00$ had adverse yaw with its roll control.

A review of the longitudinal aerodynamic characteristics shown in figures 6 to 11 shows that the ram-air-jet spoiler configurations are accompanied by axial-force penalties. Therefore, it may be of interest to show the axial-force coefficient penalty of each roll control system operating; although for short-range applications, axial force is usually of secondary importance compared with other control characteristics. A summary comparison of the total axial-force coefficient characteristics for each roll control system operating and not operating is shown in figure 18. These data show that the ram-air-jet spoiler has the disadvantage of significantly larger axial-force coefficients compared to the plain fin configuration. When comparing the closed plenum exit configuration to that of the configuration for $A_e/A_i = 0.75$, only negligible differences in total axial-force coefficients are observed. The axial-force

coefficient increment between the flow-through nacelle and the open or closed plenum exit configurations is about equal to the pressure rise generated by the normal shock in front of the ram-air-jet spoiler inlets. For example, by substituting in the expression $\frac{4A_i(p_{t,2} - p_\infty)}{q_\infty A}$ the free-stream tunnel conditions for free-stream Mach numbers of 1.90 and 2.86, respectively, one can compute coefficient values of 0.182 and 0.194 which approximate the axial-force coefficient increment between the flow-through nacelle and the closed plenum exit configurations shown in figure 18. Therefore, it can be concluded that the axial-force coefficient penalty increment associated with the inlet-duct-plenum manifolds (e.g., an operating ram-air-jet spoiler) results primarily from the total pressure behind a normal shock in front of each nacelle inlet.

CONCLUSIONS

A wind-tunnel investigation was made at free-stream Mach numbers from 1.90 to 2.86 to determine the efficacy of using a ram-jet spoiler roll control device on a typical canard-controlled missile configuration. For roll control comparisons, conventional aileron controls on the tail fins were also tested. The results of the investigation are as follows:

1. The roll control of the ram-air-jet spoiler tail fins at the highest free-stream Mach number compared favorably with that of conventional 11-percent area-ratio tail fin ailerons, each deflected 10°. The roll control of the tail fin ailerons decreased while that of the ram-air-jet spoiler increased with free-stream Mach number.

2. The addition of ram-air-jet spoiler tail fins or flow-through tip chord nacelles on the tail fins resulted in only small changes in basic missile longitudinal stability.

3. The axial-force coefficient of the operating ram-air-jet spoiler tail fins is significantly larger than that of the plain tail fins with conventional ailerons and results primarily from the total pressure behind a normal shock in front of the nacelle inlets.

Langley Research Center
National Aeronautics and Space Administration
Hampton, VA 23665
January 16, 1978

REFERENCES

1. Turner, Thomas R.; and Vogler, Raynond D.: Wind-Tunnel Investigation at Transonic Speeds of a Jet Control on an 80° Delta-Wing Missile. NACA RM L55H22, 1955.

2. Lowry, John G.: Recent Control Studies. NACA RM L55L22a, 1956.

3. Schult, Eugene D.: Free-Flight Roll Performance of a Steady-Flow Jet-Spoiler Control on an 80° Delta-Wing Missile Between Mach Numbers of 0.6 and 1.8. NACA RM L57J28, 1958.

4. Schult, Eugene D.: Free-Flight Investigation at Mach Numbers Between 0.5 and 1.7 of the Zero-Lift Rolling Effectiveness and Drag of Various Surface, Spoiler, and Jet Controls on an 80° Delta-Wing Missile. NASA TN D-205, 1960.

5. Durham, Mark: Feasibility of a "Fluidic Rolleron" for Application to the Chaparral Missile. NWC Tech. Note 4063-224, U.S. Navy, Nov. 1970.

6. Young, R.: Final Report. Fluidic Roll Rate Damping System. Doc. No. 73SD2110, Gen. Elec. Co., July 1973. (Available from DDC as AD B007 800L.)

7. Mechtly, E. A.: The International System of Units - Physical Constants and Conversion Factors (Second Revision). NASA SP-7012, 1973.

TABLE I.- RAM-AIR-JET SPOILER TAIL FIN INLET-PLENUM

CONSTANTS, PER FIN

Inlet area, A_i, cm^2 (in^2)	1.29 (0.20)
Plenum entrance area, cm^2 (in^2)	1.74 (0.27)
Nozzle block	None
A_e/A_i = 0.75, A_e, cm^2 (in^2)	0.97 (0.15)
A_e/A_i = 1.00, A_e, cm^2 (in^2)	1.29 (0.20)

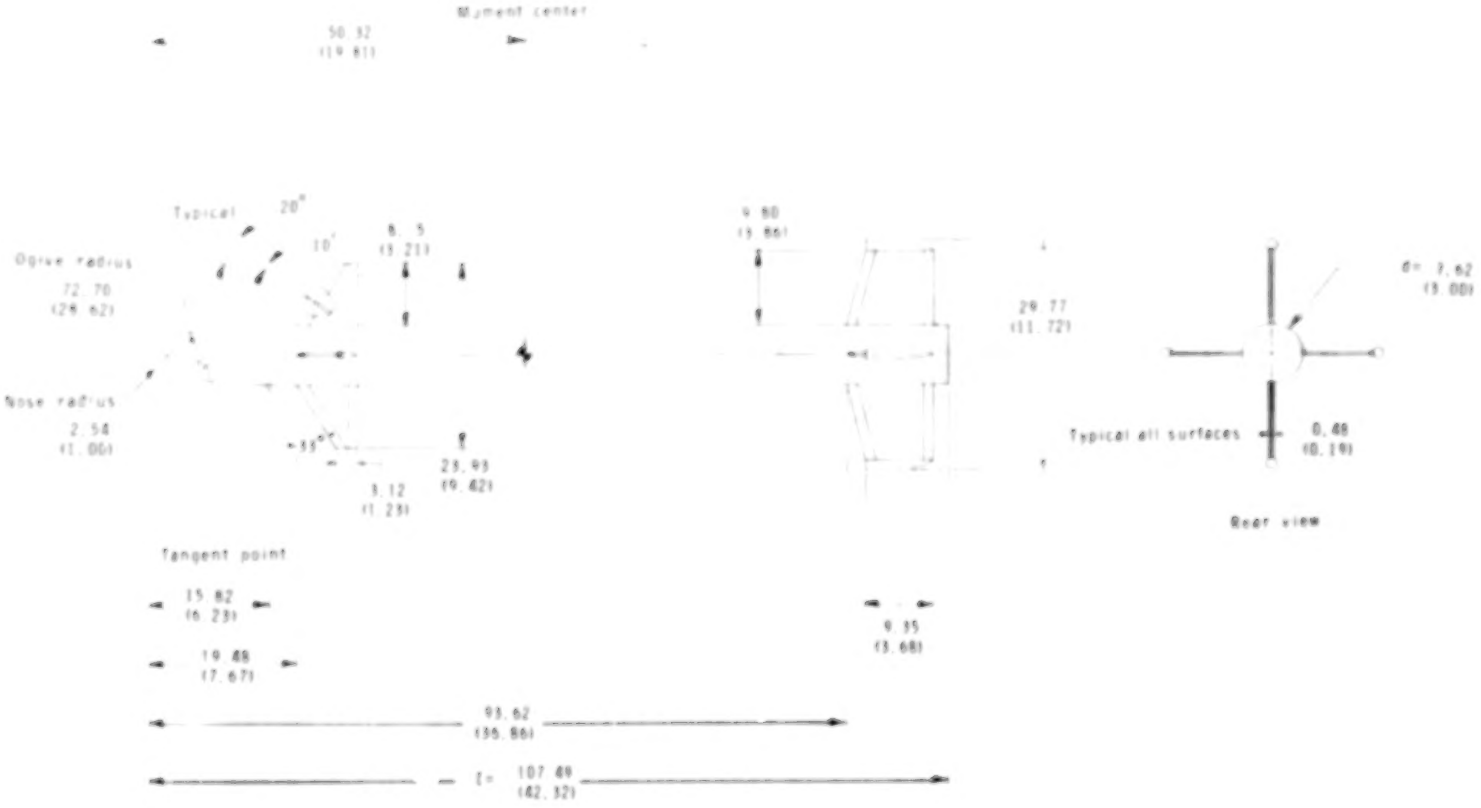

(a) Complete model.

Figure 1.- Model details. All dimensions are in cm (in.) unless otherwise indicated.

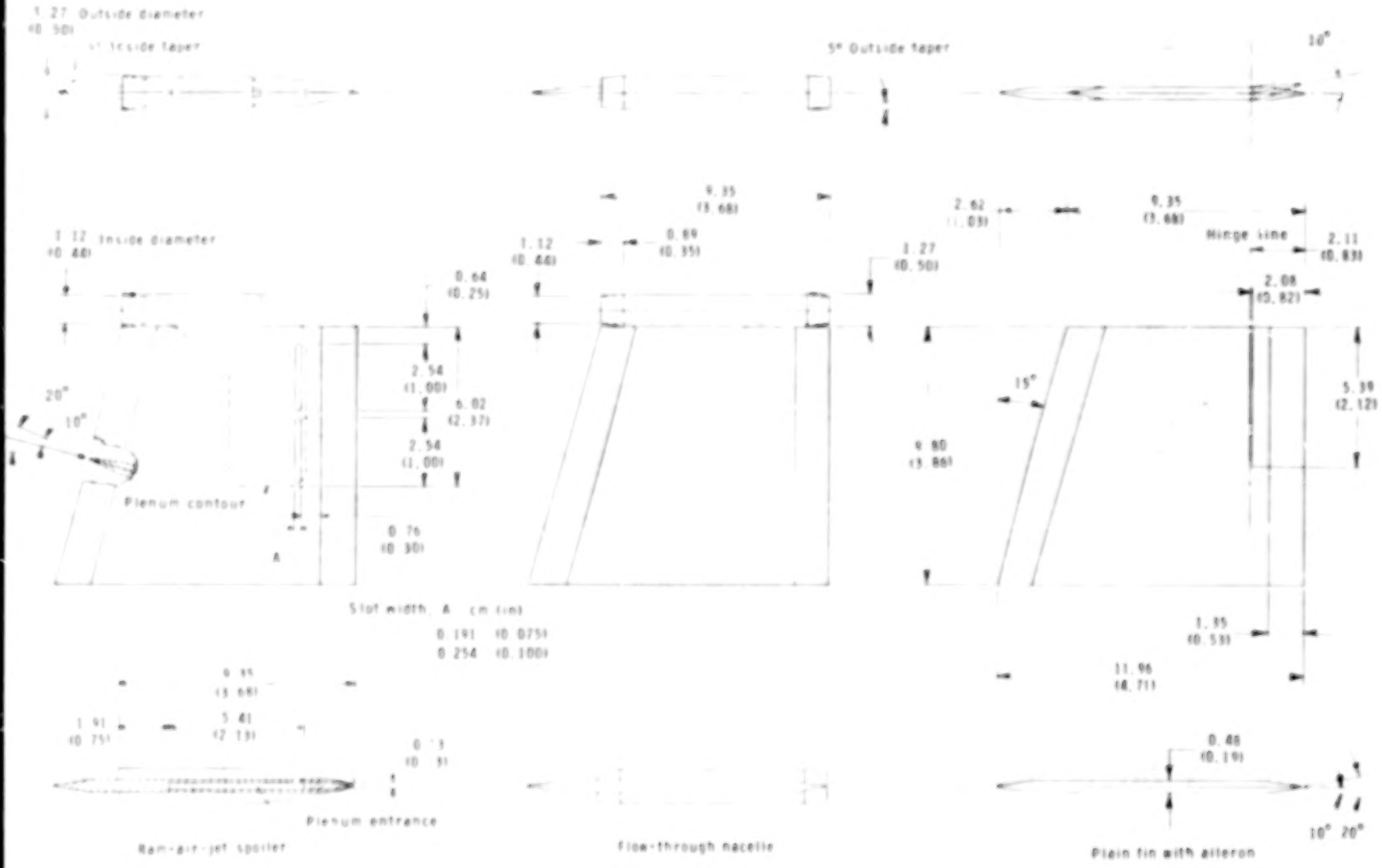

(b) Tail fins.

Figure 1.- Concluded.

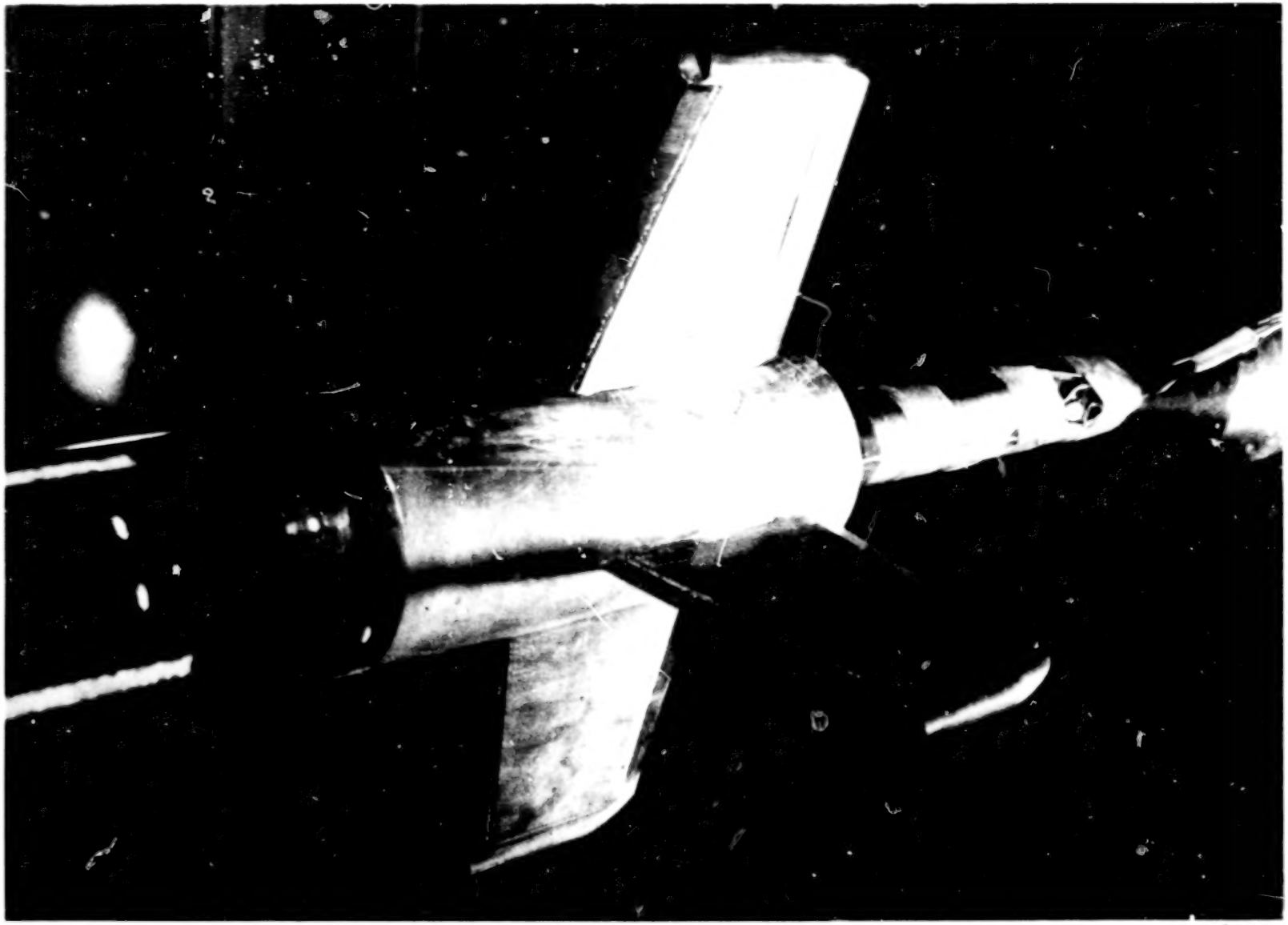

L-76-492

(a) Four ram-air-jet spoiler tail fins.

Figure 2.- Model photographs.

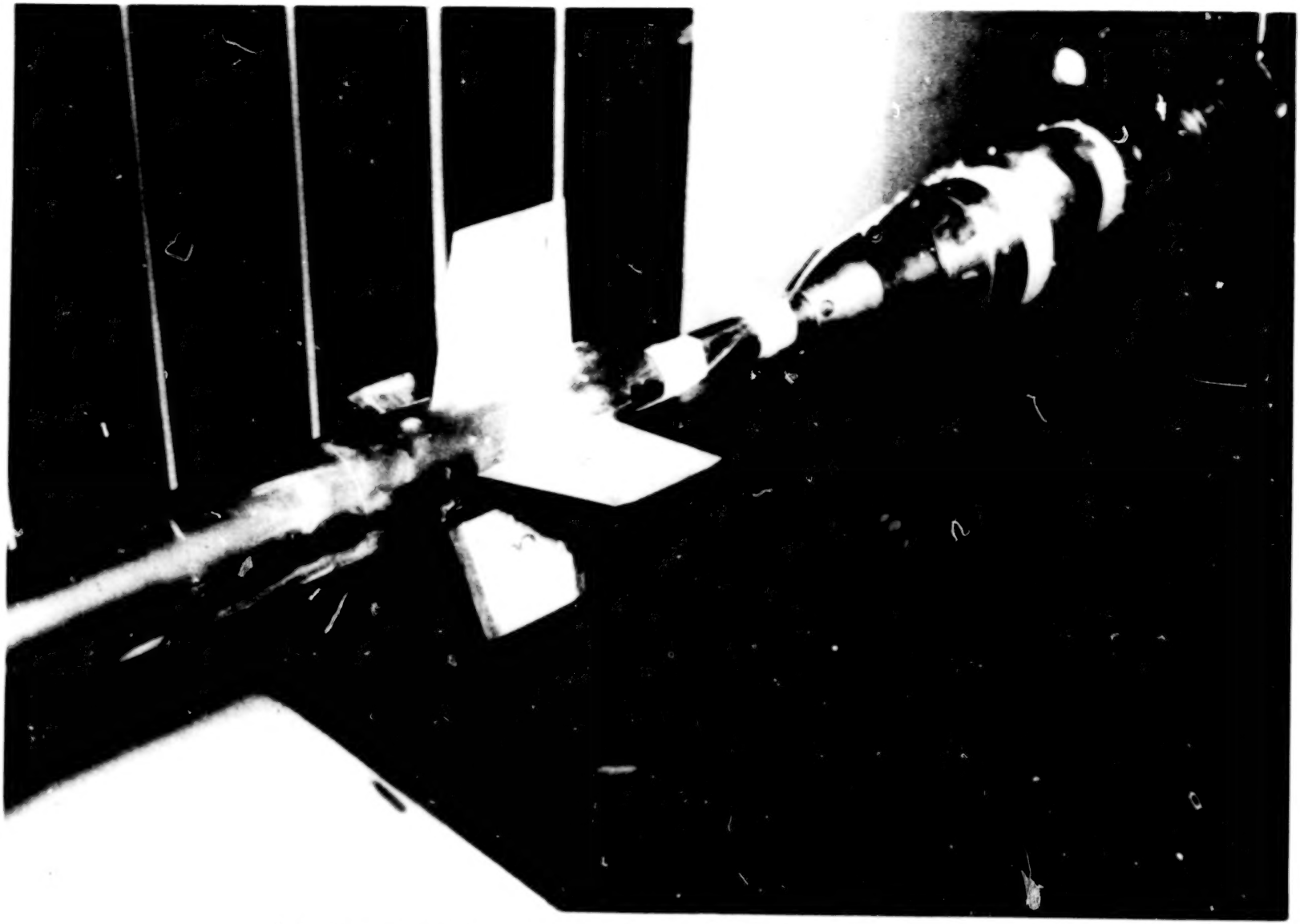

(b) Four plain tail fins each with trailing-edge ailerons. L-76-4905

Figure 2.- Continued.

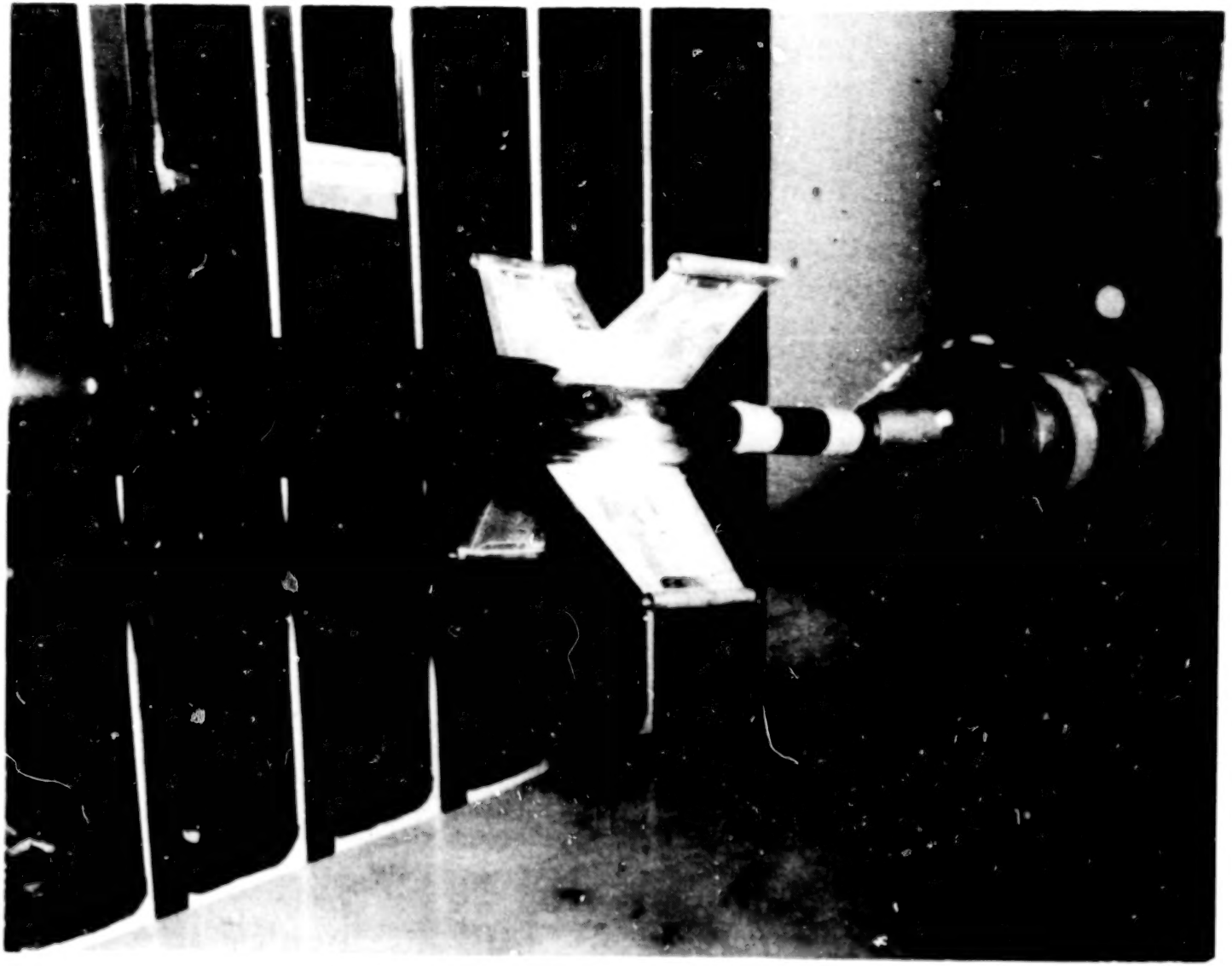

(c) Four flow-through tail fin tip chord nacelles. L-78-1

Figure 2.- Concluded.

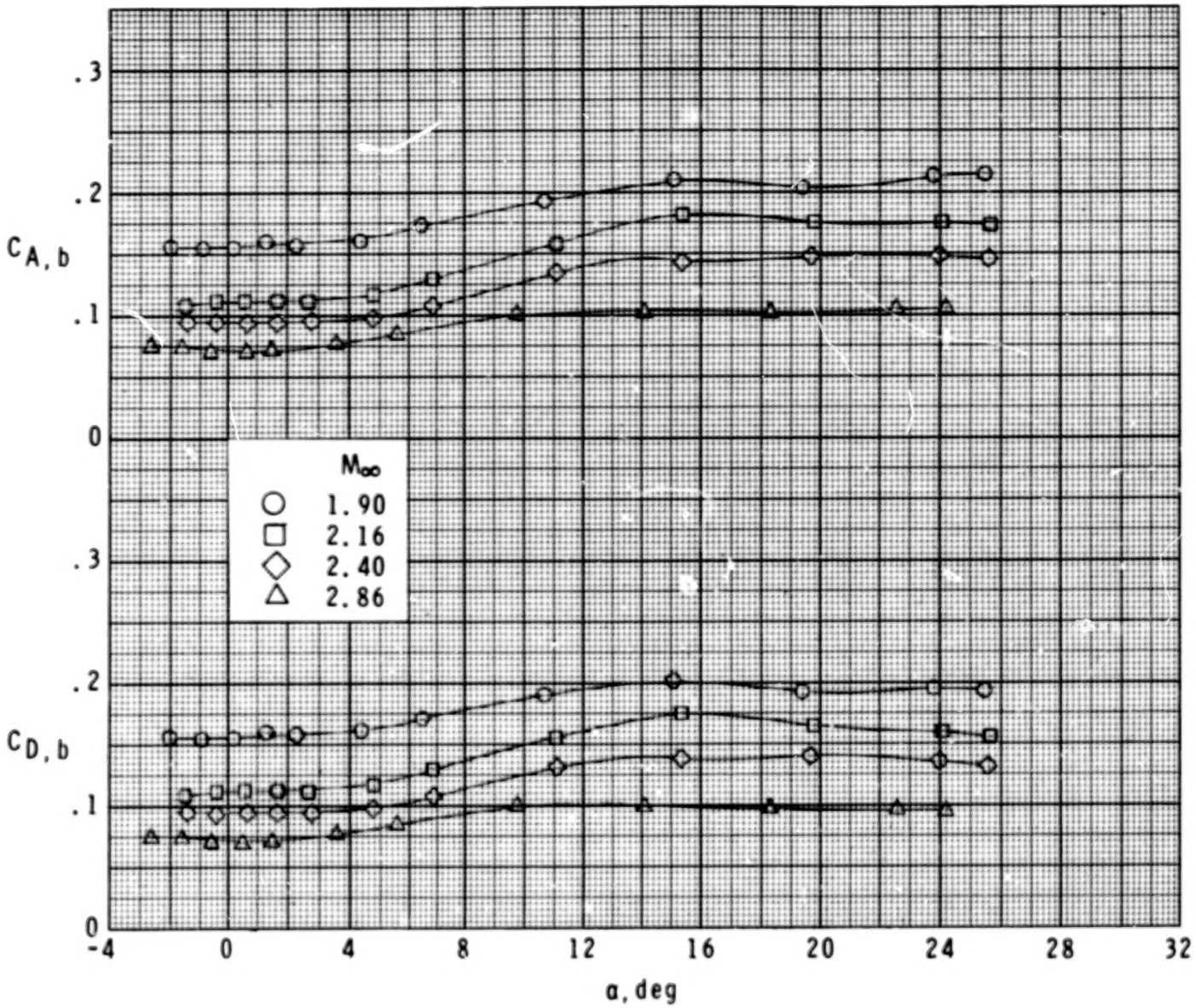

Figure 3.- Typical variation of $C_{A,b}$ and $C_{D,b}$ with angle of attack.

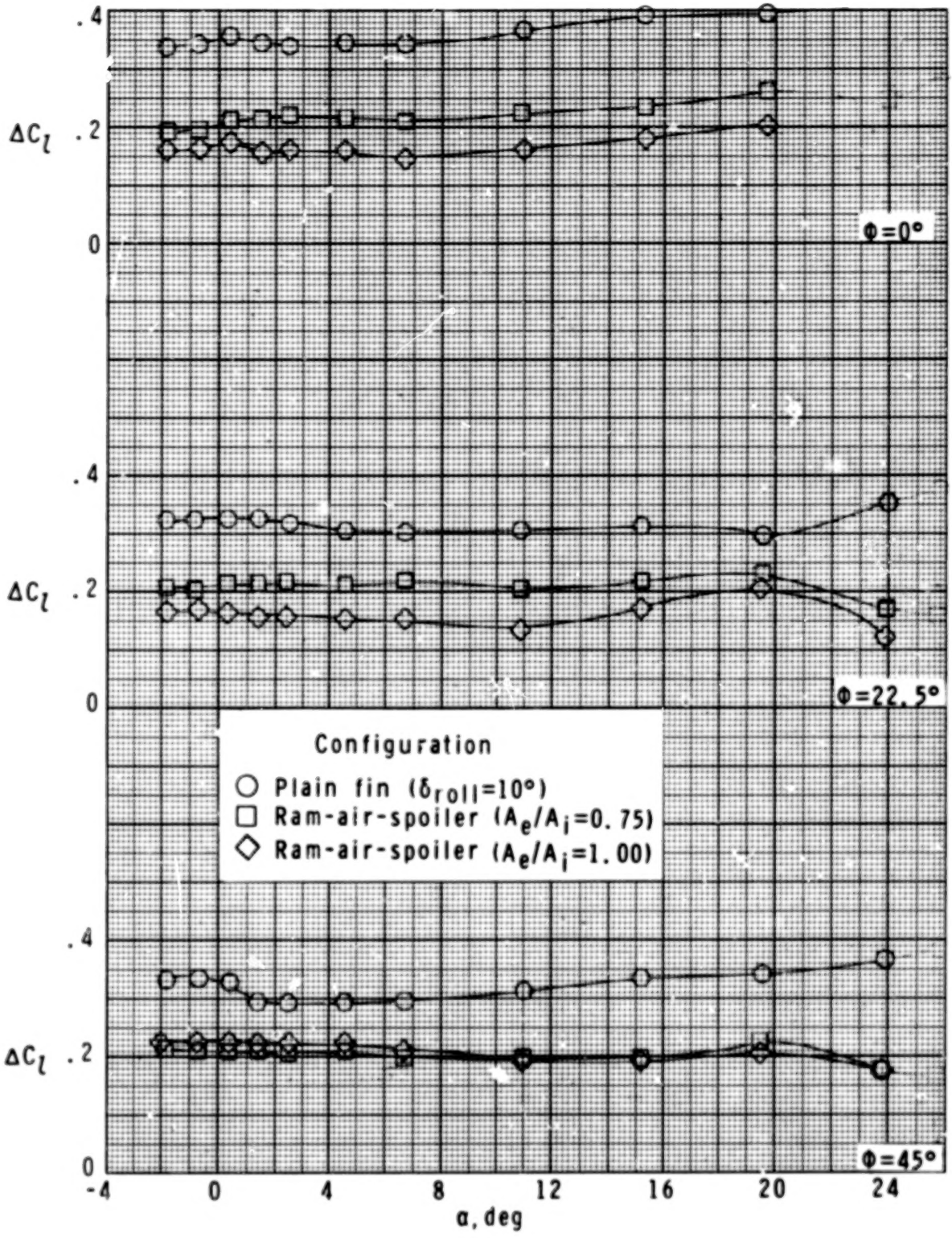

(a) $M_\infty = 1.90$.

Figure 4.- Comparison of roll control for four ram-jet spoiler tail fins and four plain tail fins with trailing-edge ailerons.

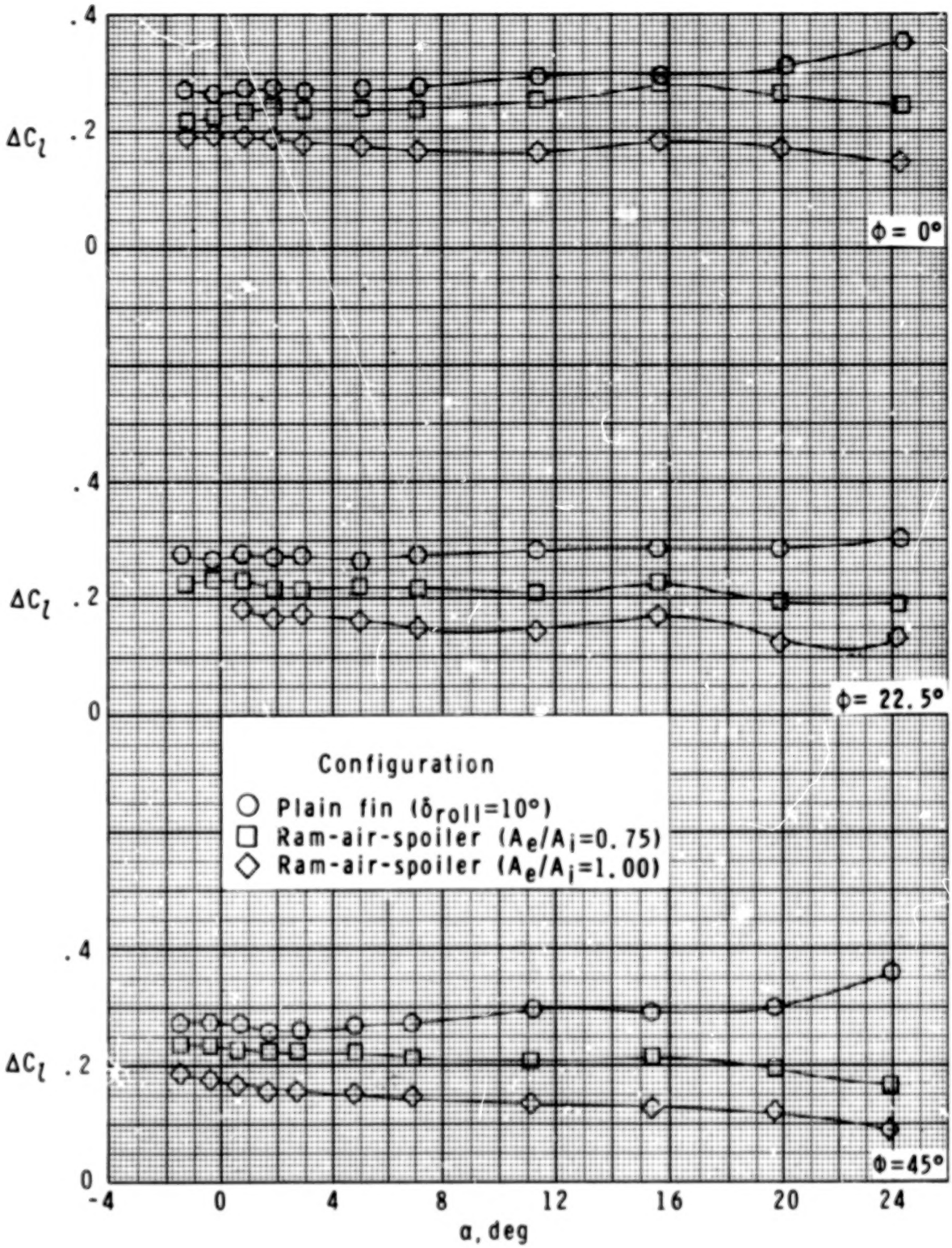

(b) $M_\infty = 2.16$.

Figure 4.- Continued.

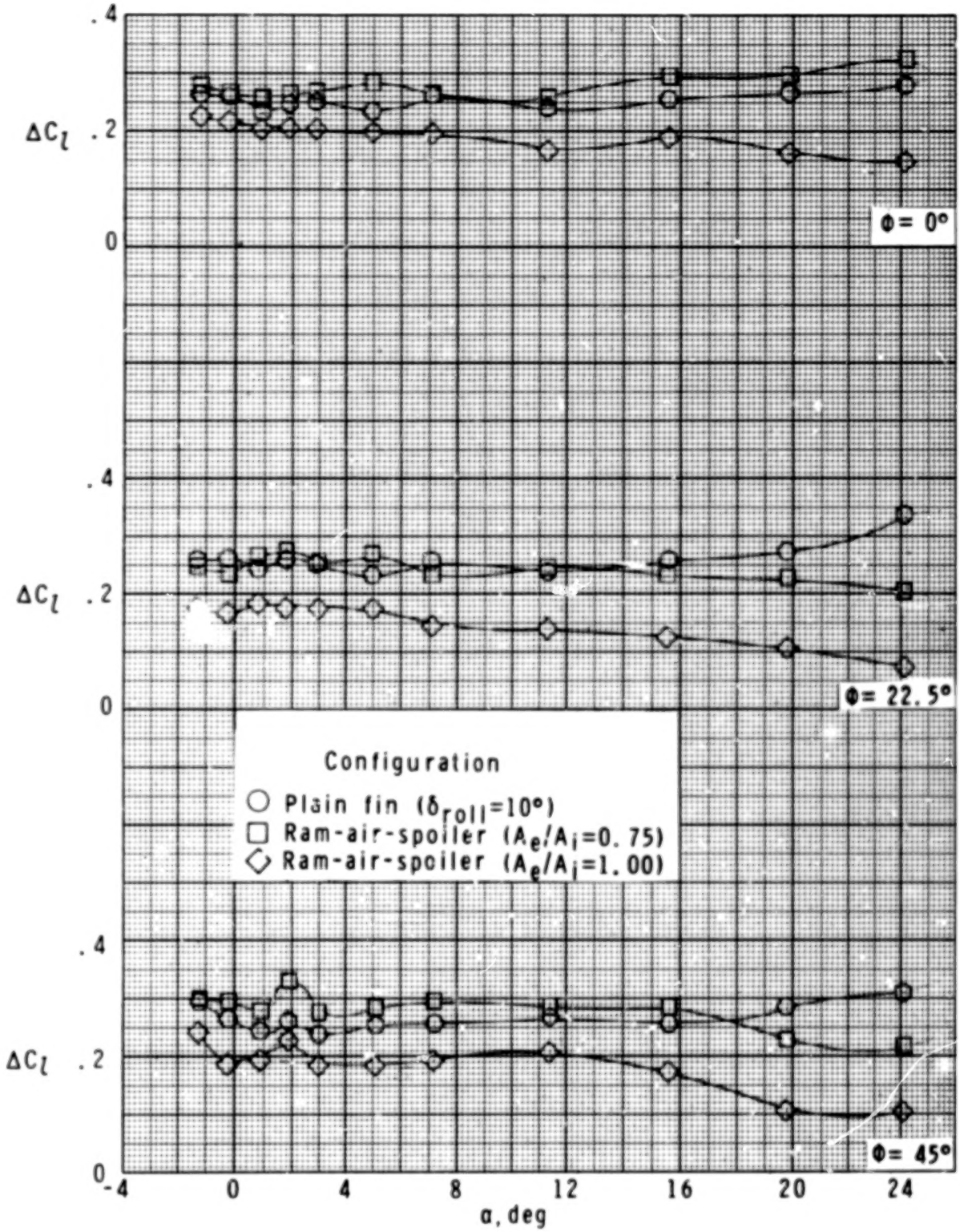

(c) $M_\infty = 2.40$.

Figure 4.- Continued.

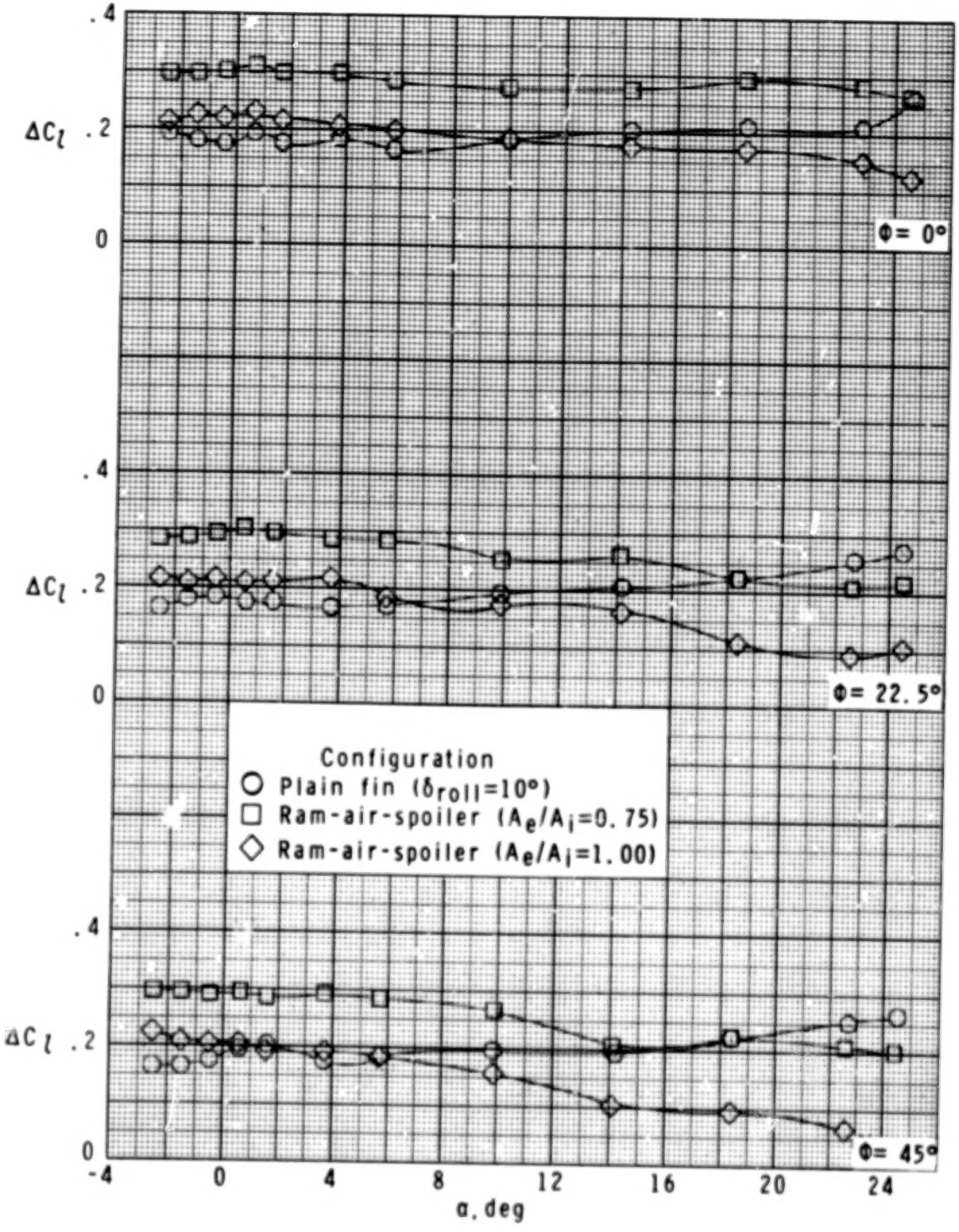

(d) $M_\infty = 2.86$.

Figure 4.- Concluded.

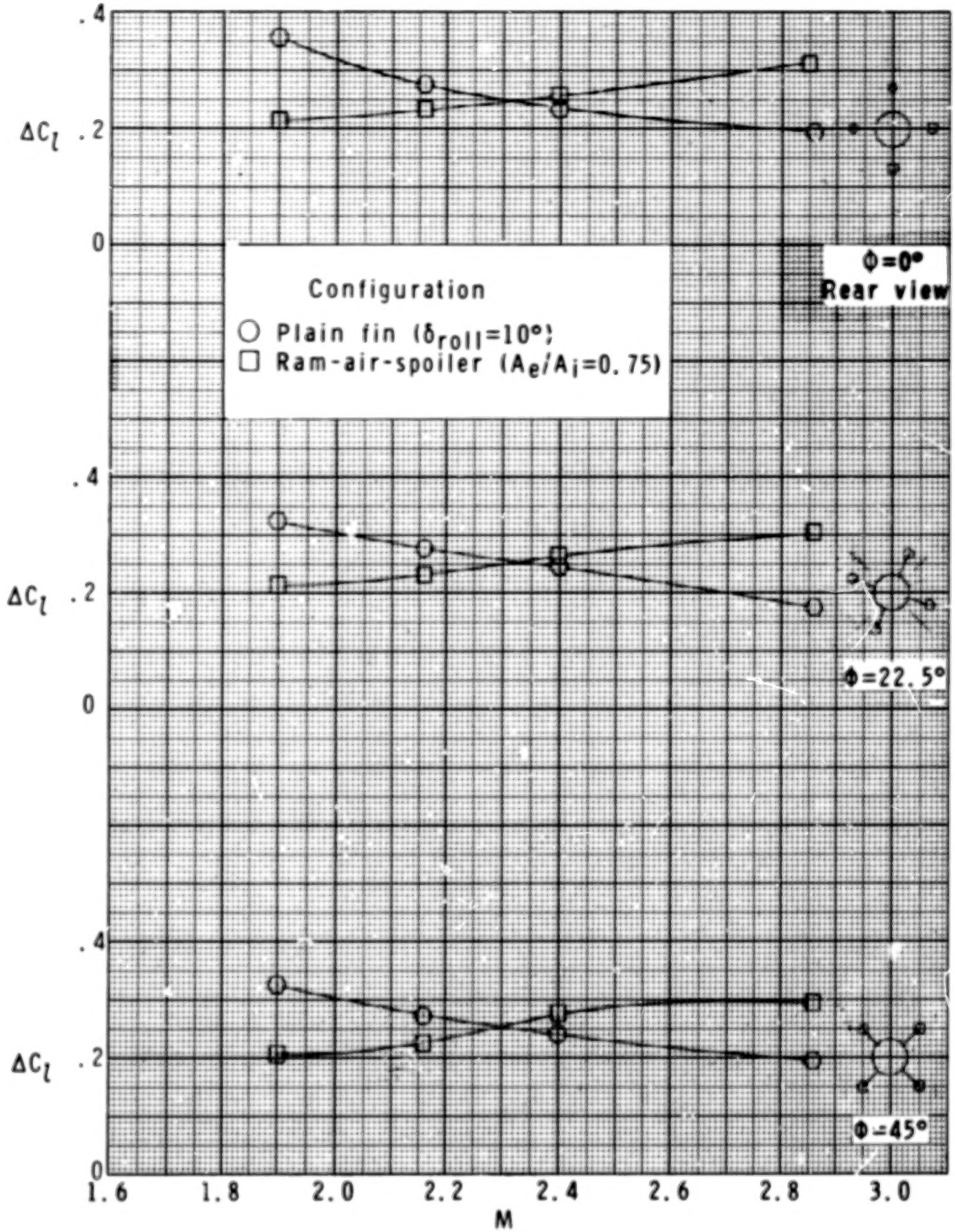

Figure 5.- Summary of zero-lift roll control for four ram-air-jet spoiler tail fins and four plain tail fins with trailing-edge aileron. $\alpha \approx 0^{\circ}$.

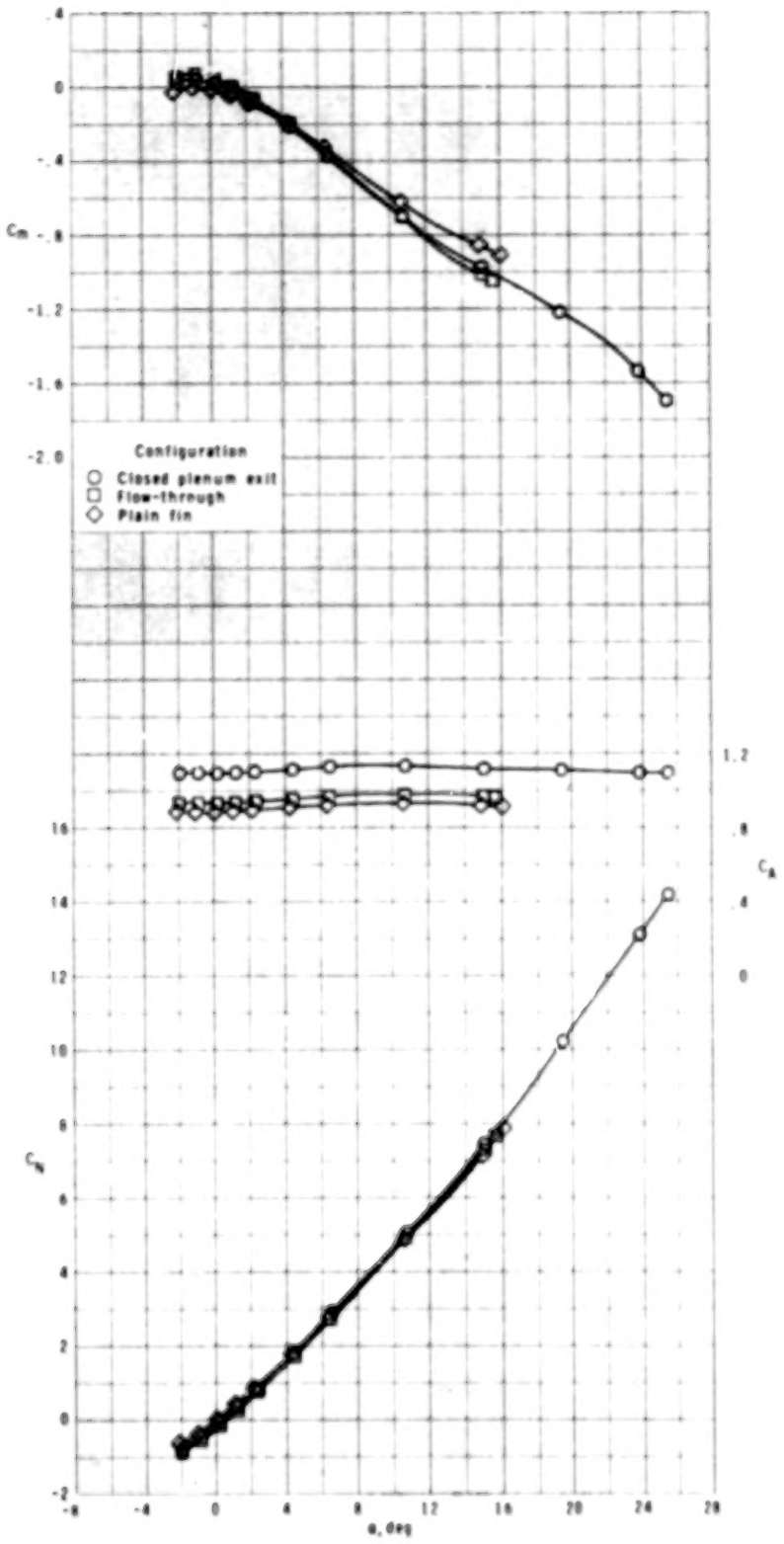

(a) $M_\infty = 1.90$.

Figure 6.- Effect of closed plenum exit and flow-through nacelle configurations on longitudinal aerodynamic characteristics of model. $\phi = 0^\circ$.

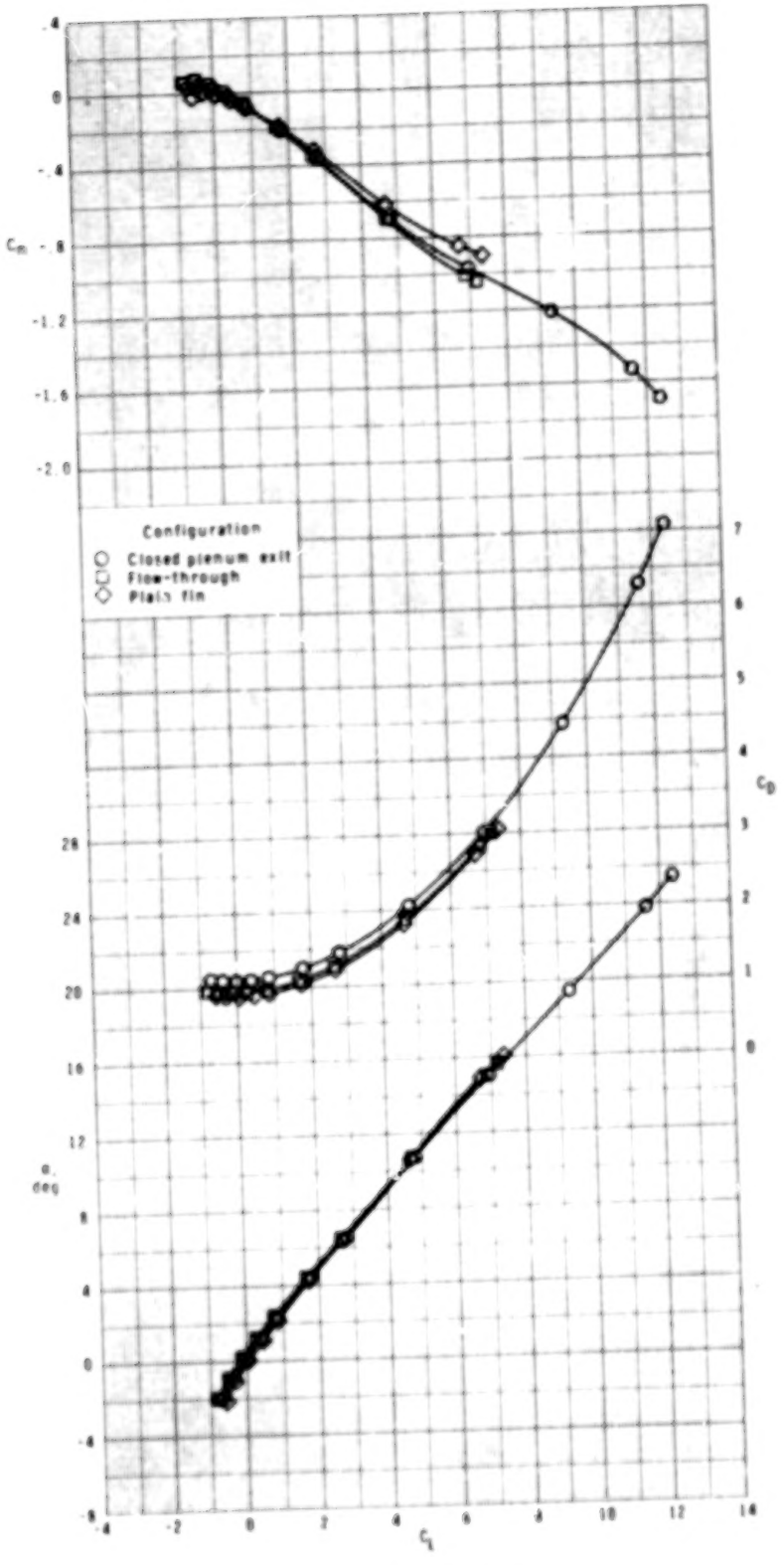

(a) Concluded.

Figure 6.- Continued.

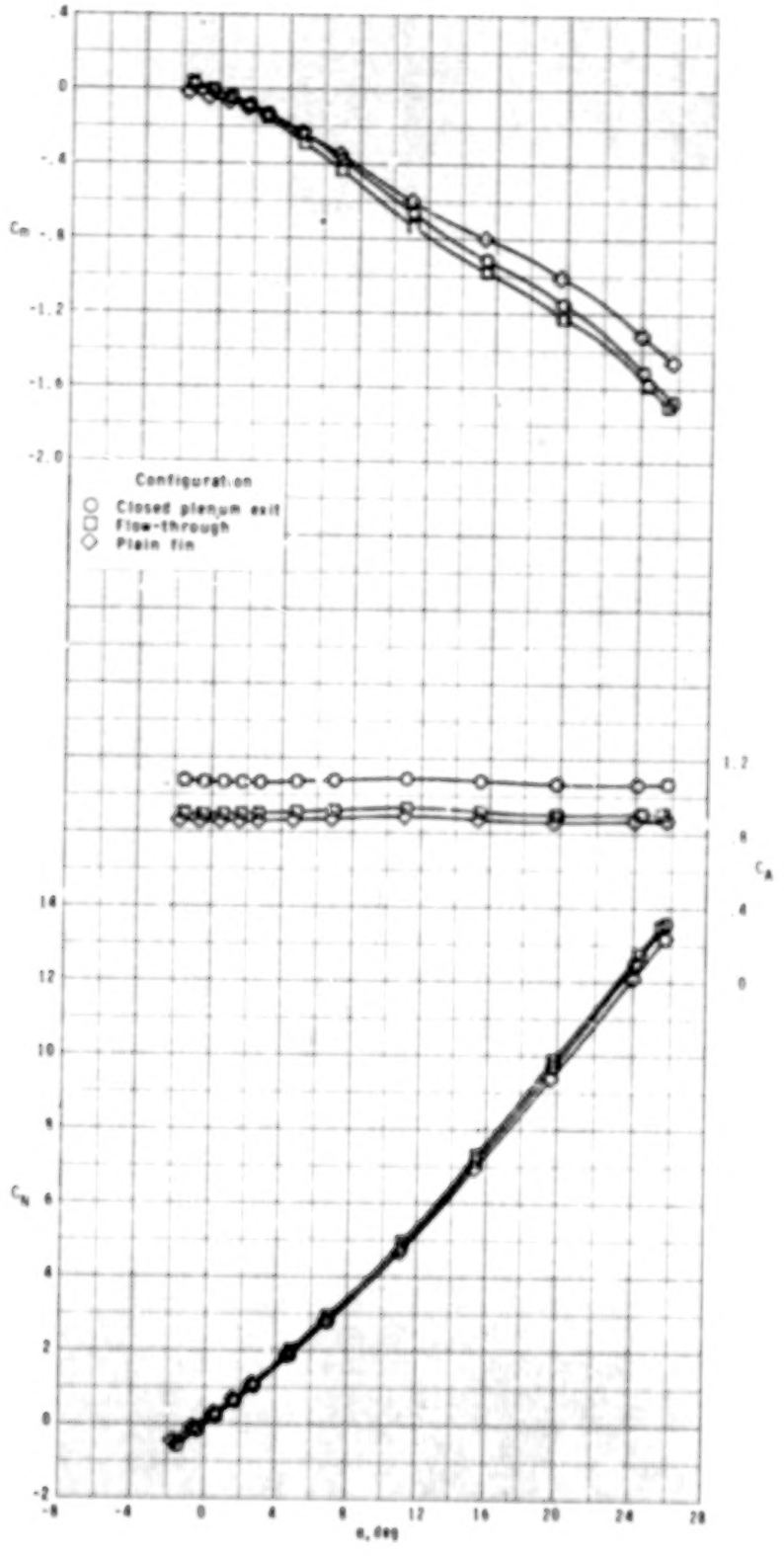

(b) $M_\infty = 2.16$.

Figure 6.- Continued.

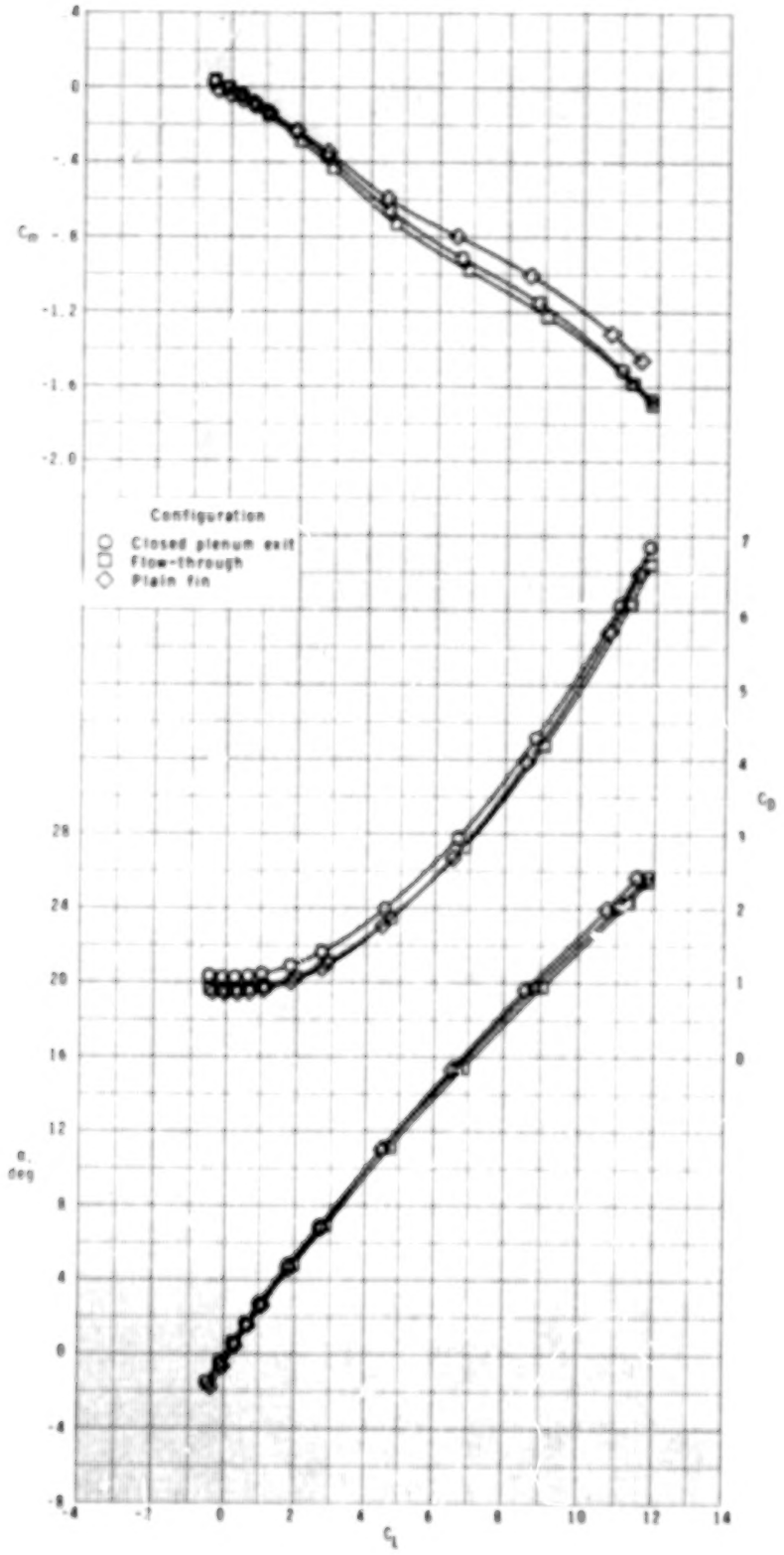

(b) Concluded.

Figure 6.- Continued.

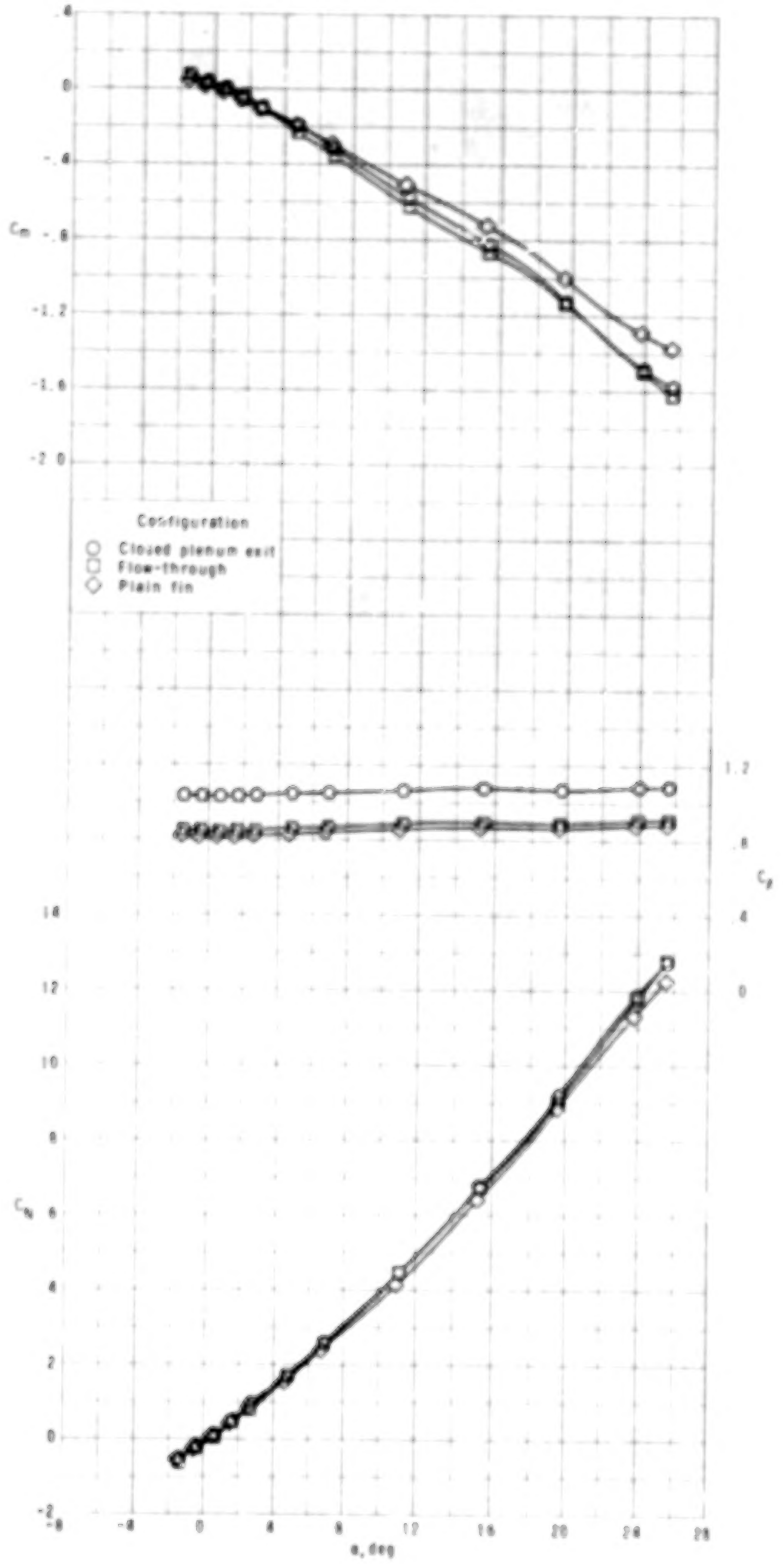

(c) $M_\infty = 2.40$.

Figure 6.- Continued.

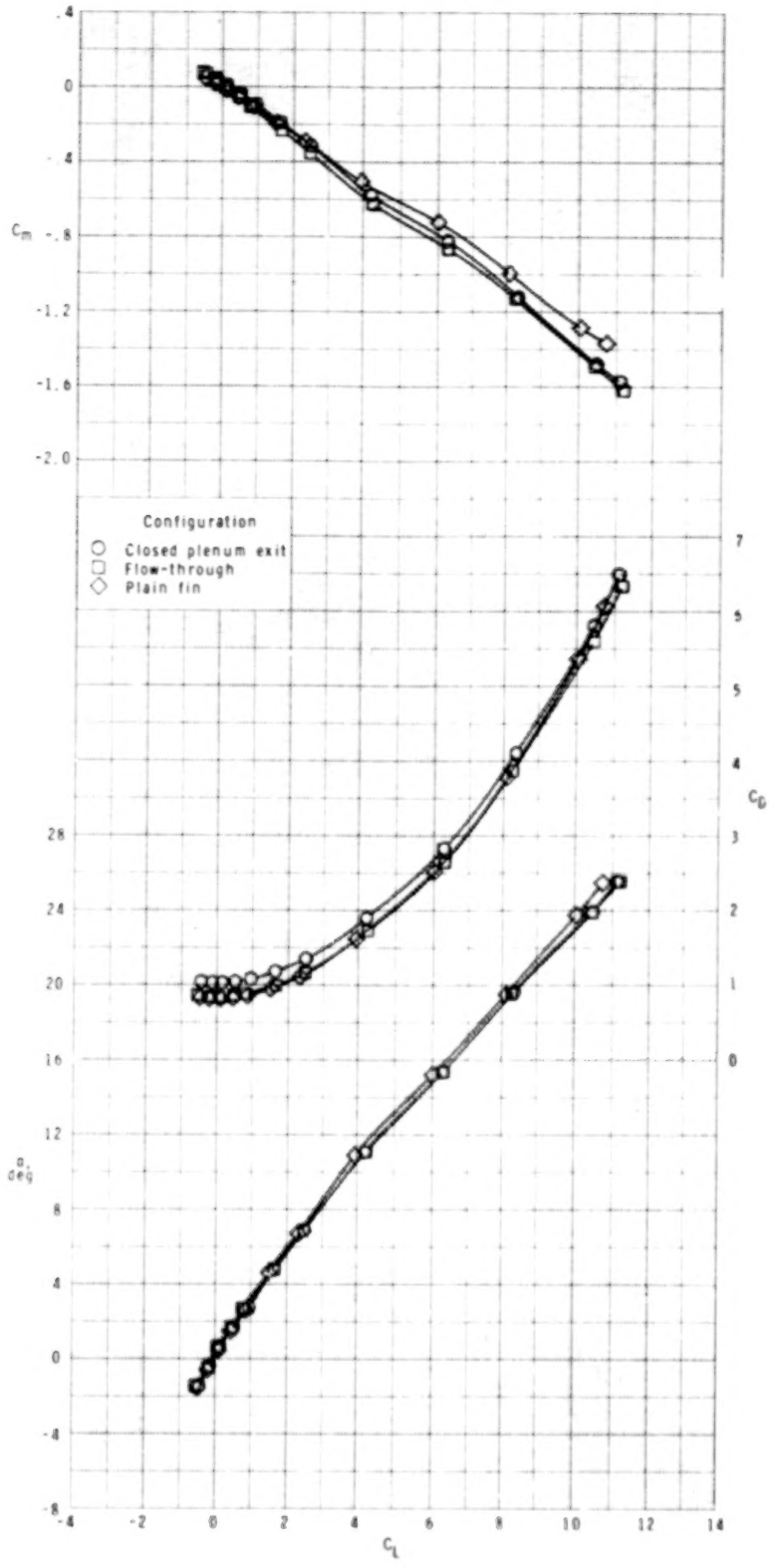

(c) Concluded.

Figure 6.- Continued.

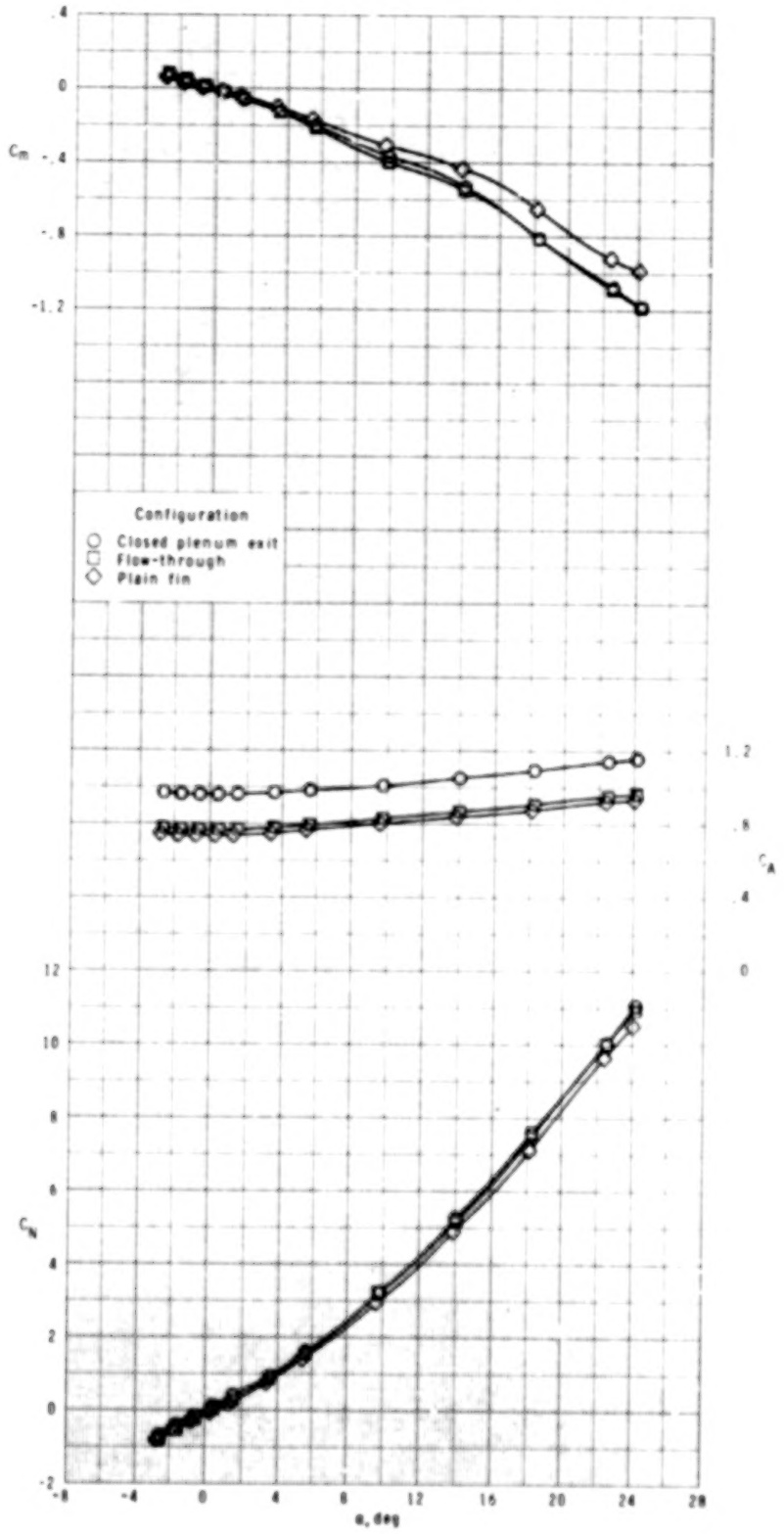

(d) $M_\infty = 2.86$.

Figure 6.- Continued.

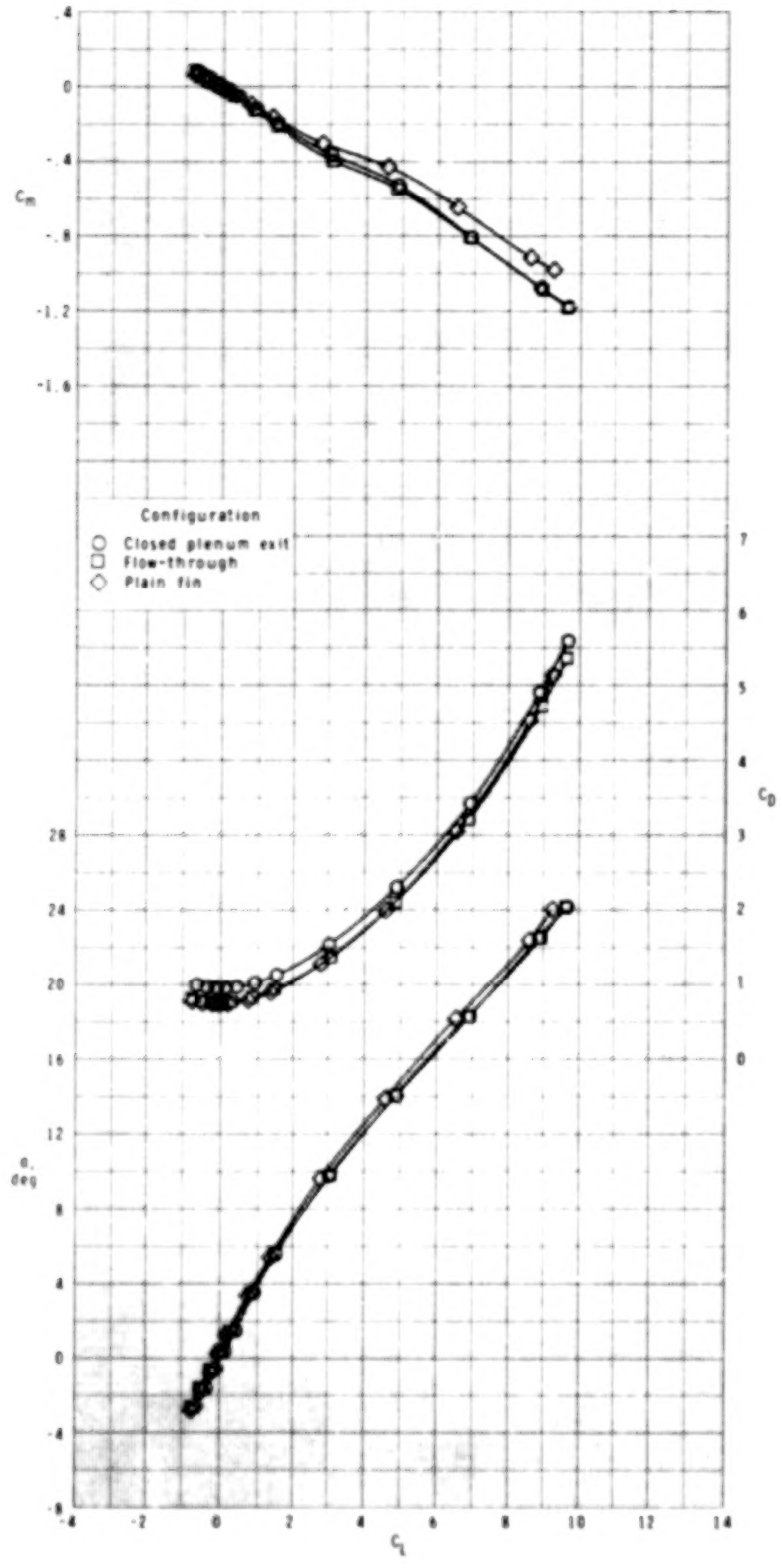

(d) Concluded.

Figure 6.- Concluded.

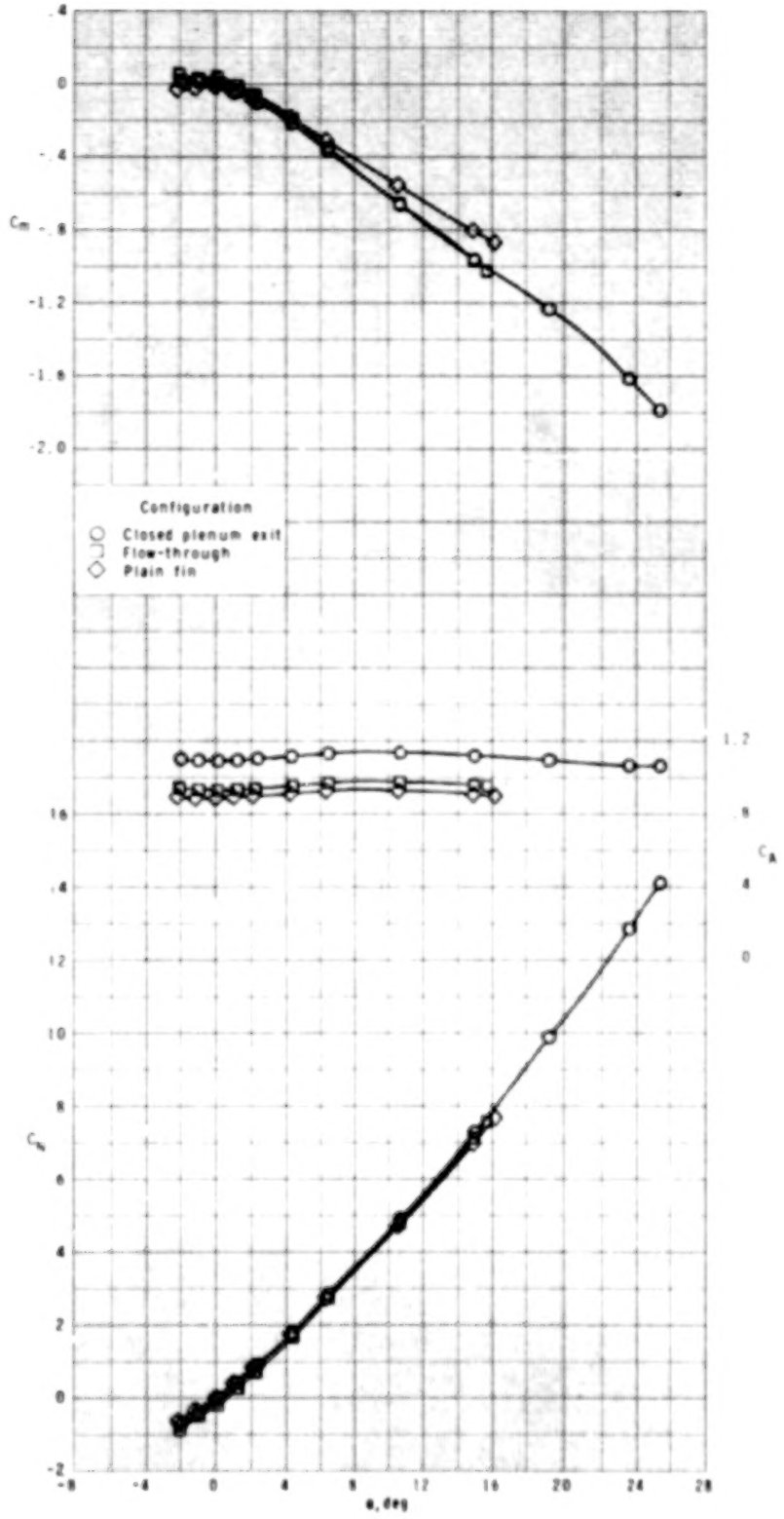

(a) $M_\infty = 1.90$.

Figure 7.- Effect of closed plenum exit and flow-through nacelle configurations on longitudinal aerodynamic characteristics of model. $\phi = 22.5^\circ$.

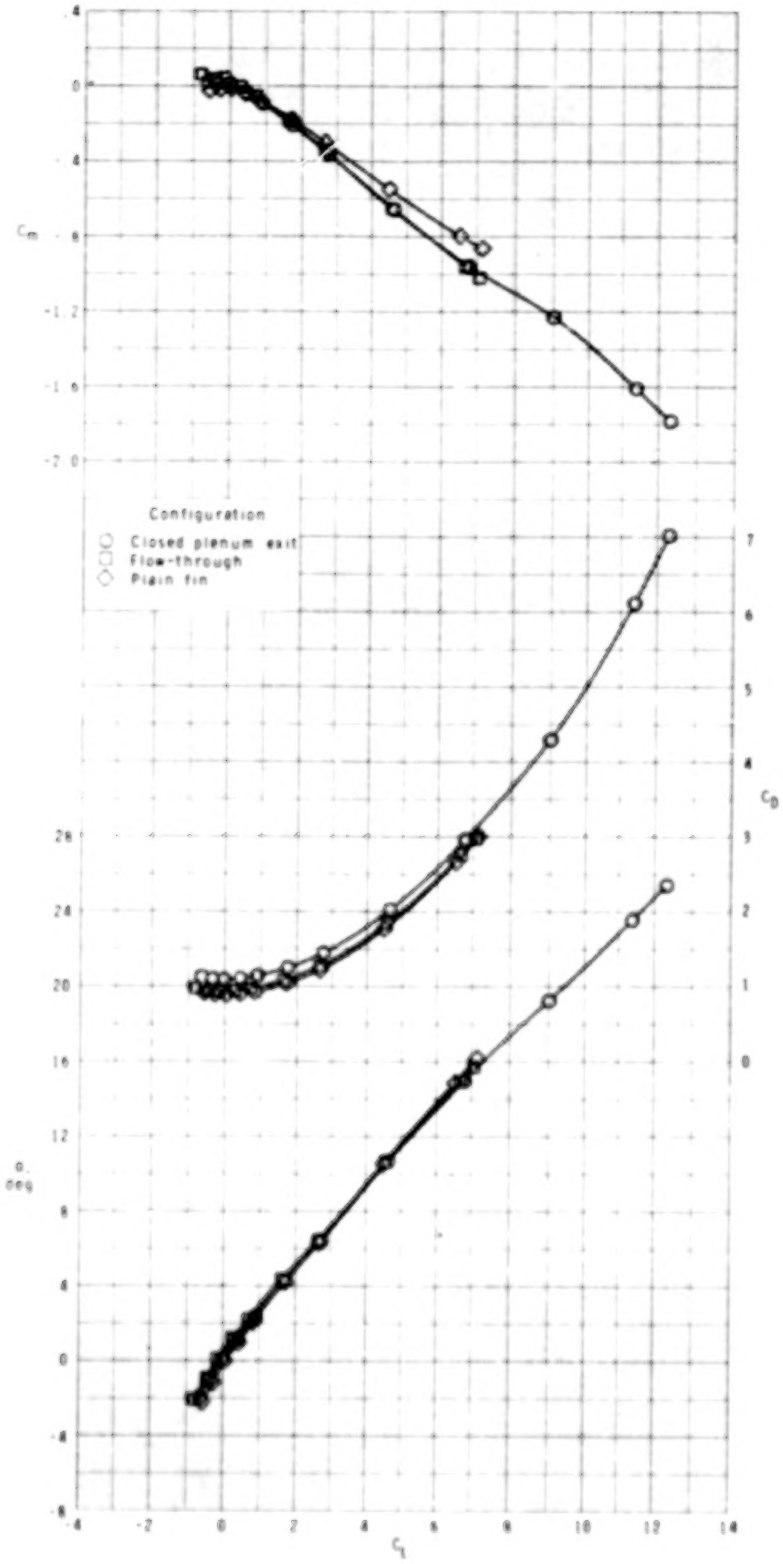

(a) Concluded.

Figure 7.- Continued.

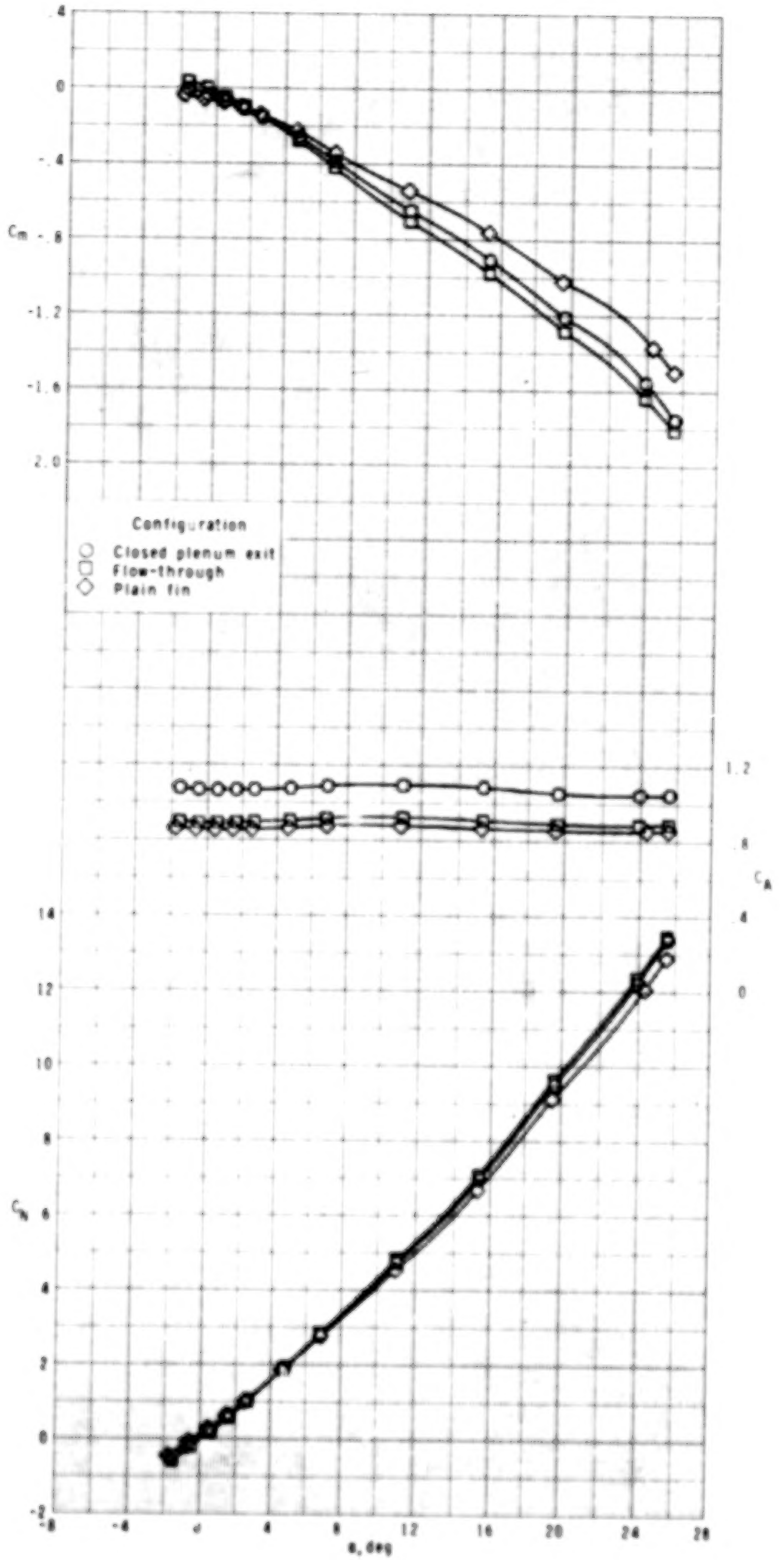

(b) $M_\infty = 2.16$.

Figure 7.- Continued.

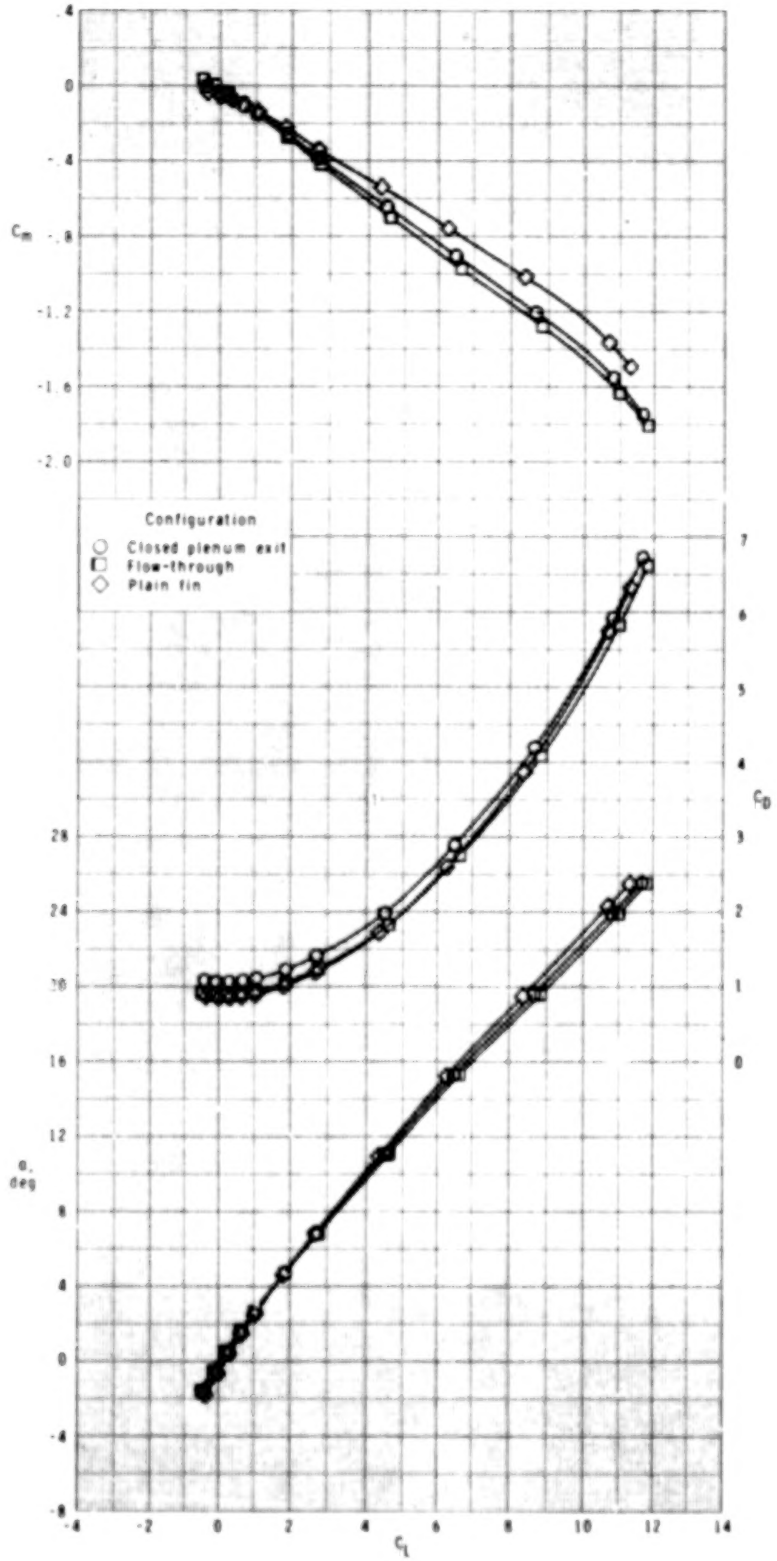

(b) Concluded.

Figure 7.- Continued.

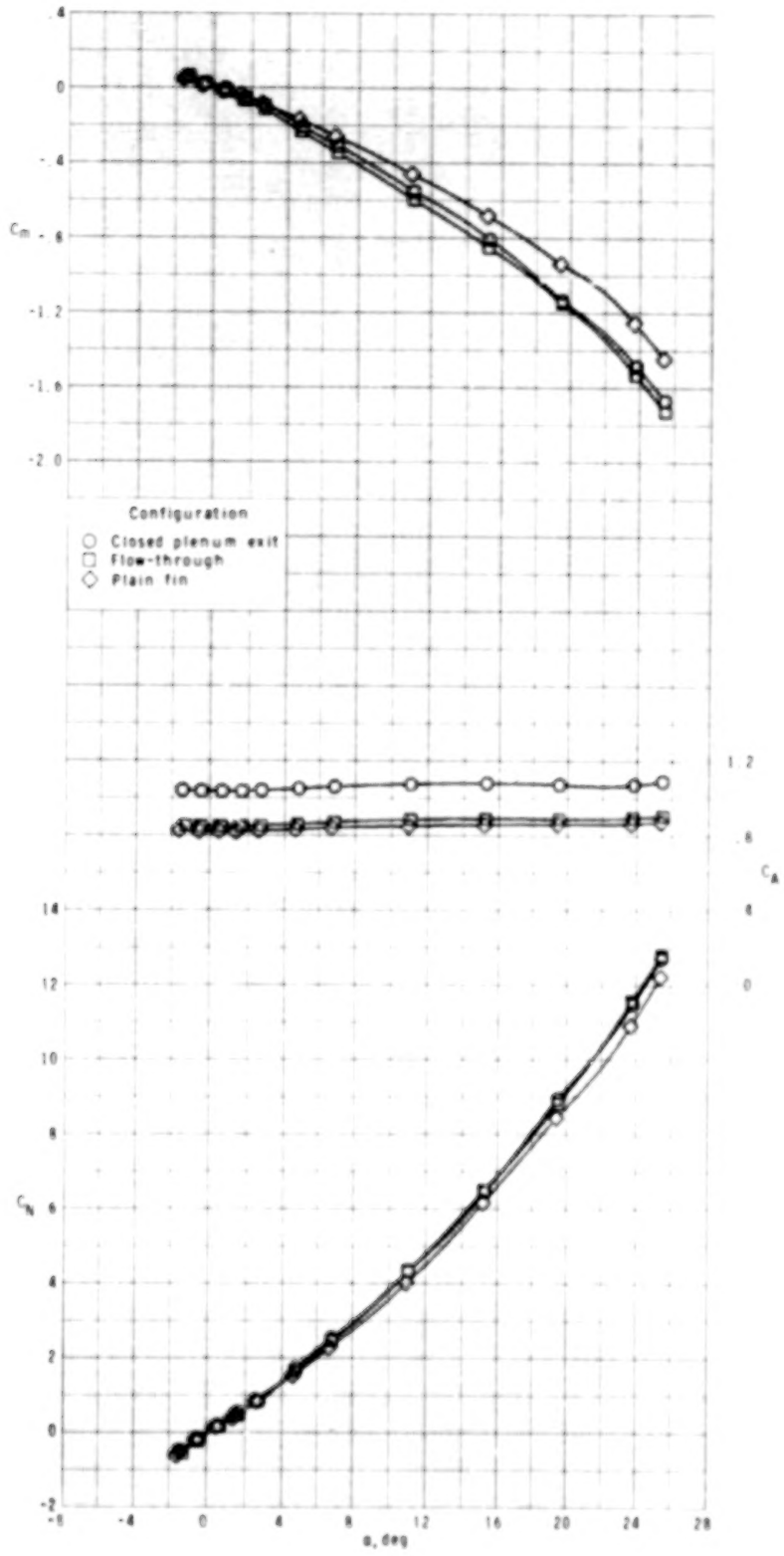

(c) $M_\infty = 2.40$.

Figure 7.- Continued.

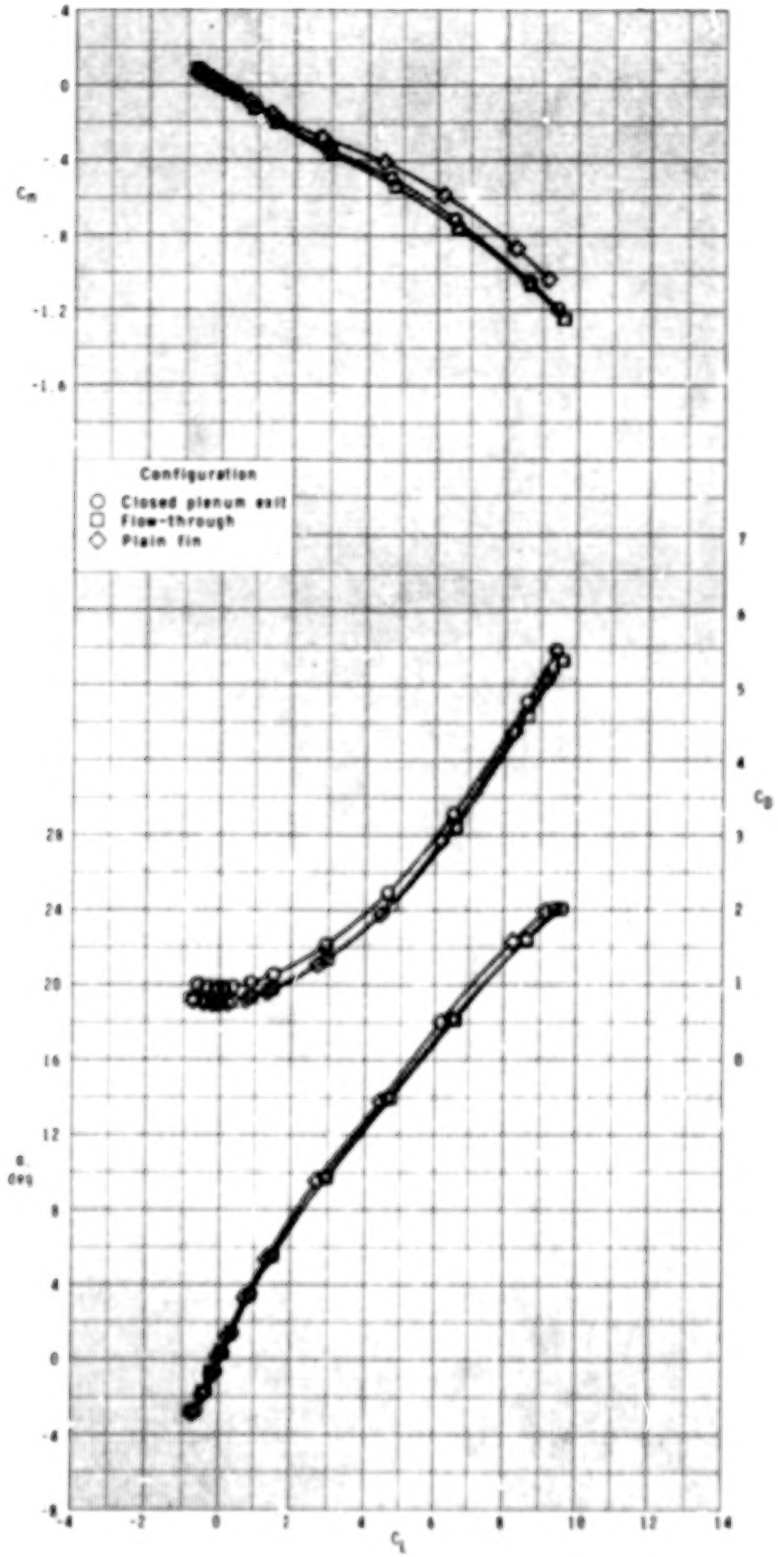

(c) Concluded.

Figure 7.- Continued.

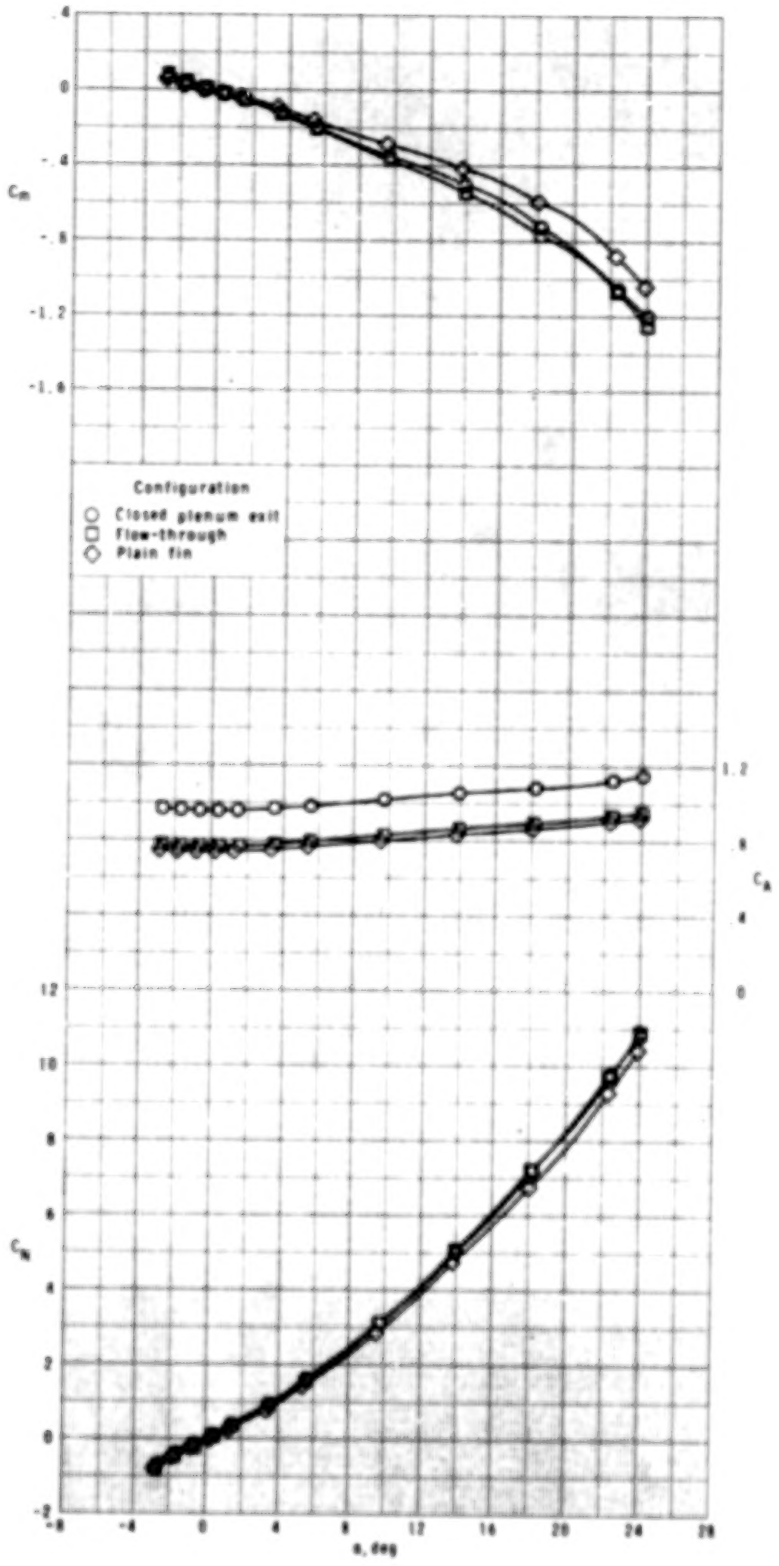

(d) $M_\infty = 2.86$.

Figure 7.- Continued.

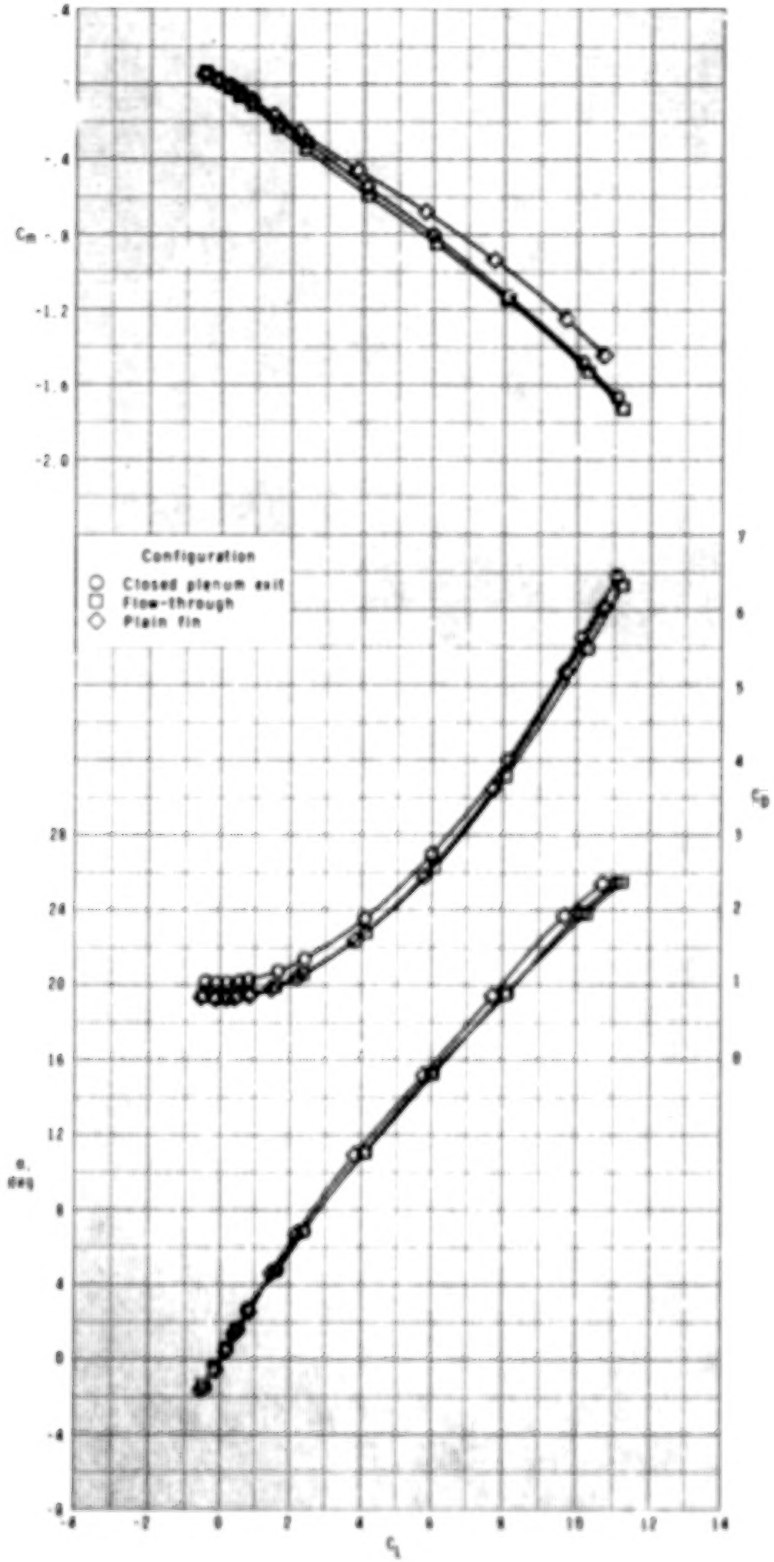

(d) Concluded.

Figure 7.- Concluded.

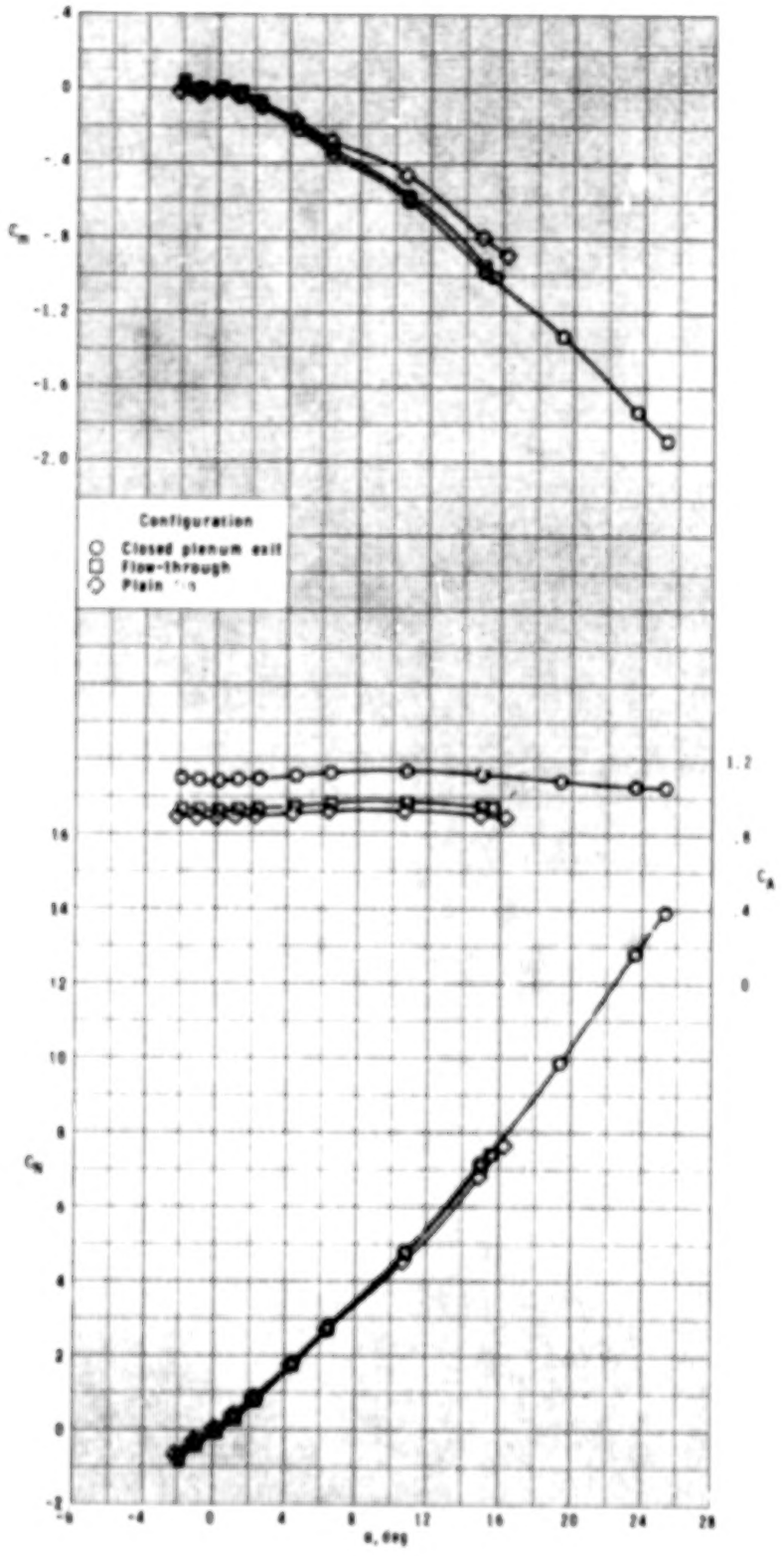

(a) $M_\infty = 1.90$.

Figure 8.- Effect of closed plenum exit and flow-through nacelle configurations on longitudinal aerodynamic characteristics of model. $\phi = 45^\circ$.

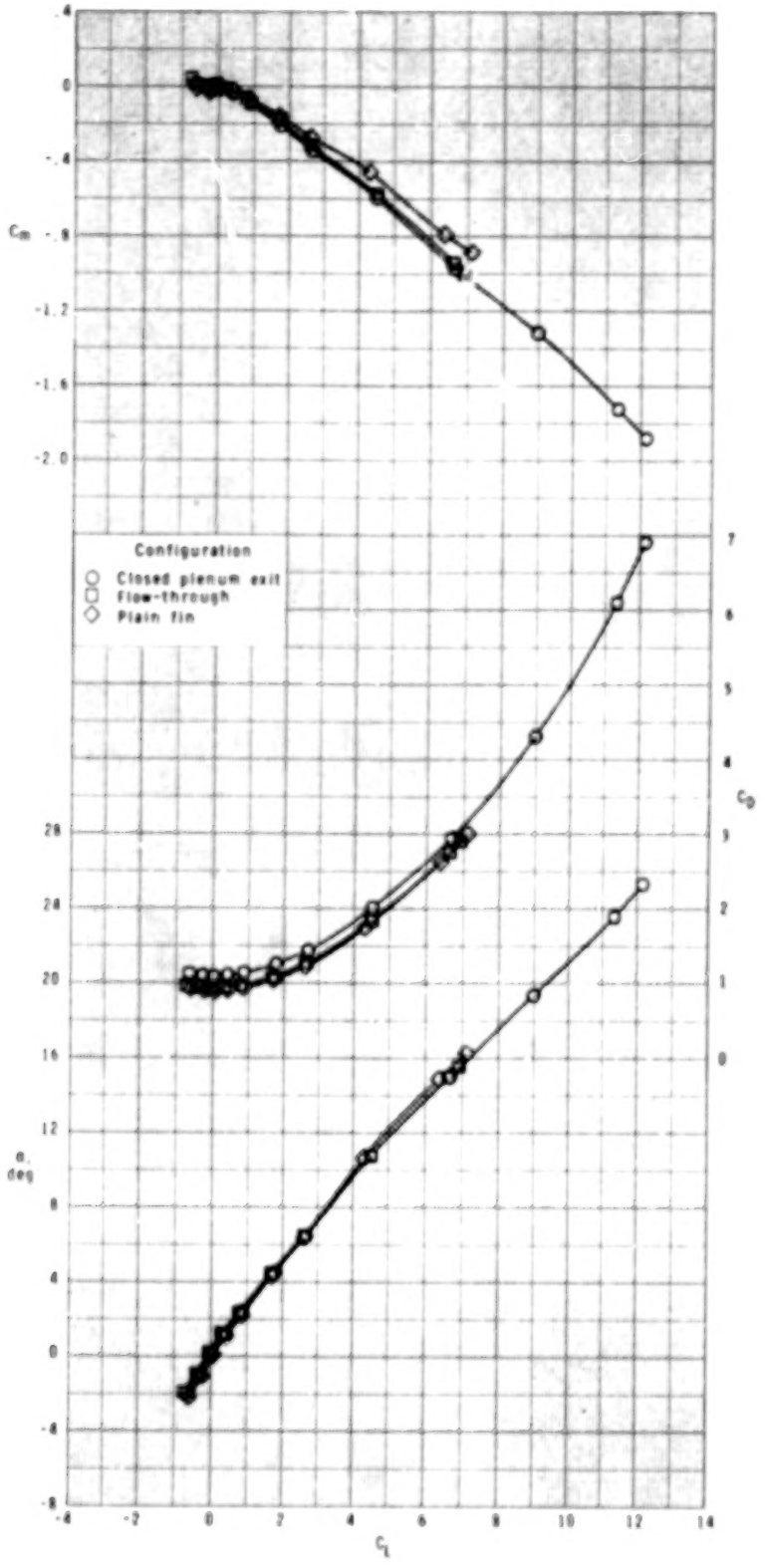

(a) Concluded.

Figure 8.- Continued.

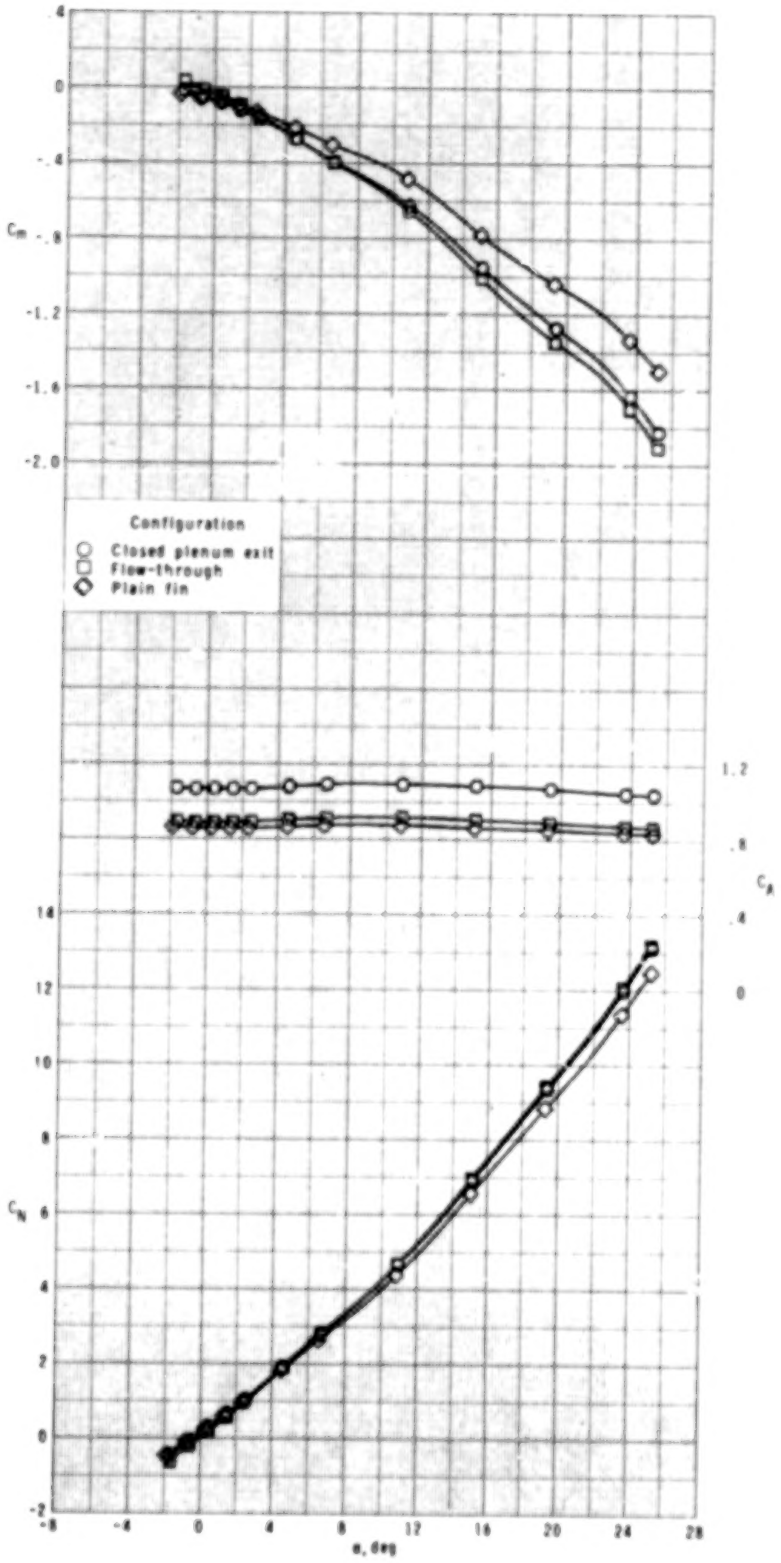

(b) $M_\infty = 2.16$.

Figure 8.- Continued.

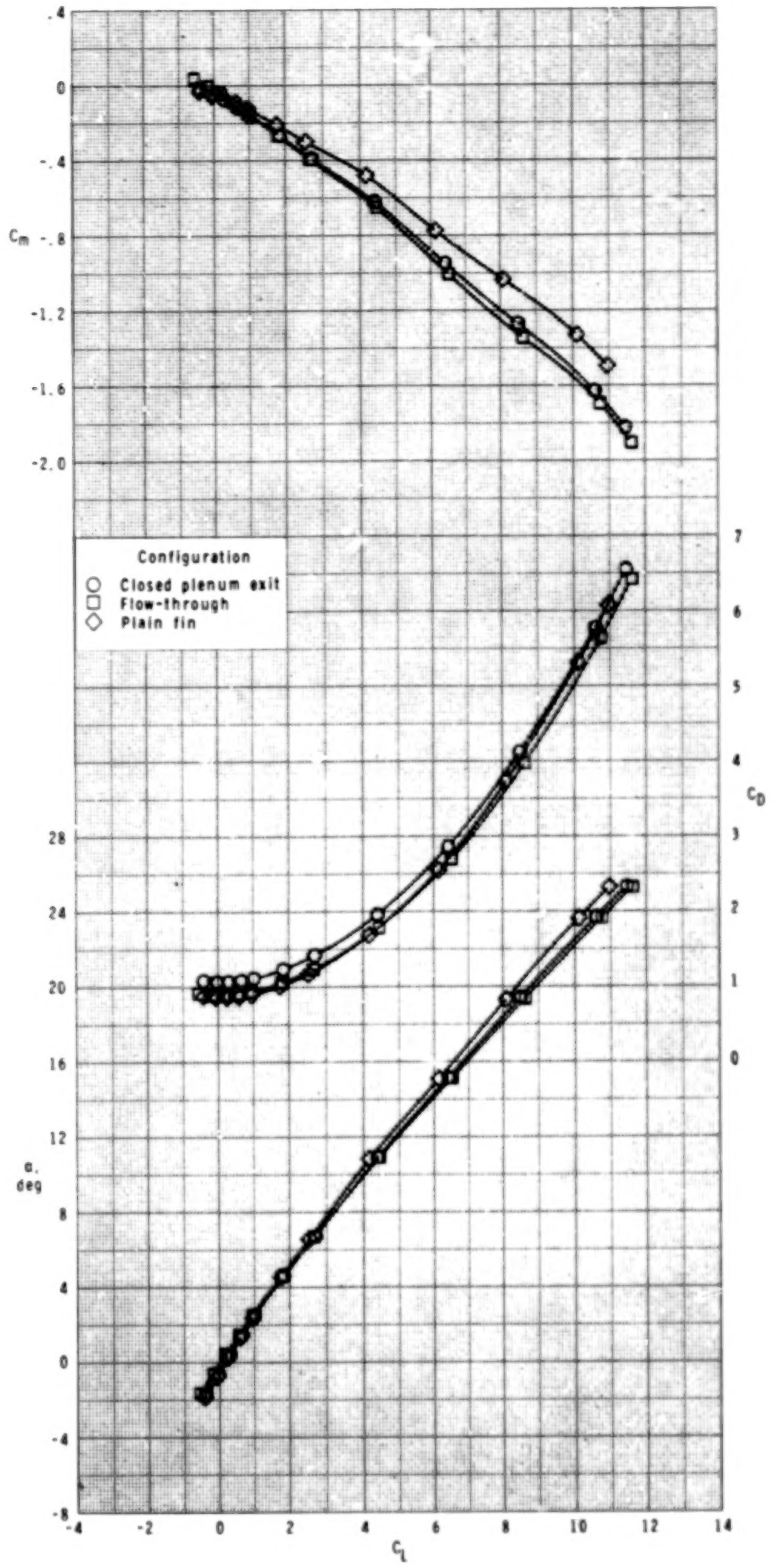

(b) Concluded.

Figure 8.- Continued.

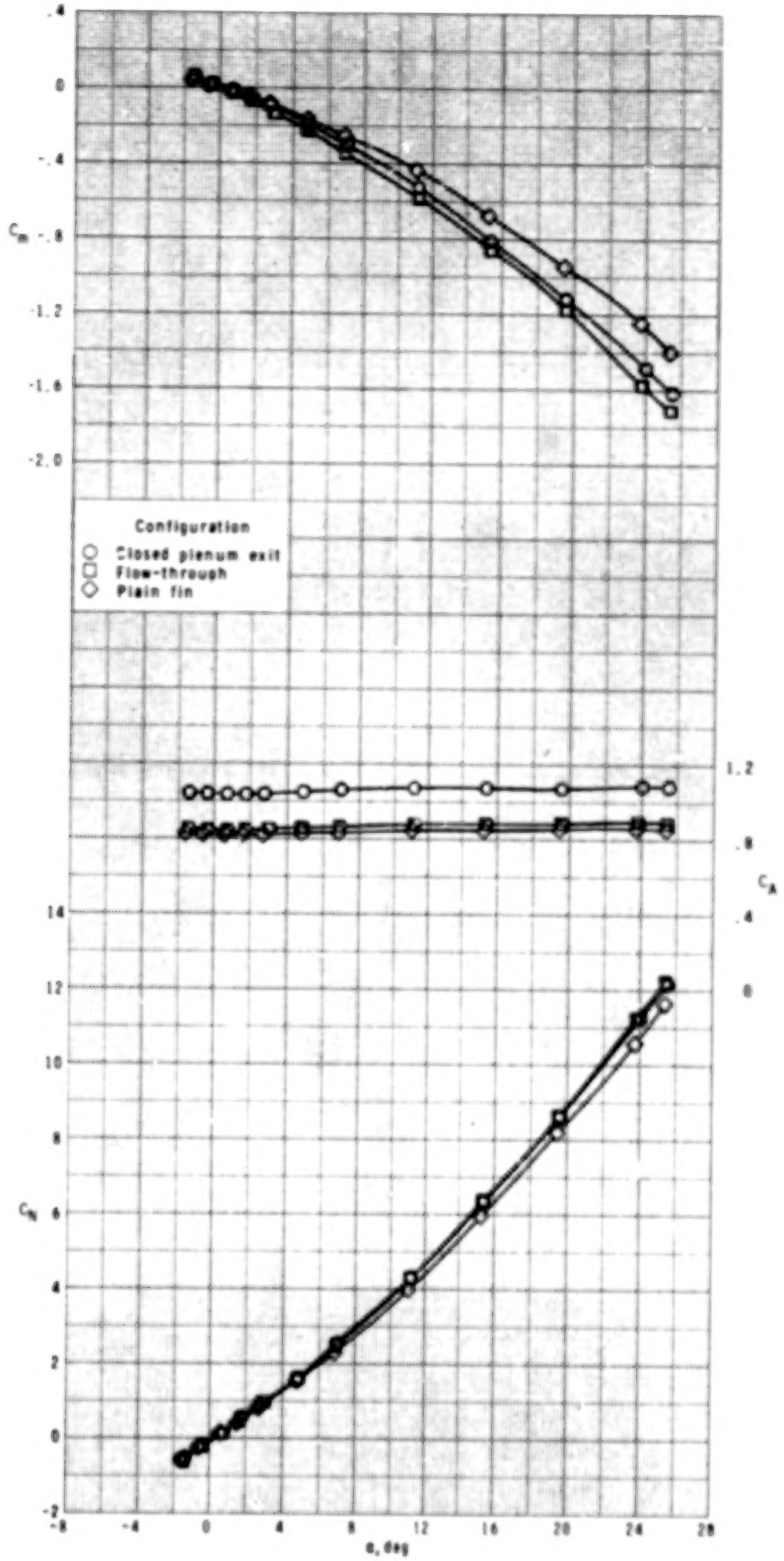

(c) $M_\infty = 2.40$.

Figure 8.- Continued.

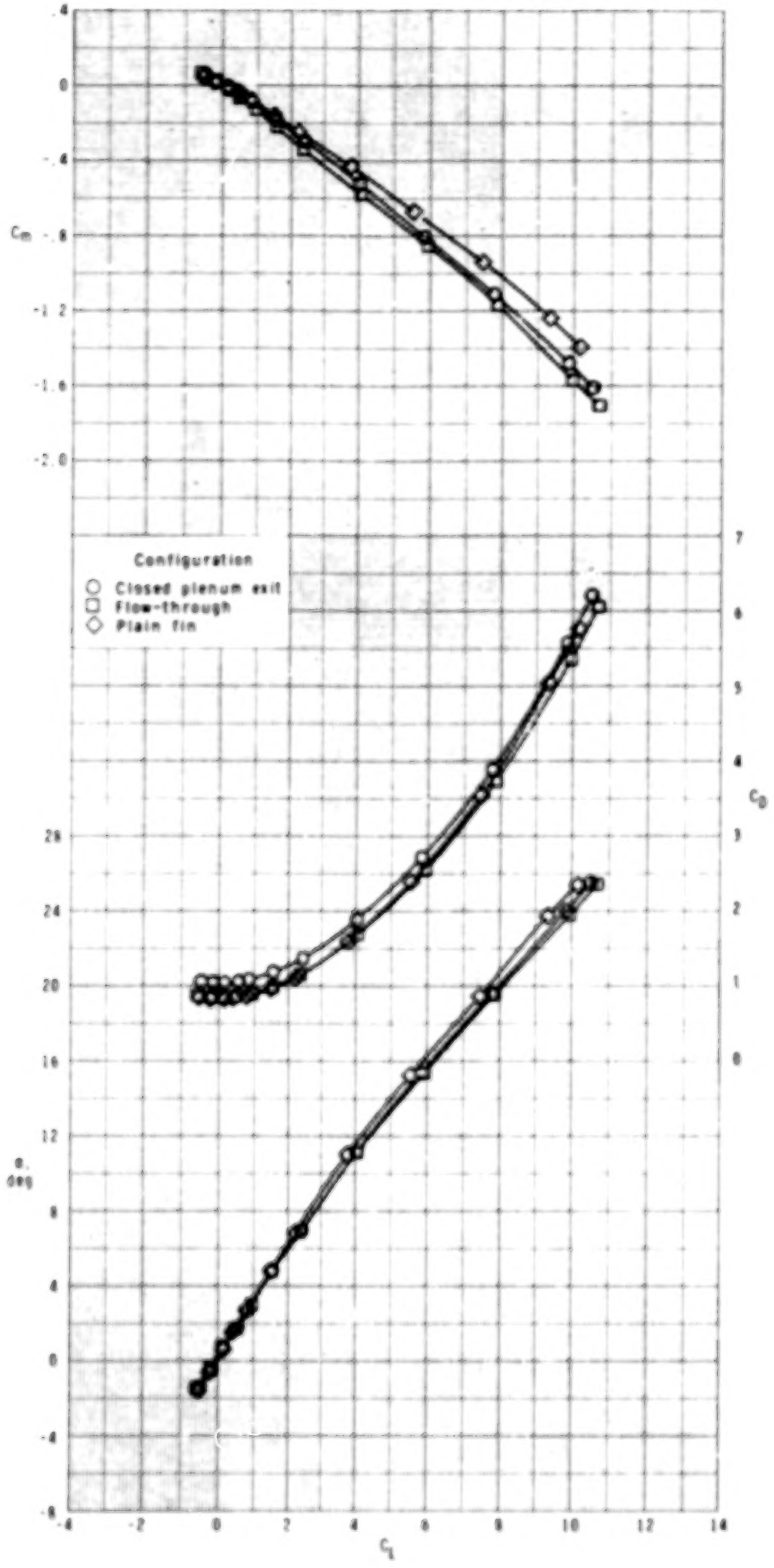

(c) Concluded.

Figure 8.- Continued.

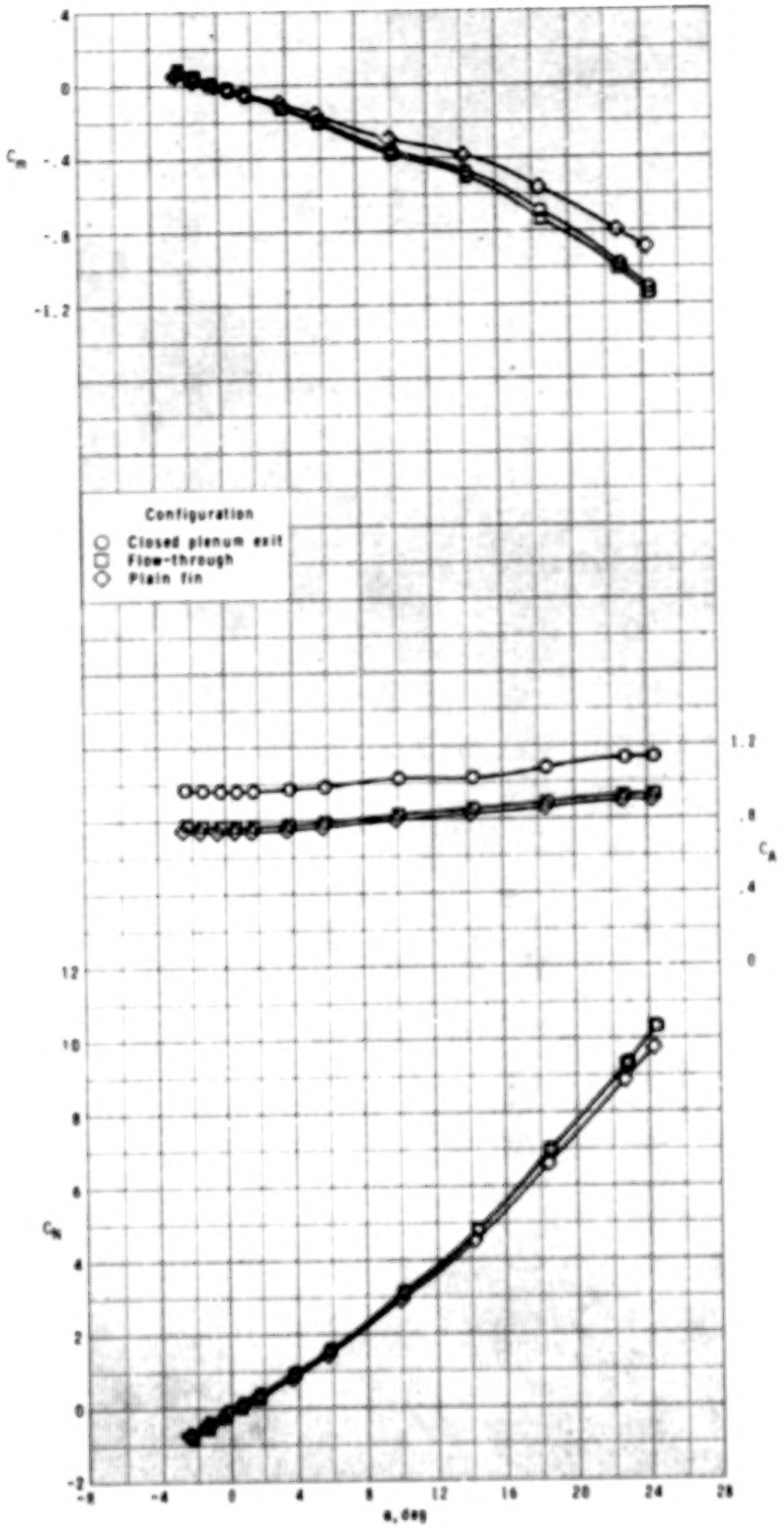

(d) $M_\infty = 2.86$.

Figure 8.- Continued.

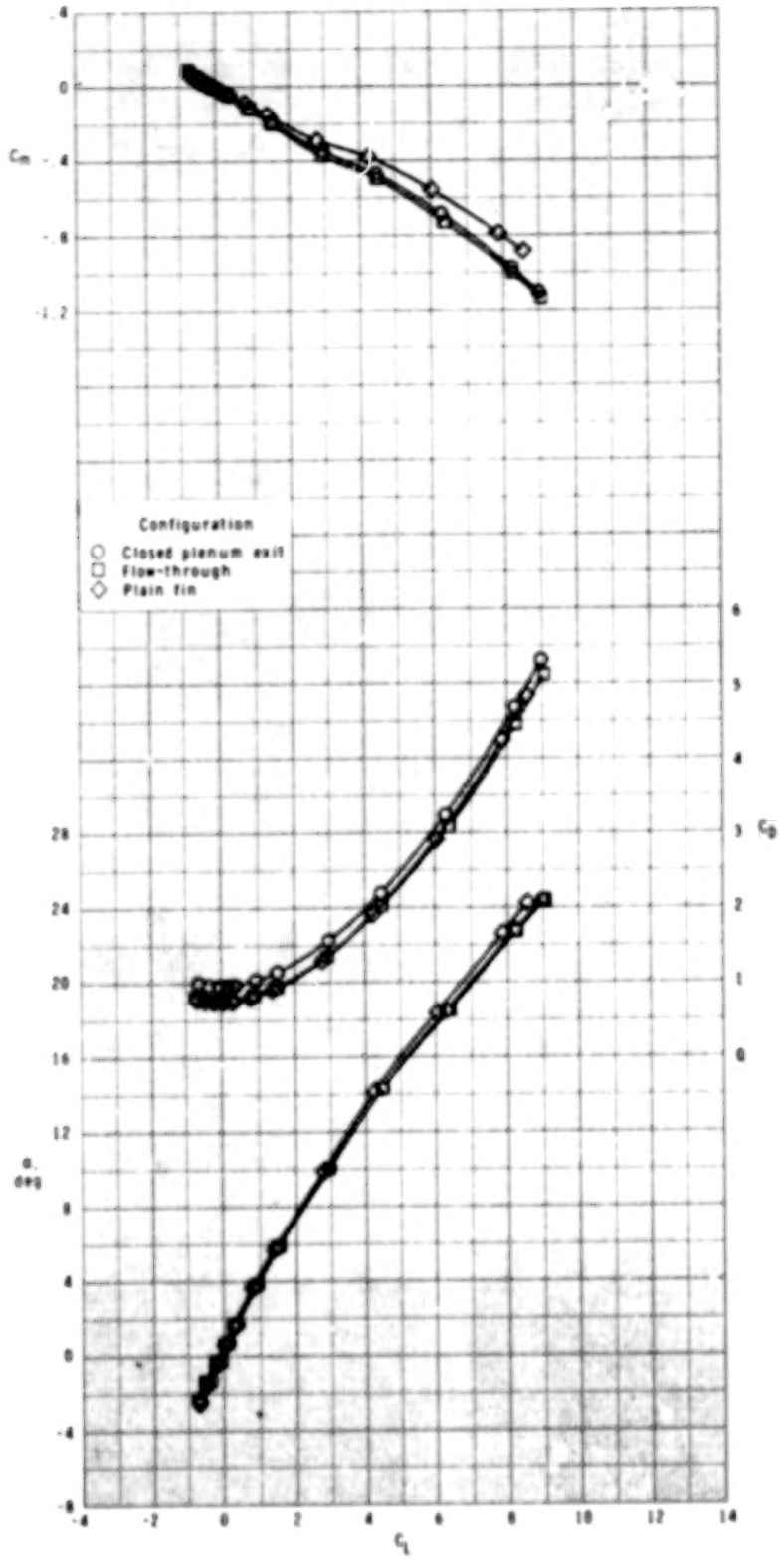

(d) Concluded.

Figure 8.- Concluded.

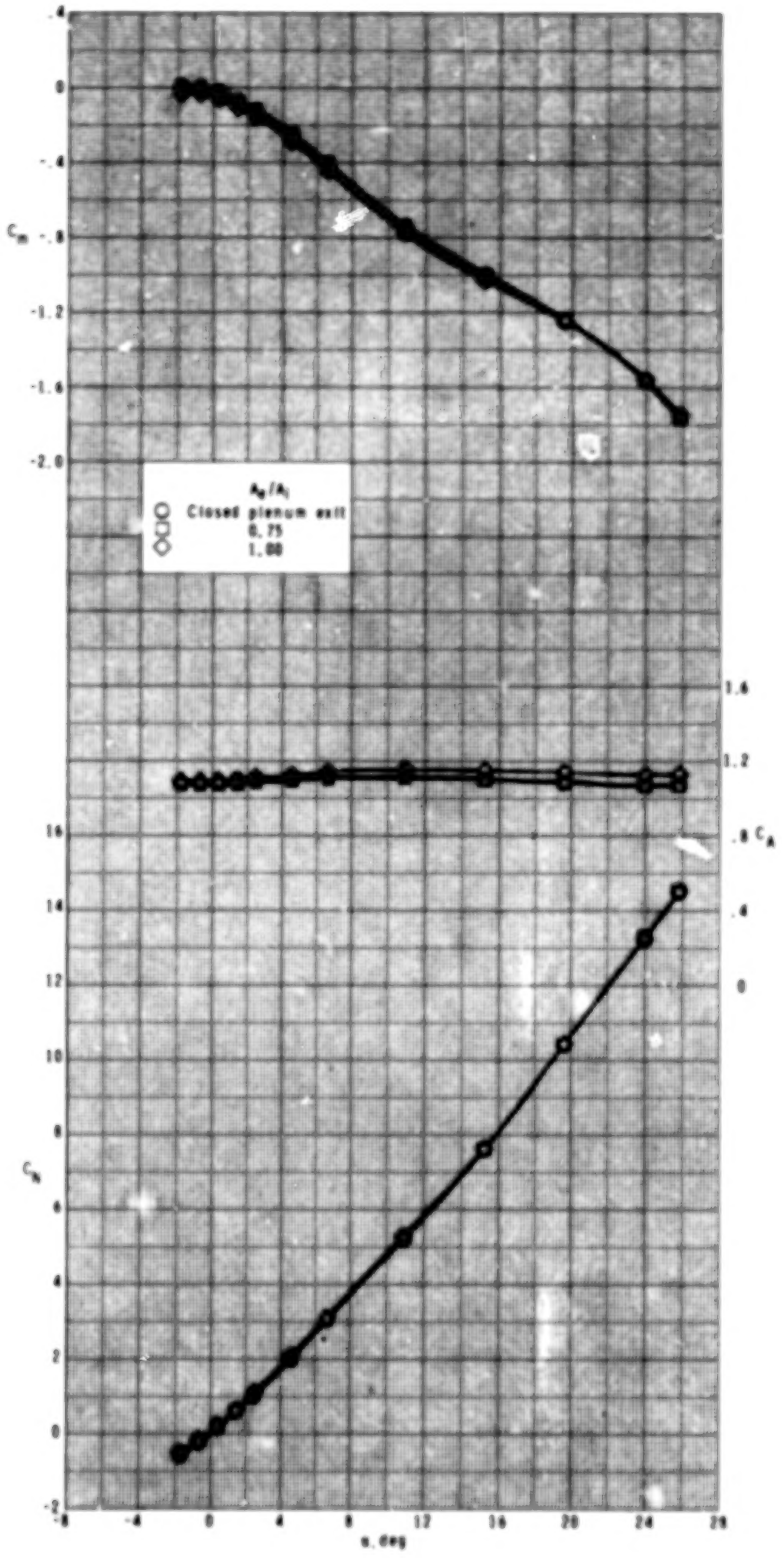

(a) $M_\infty = 1.90$.

Figure 9.- Effect of exit area to inlet area ratios for roll control on the longitudinal aerodynamic characteristics of model with four ram-air-jet spoiler tail fins. $\phi = 0^o$.

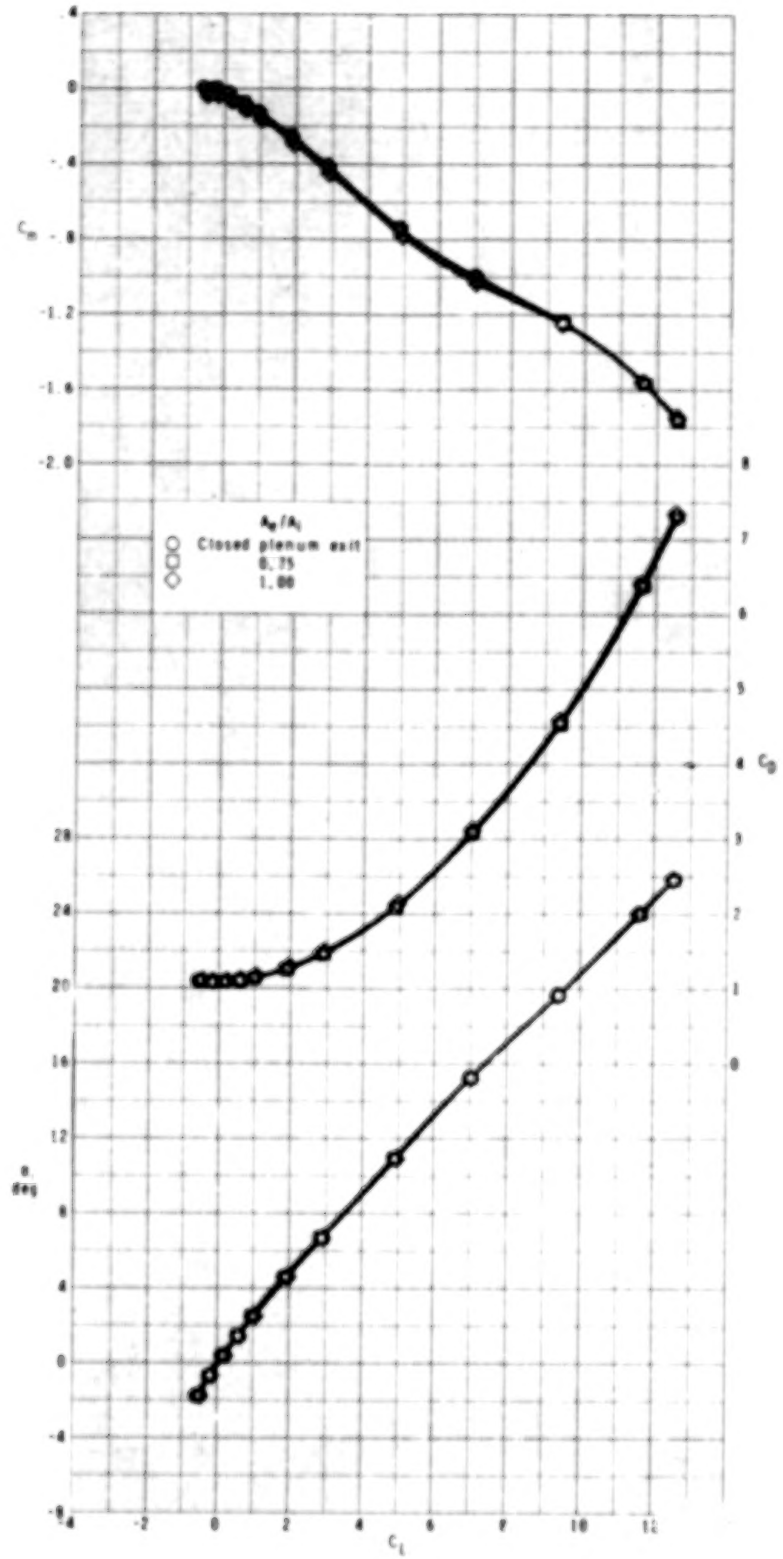

(a) Concluded.

Figure 9.- Continued.

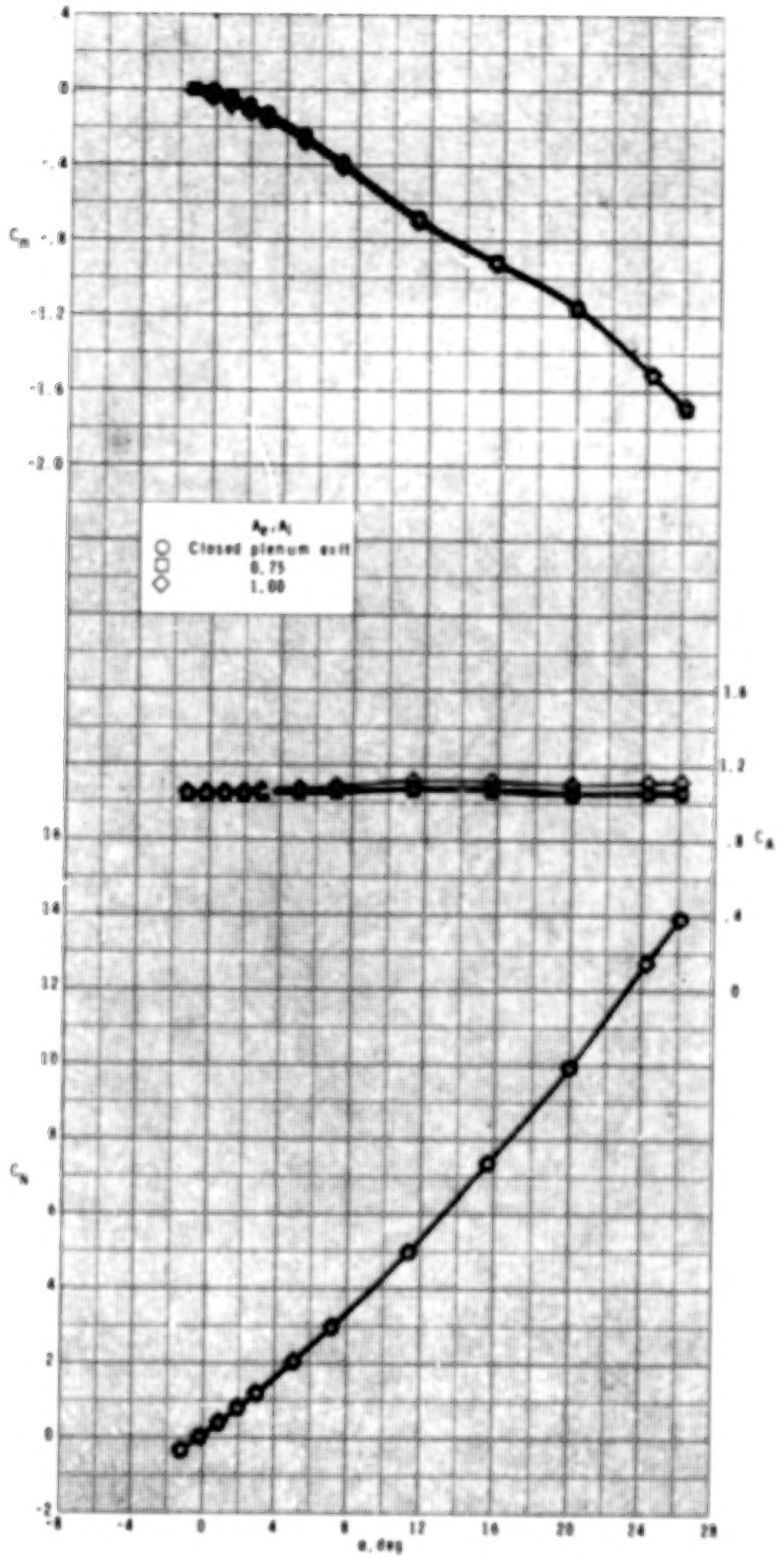

(b) $M_\infty = 2.16$.

Figure 9.- Continued.

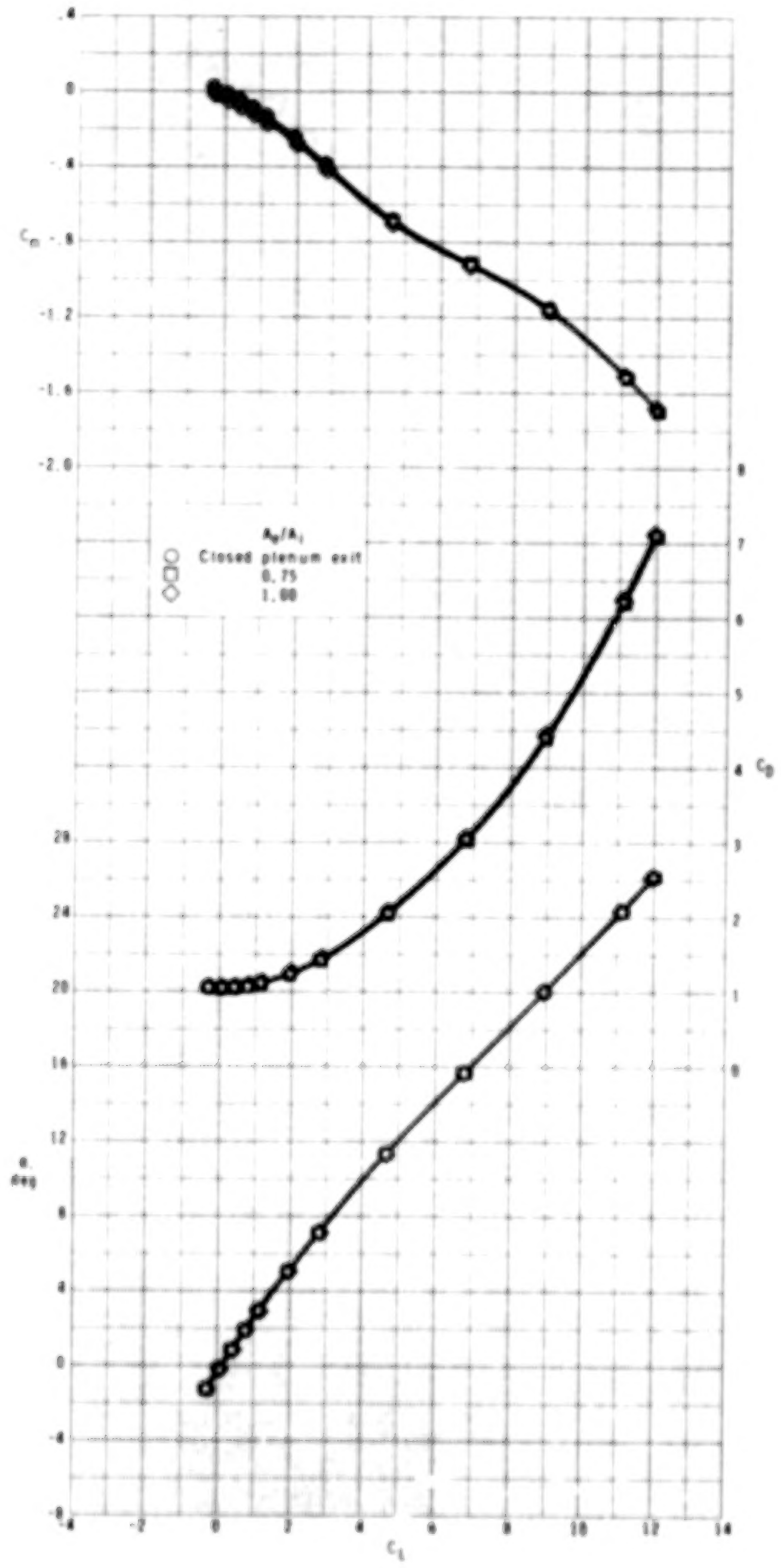

(b) Concluded.

Figure 9.- Continued.

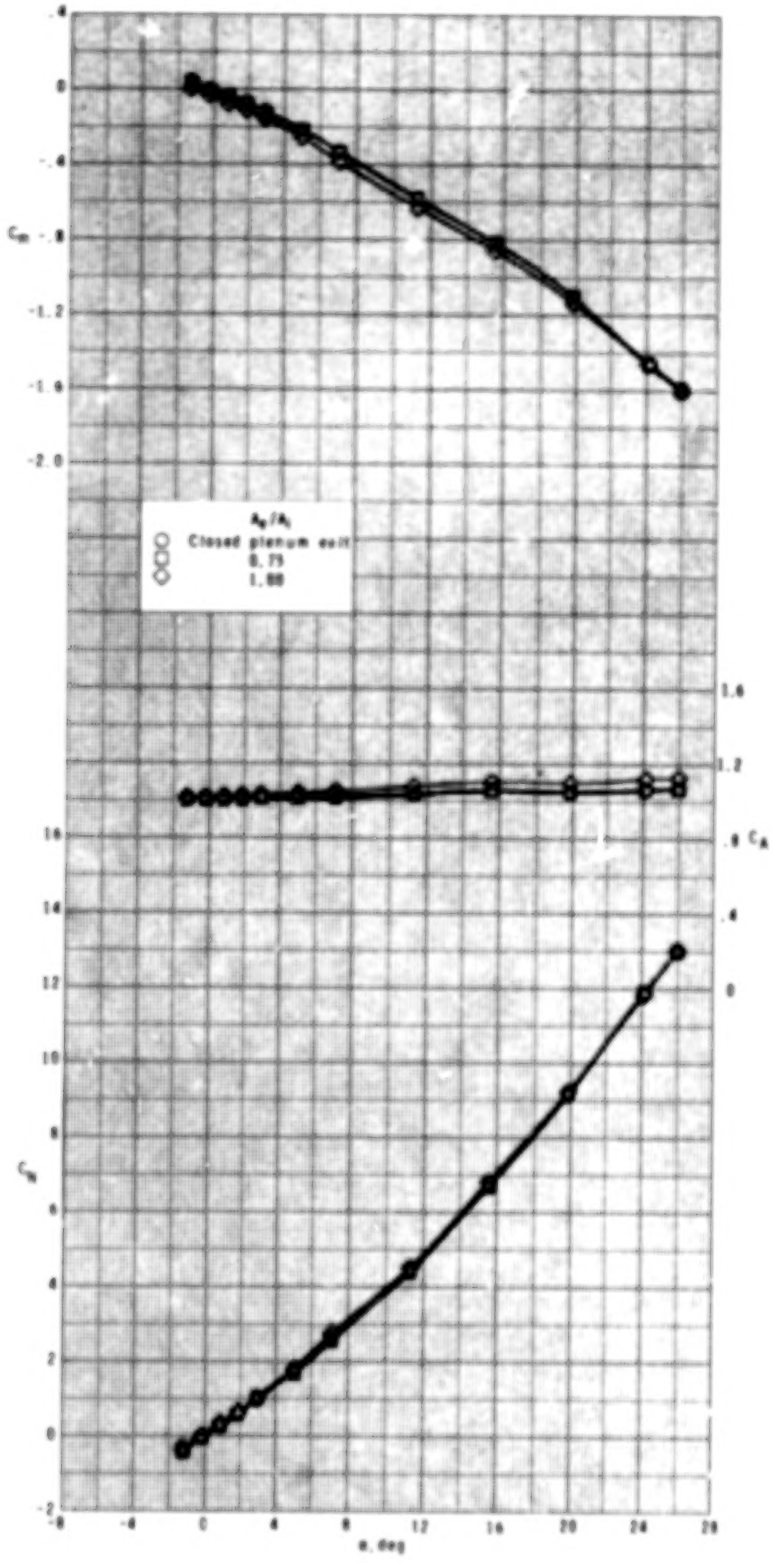

(c) $M_\infty = 2.40$.

Figure 9.- Continued.

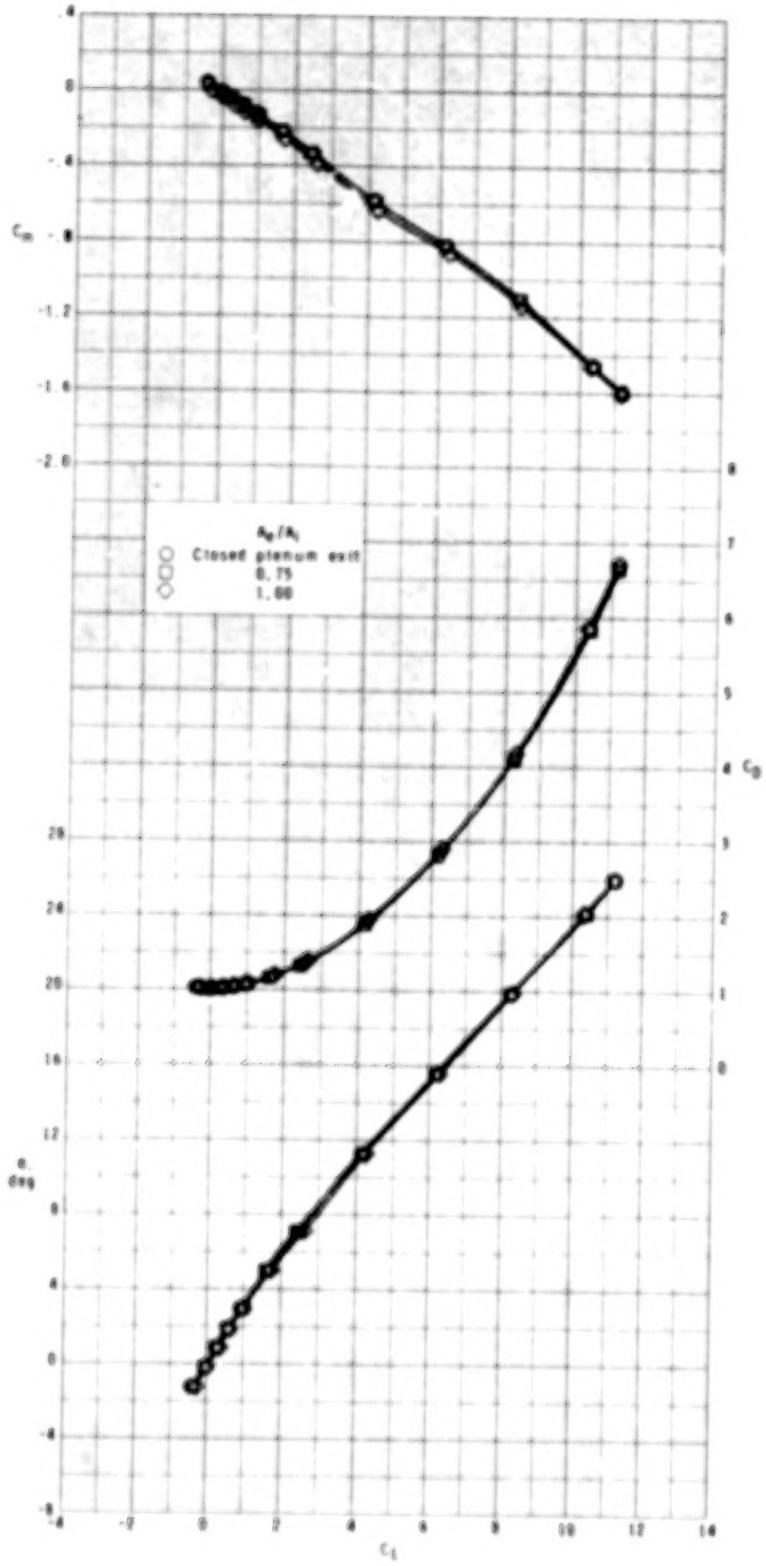

(c) Concluded.

Figure 9.- Continued.

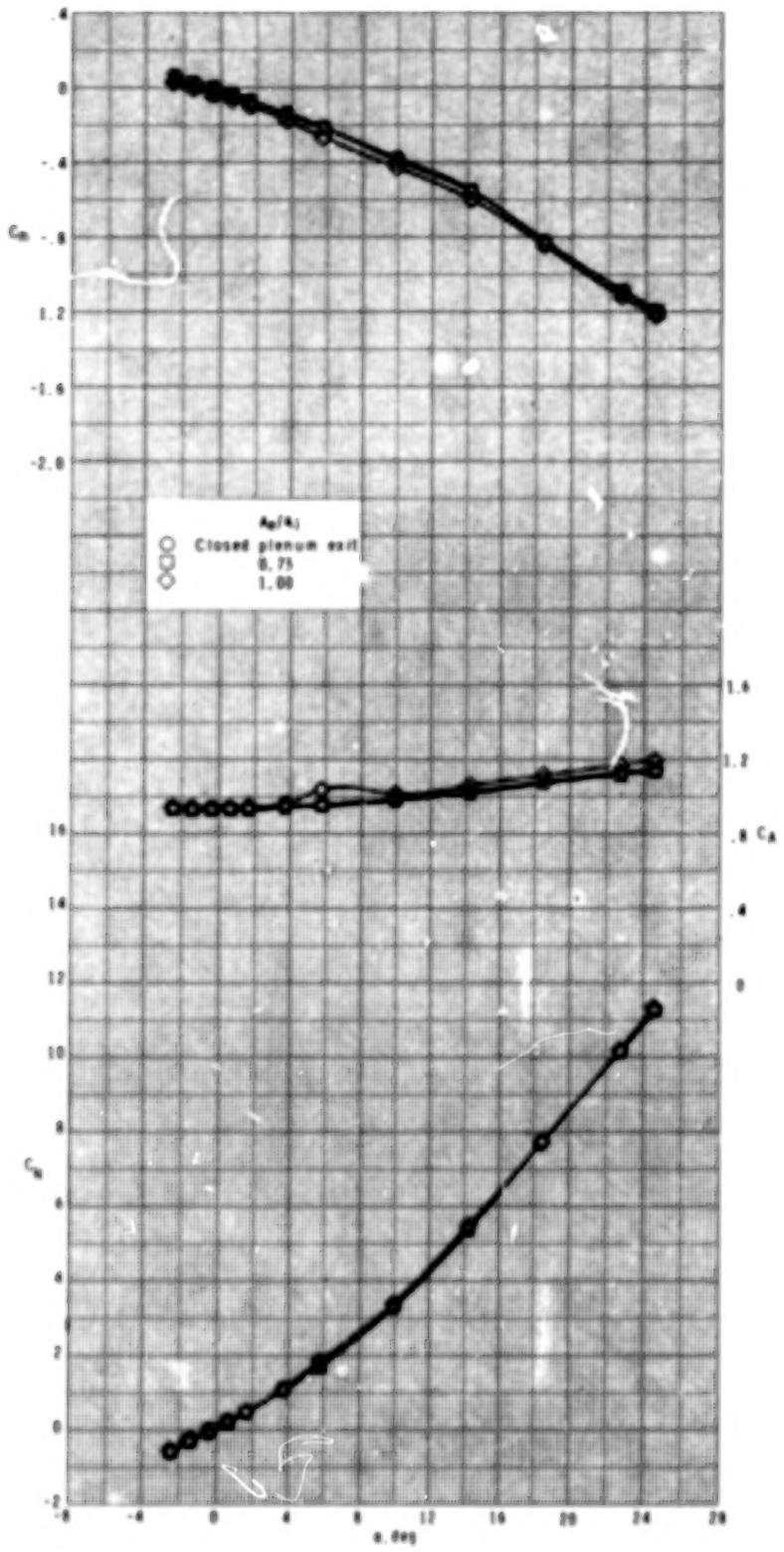

(d) $M_\infty = 2.86$.

Figure 9.- Continued.

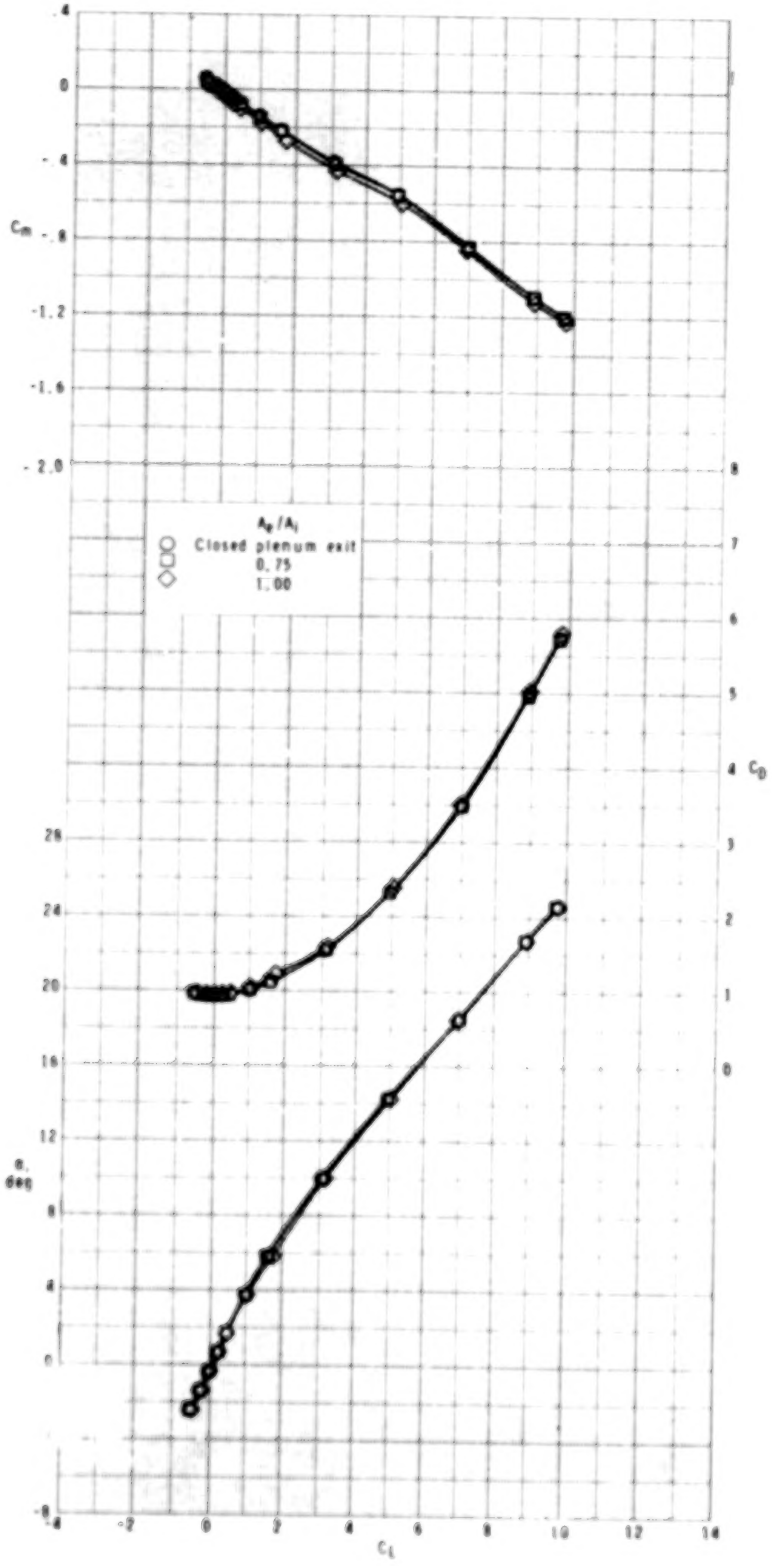

(d) Concluded.

Figure 9.- Concluded.

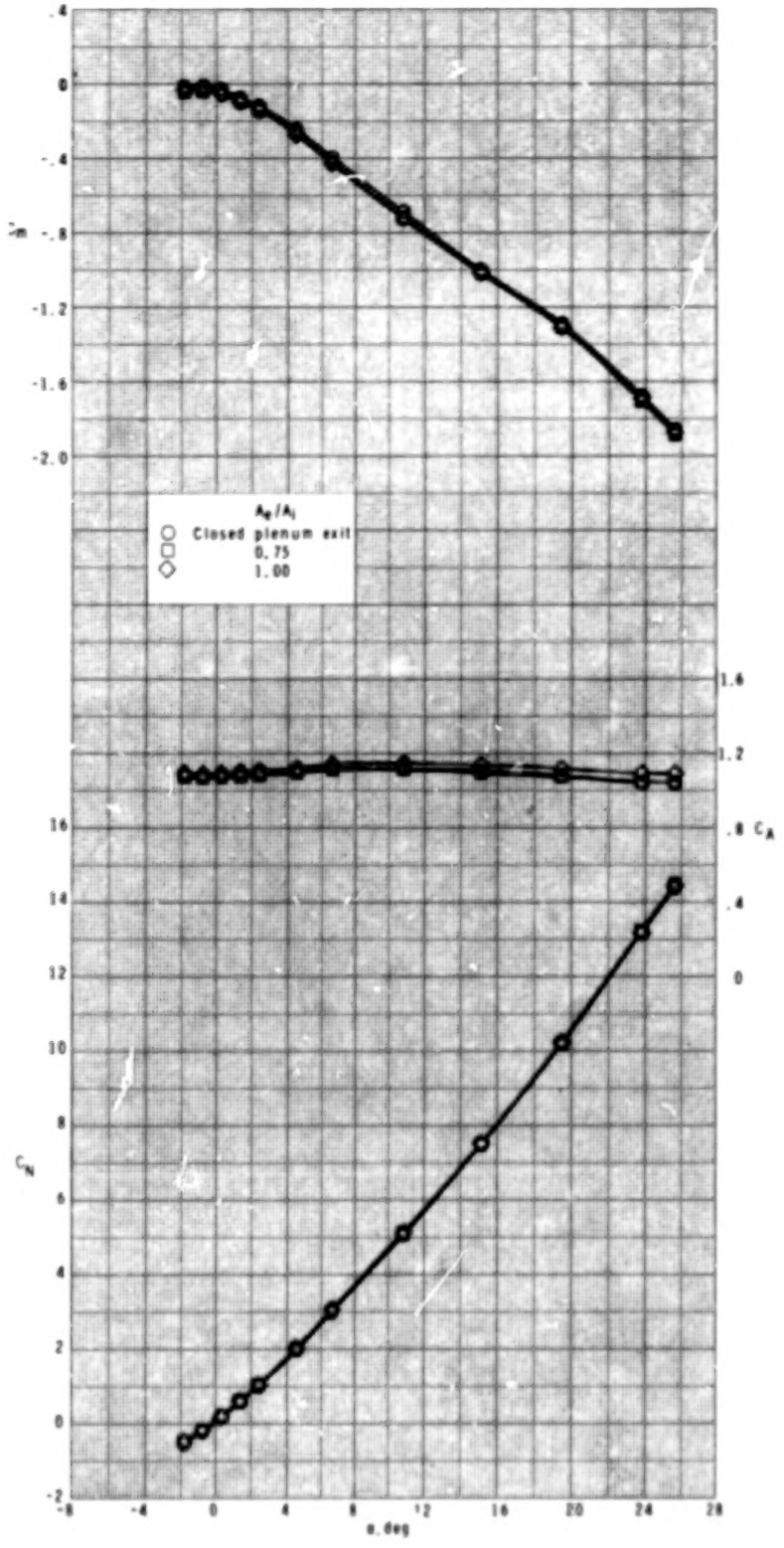

(a) $M_\infty = 1.90$.

Figure 10.- Effect of exit area to inlet area ratios for roll control on the longitudinal aerodynamic characteristics of model with four ram-air-jet spoiler tail fins. $\phi = 22.5^\circ$.

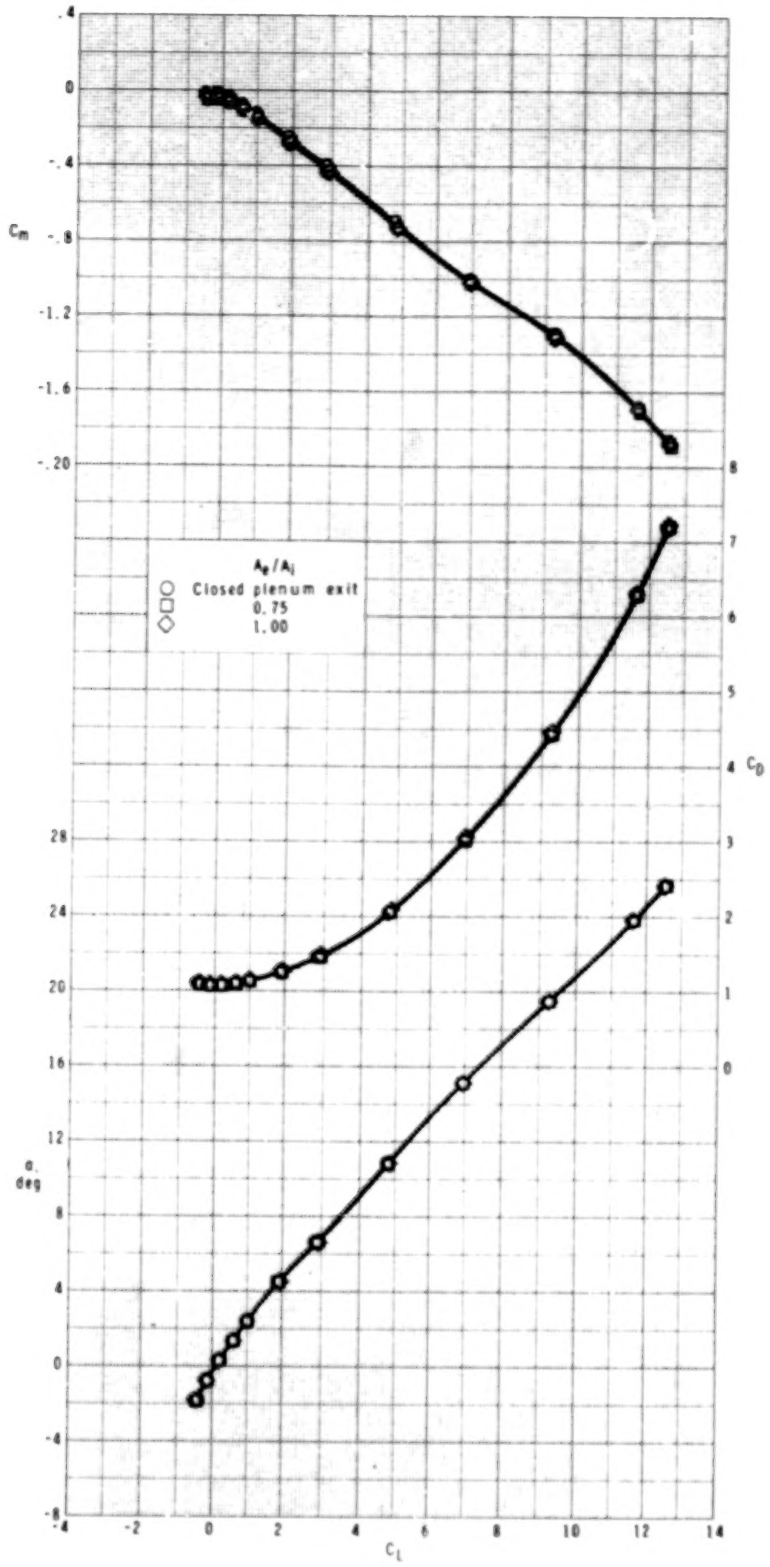

(a) Concluded.

Figure 10.- Continued.

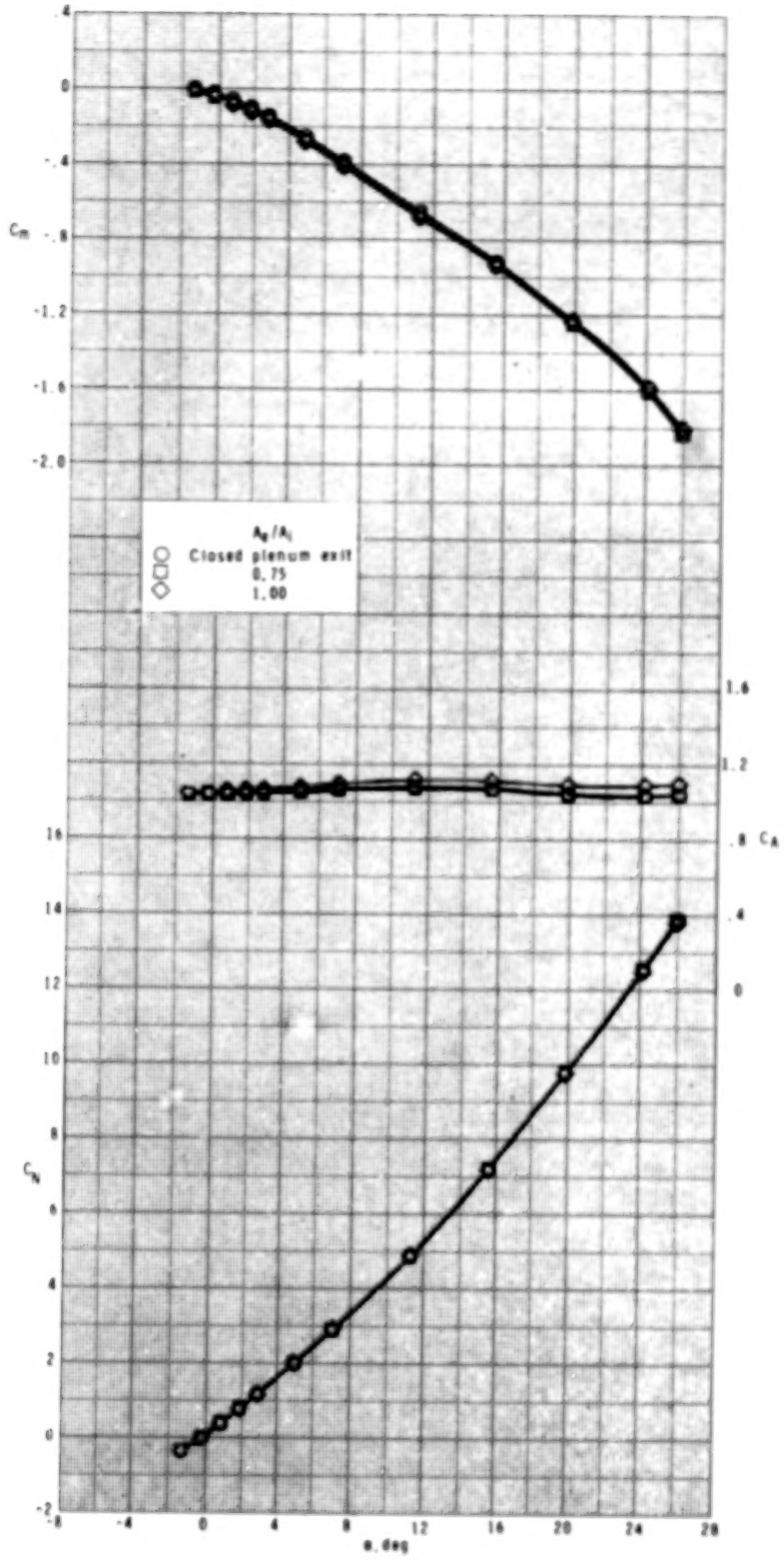

(b) $M_\infty = 2.16$.

Figure 10.- Continued.

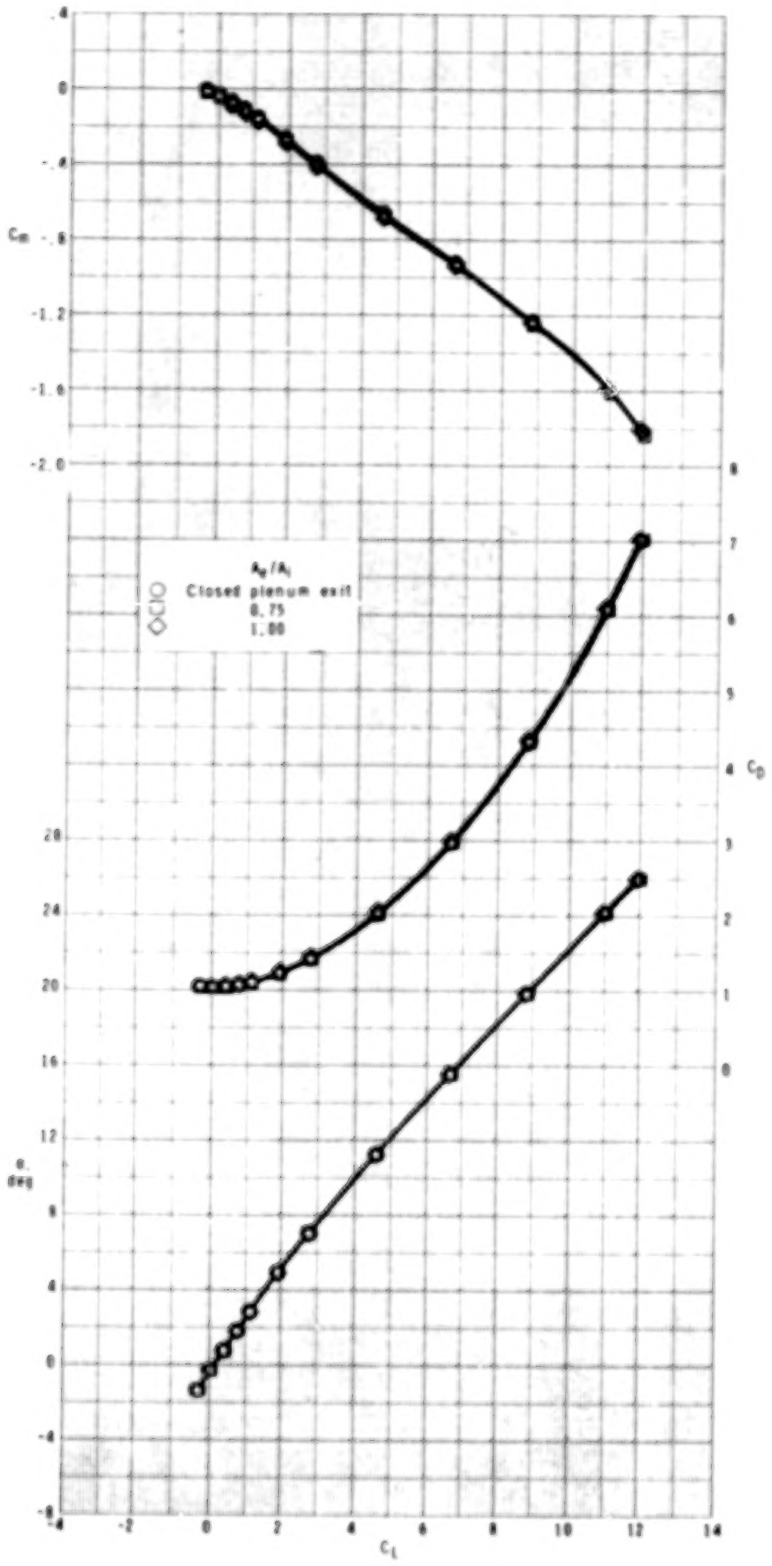

(b) Concluded.

Figure 10.- Continued.

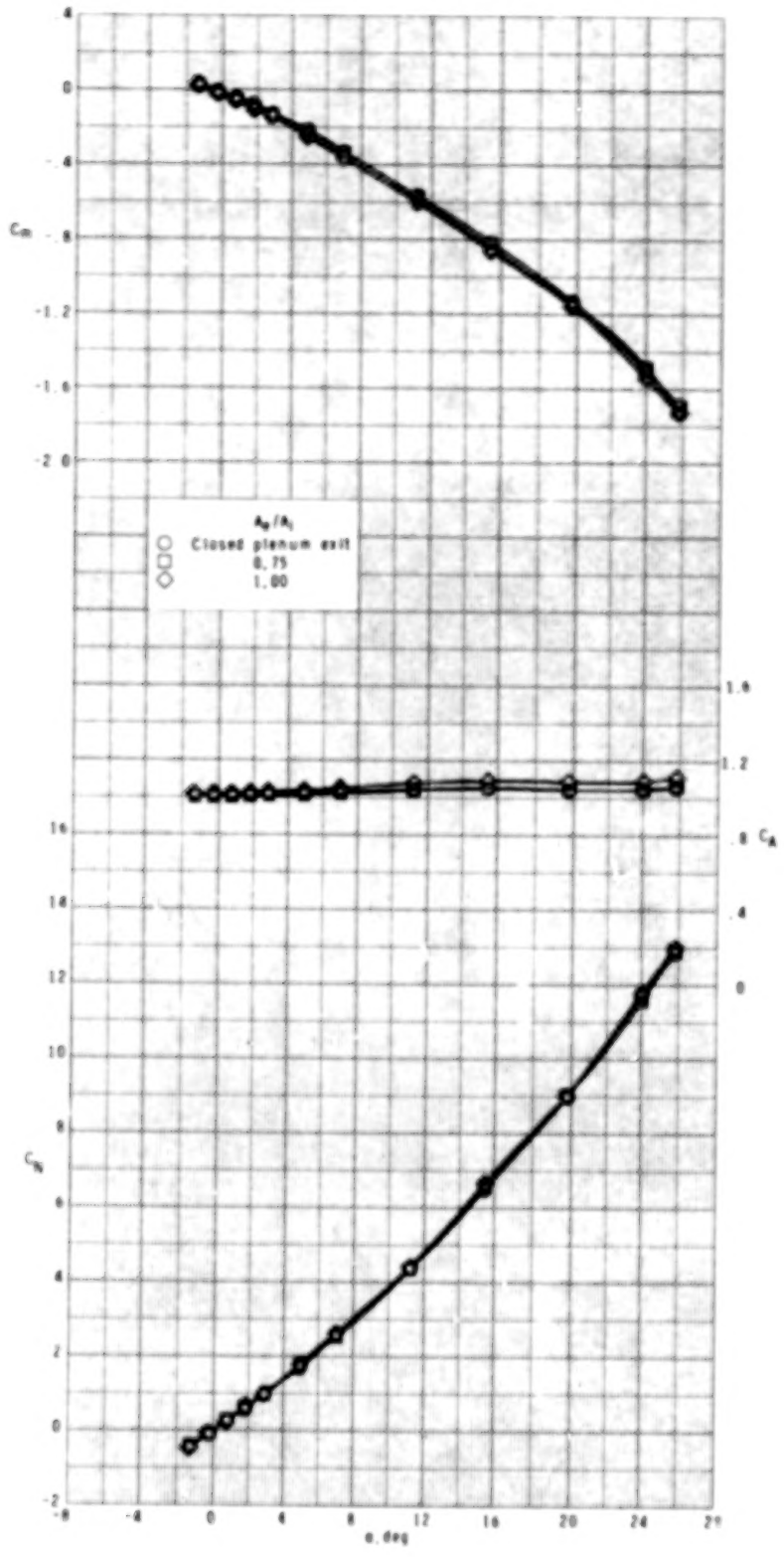

(c) $M_\infty = 2.40$.

Figure 10.- Continued.

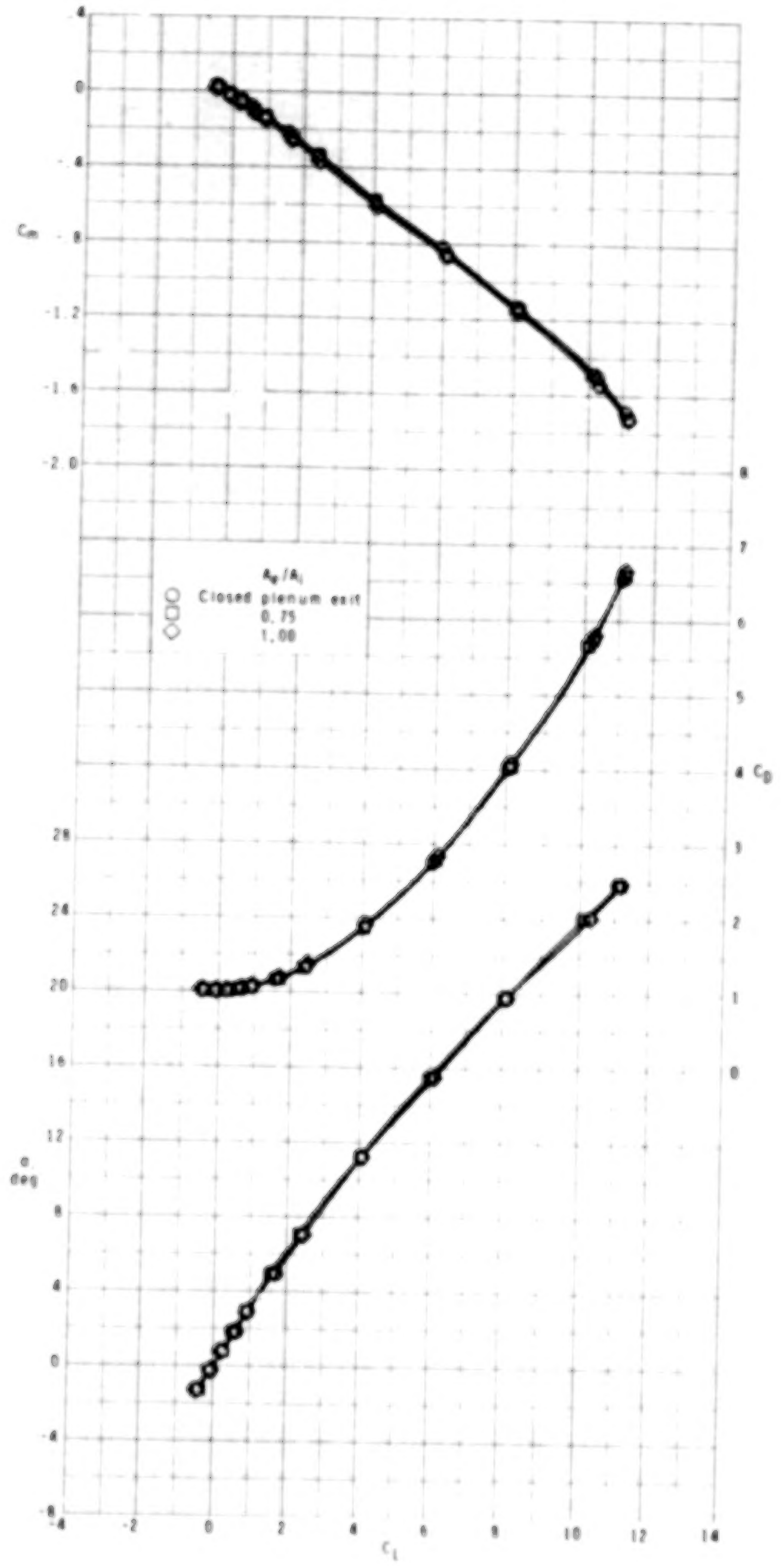

(c) Concluded.

Figure 10.- Continued.

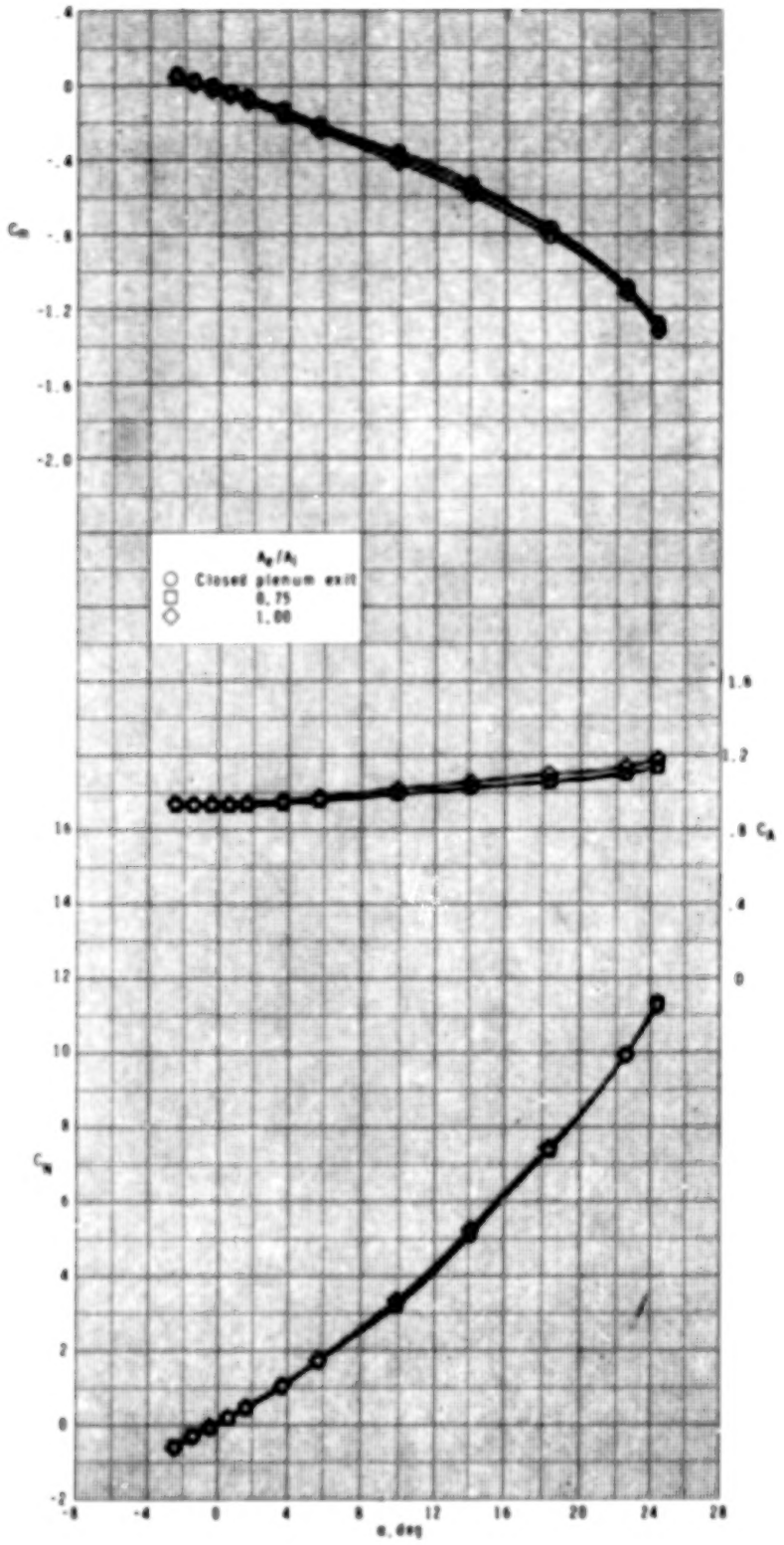

(d) $M_\infty = 2.86$.

Figure 10.- Continued.

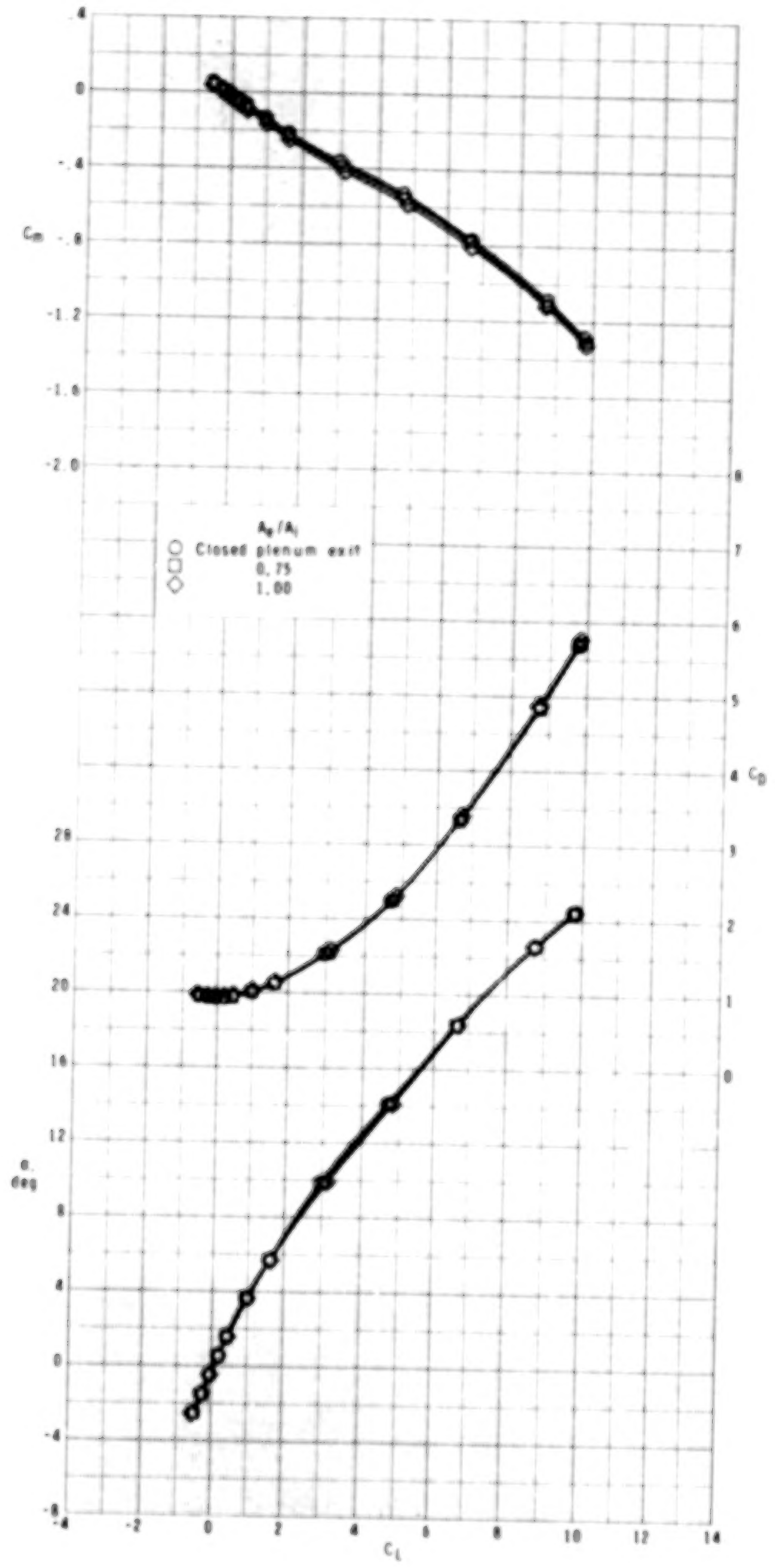

(d) Concluded.

Figure 10.- Concluded.

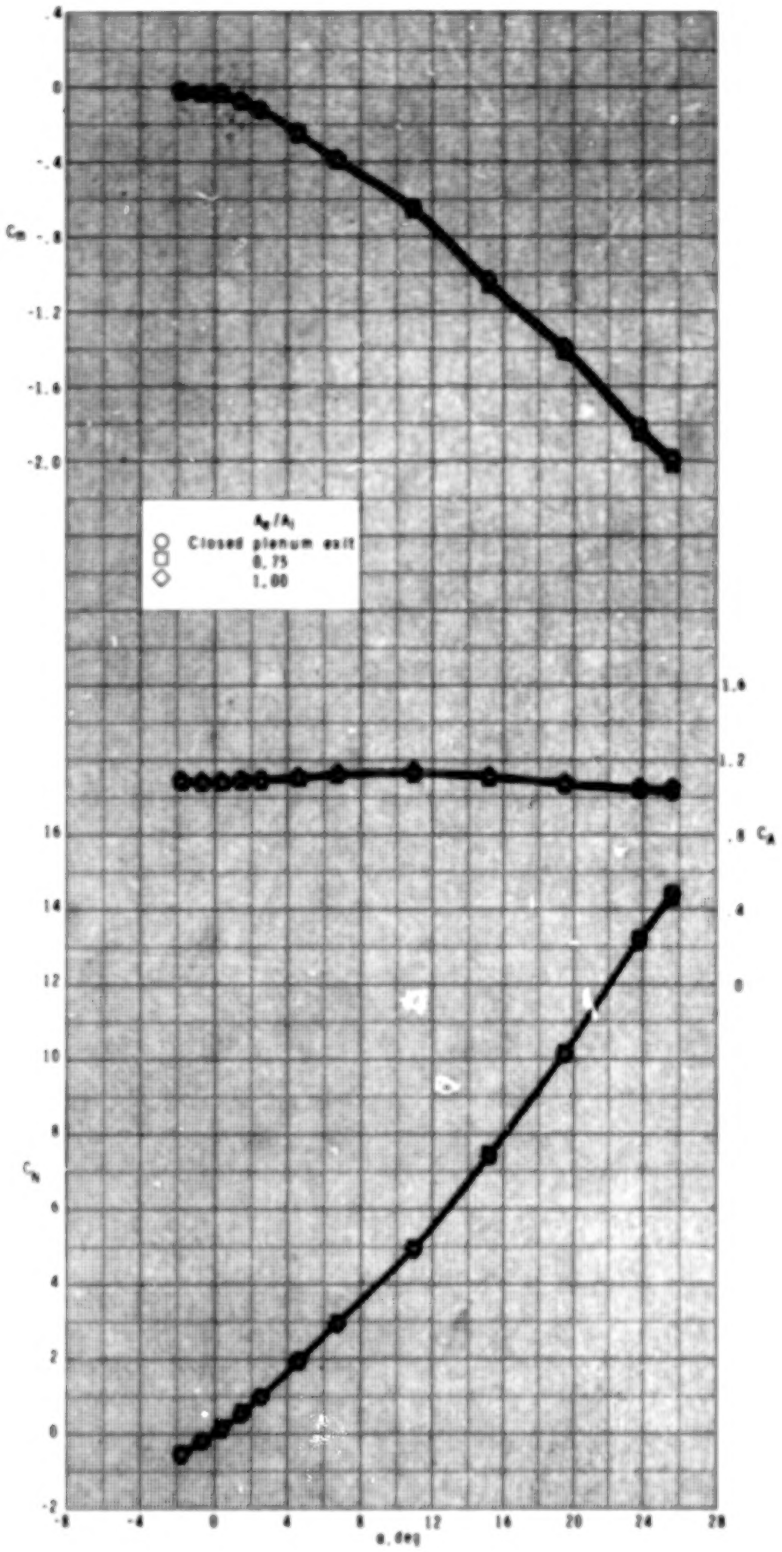

(a) $M_\infty = 1.90$.

Figure 11.- Effect of exit area to inlet area ratios for roll control on longitudinal aerodynamic characteristics of model with four ram-air-jet spoiler tail fins. $\phi = 45^\circ$.

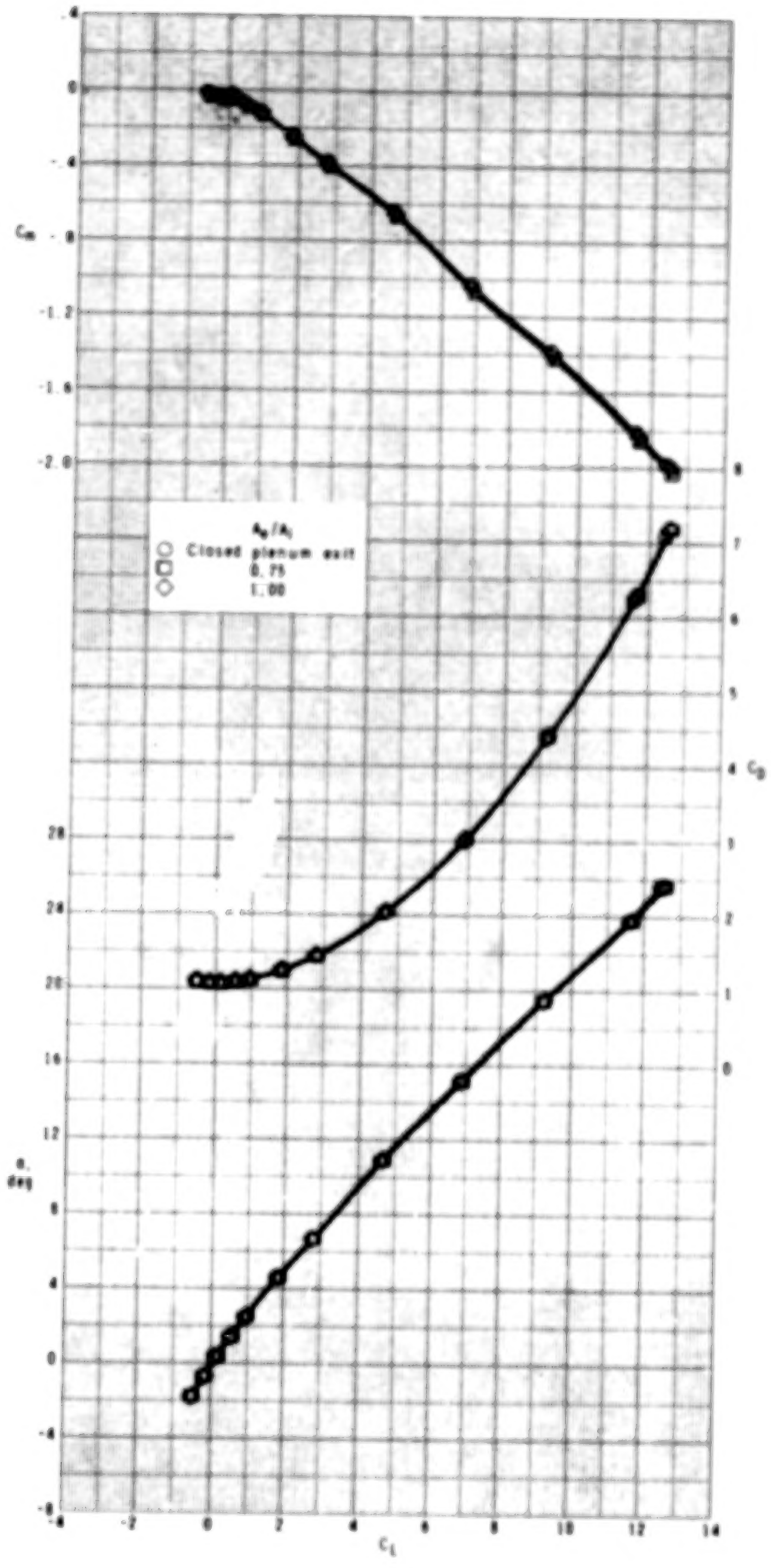

(a) Concluded.

Figure 11.- Continued.

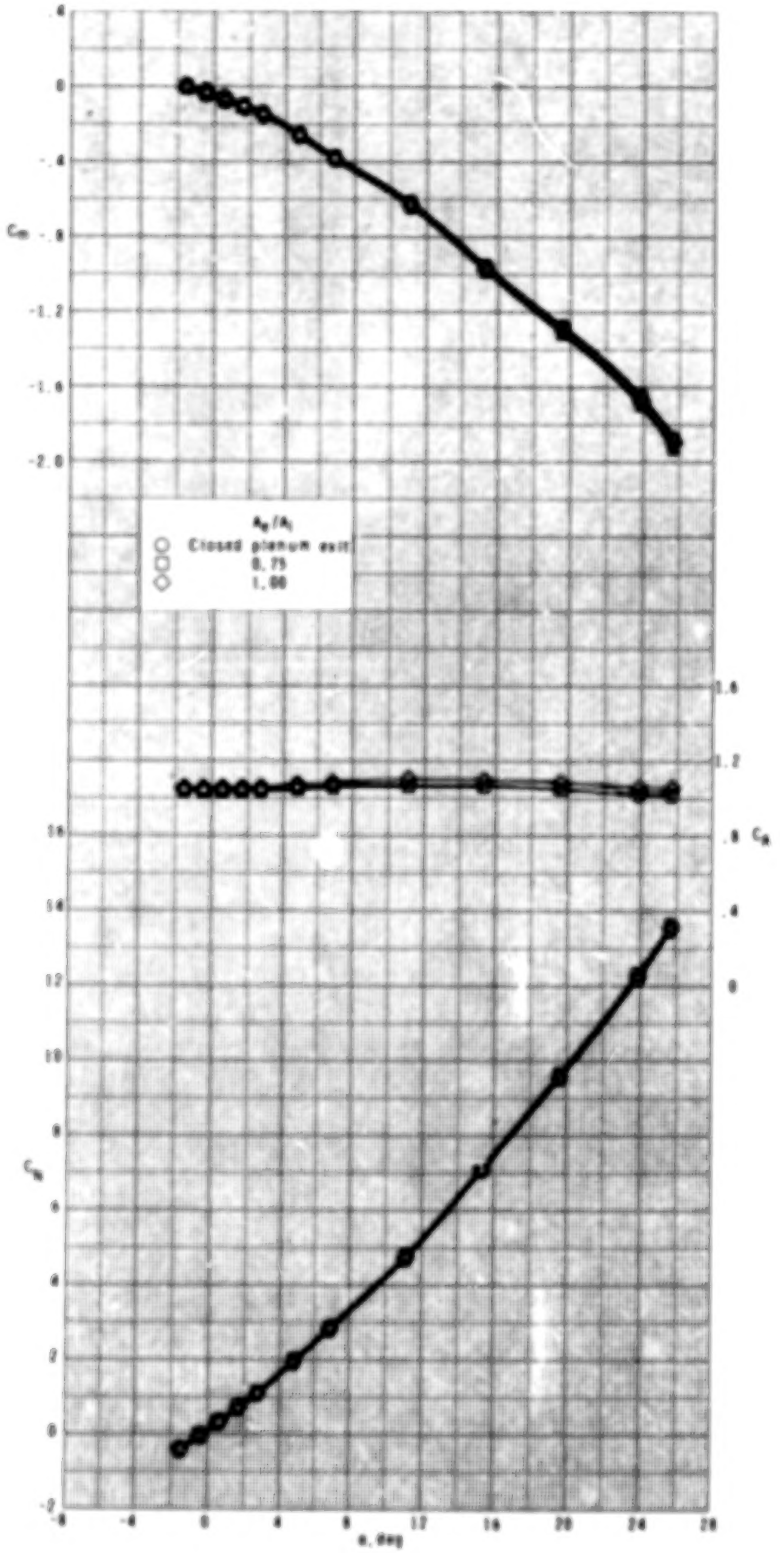

(b) $M_\infty = 2.16$.

Figure 11.- Continued.

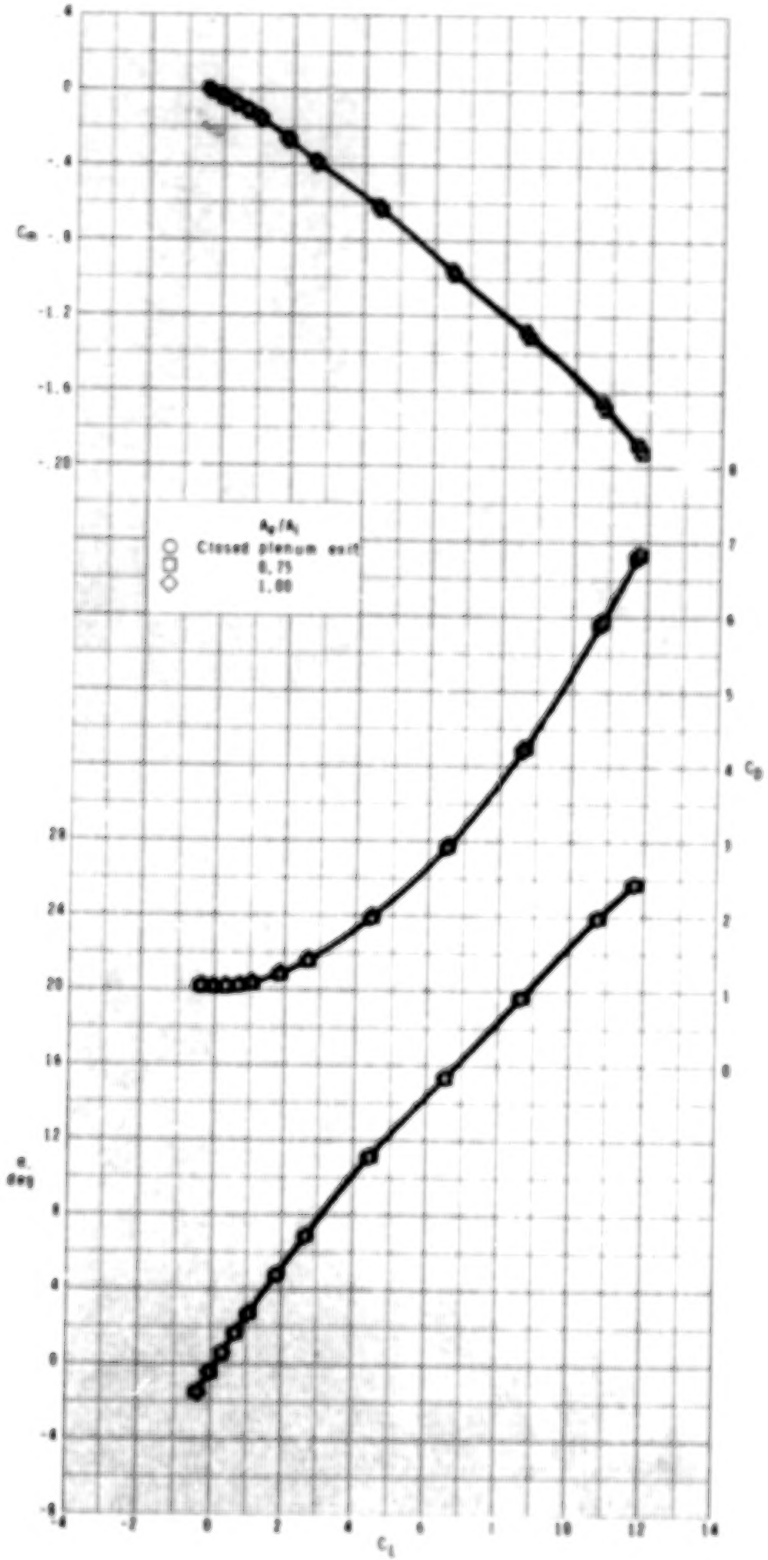

(b) Concluded.

Figure 11.- Continued.

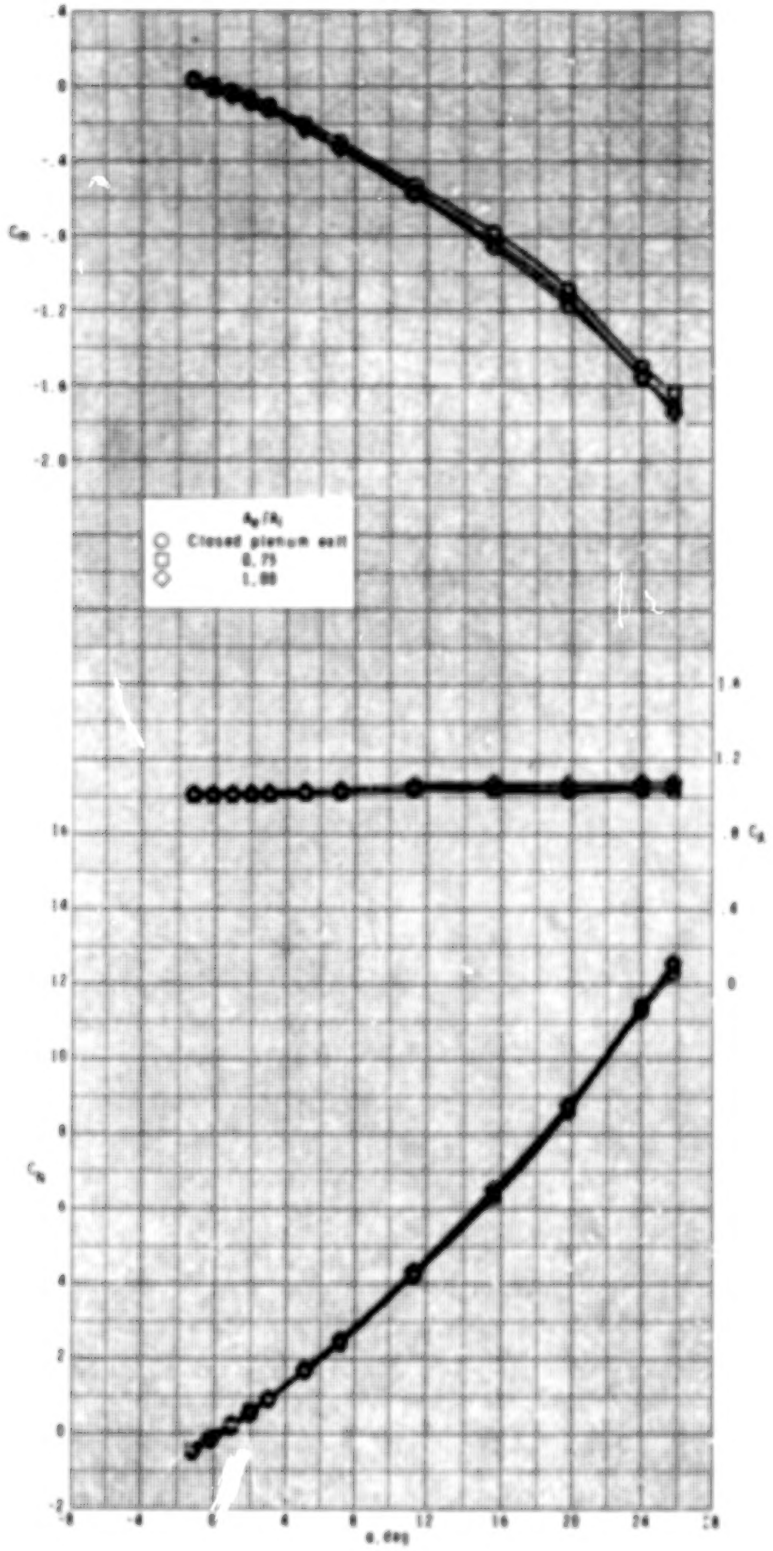

(c) $M_\infty = 2.40$.

Figure 11.- Continued.

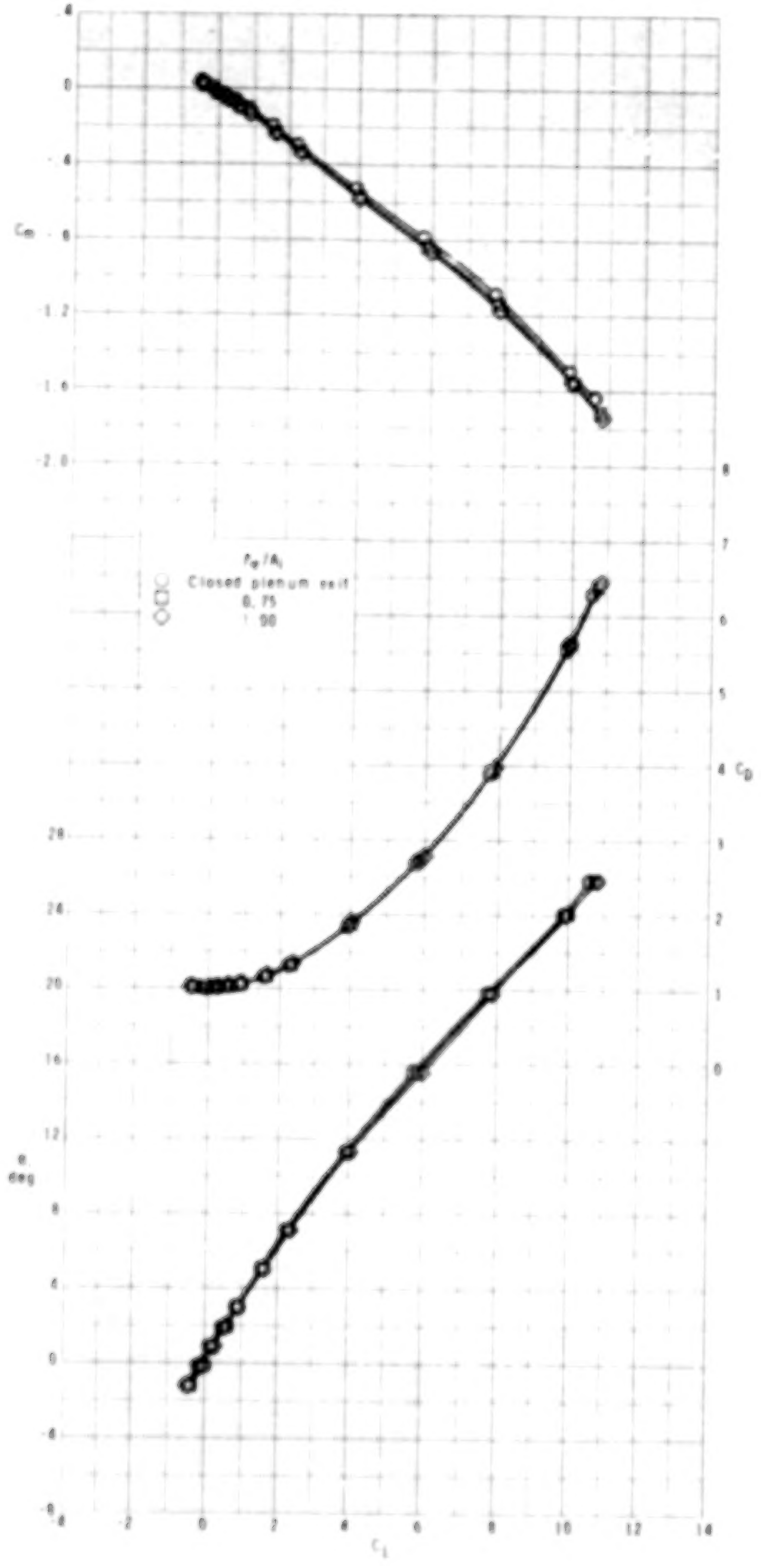

(c) Concluded.

Figure 11.- Continued.

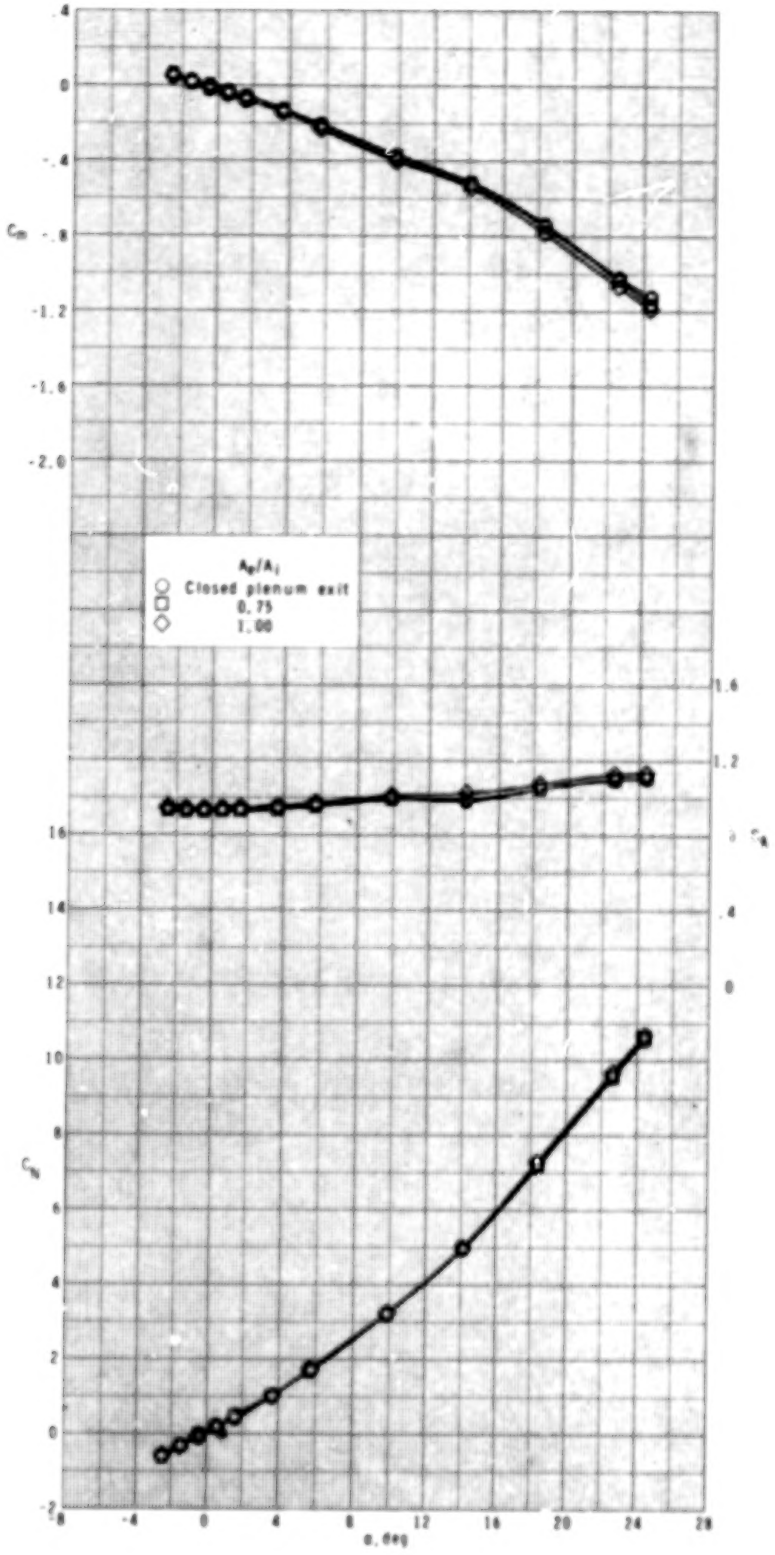

(d) $M_\infty = 2.86$.

Figure 11.- Continued.

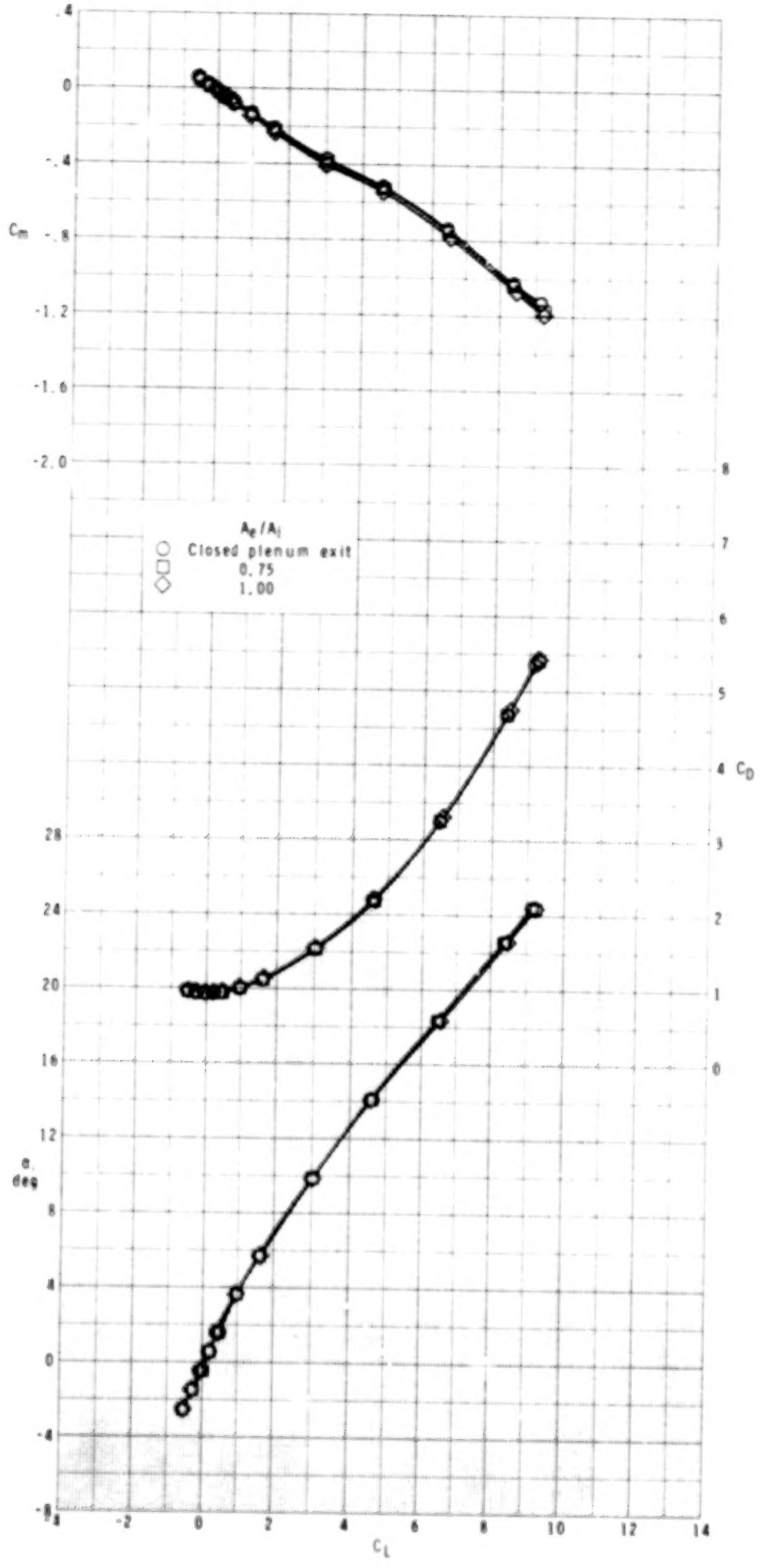

(d) Concluded.

Figure 11.- Concluded.

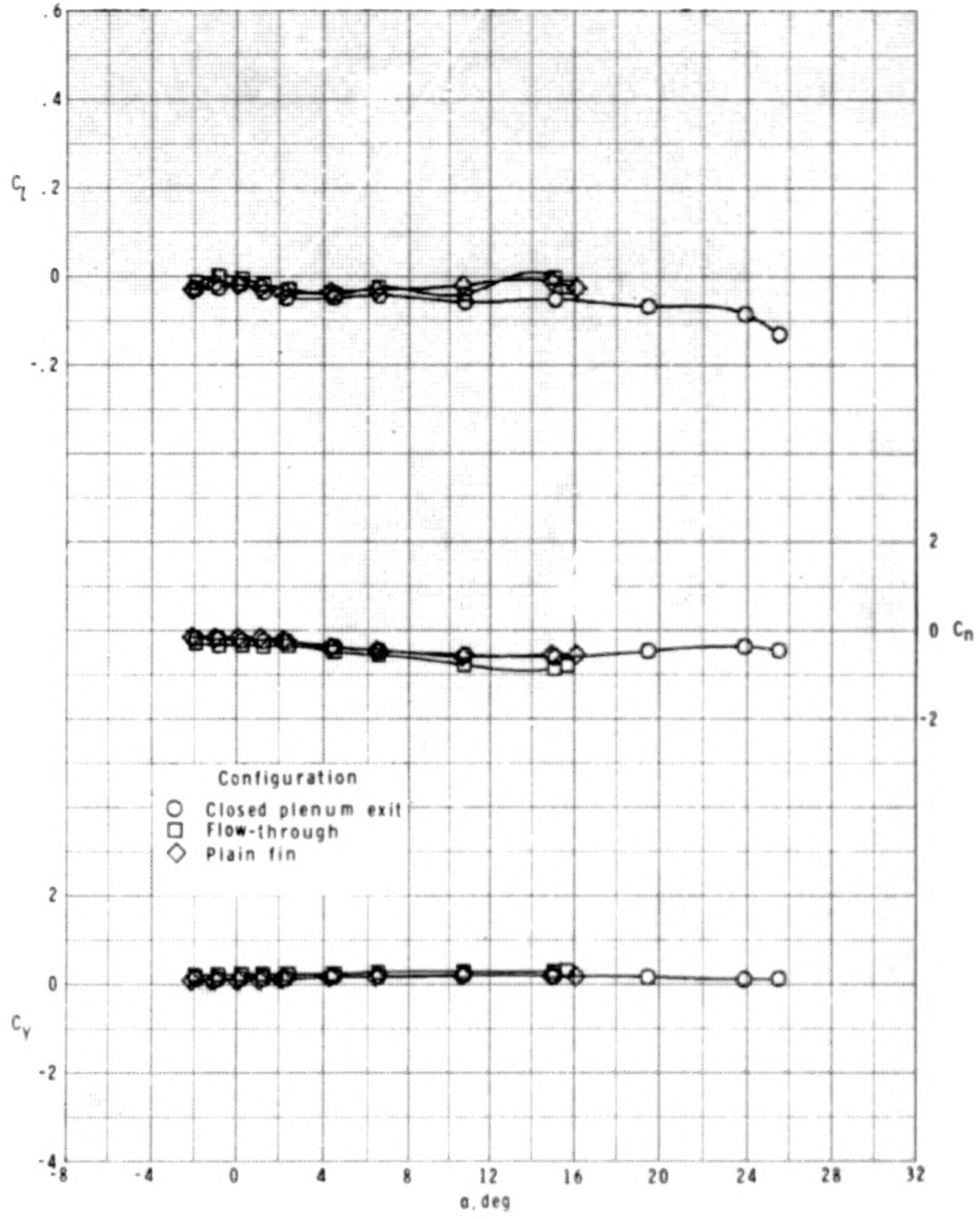

(a) $M_\infty = 1.90$.

Figure 12.- Effect of closed plenum exit and flow-through nacelle configurations on lateral aerodynamic characteristics of model. $\phi = 0^o$.

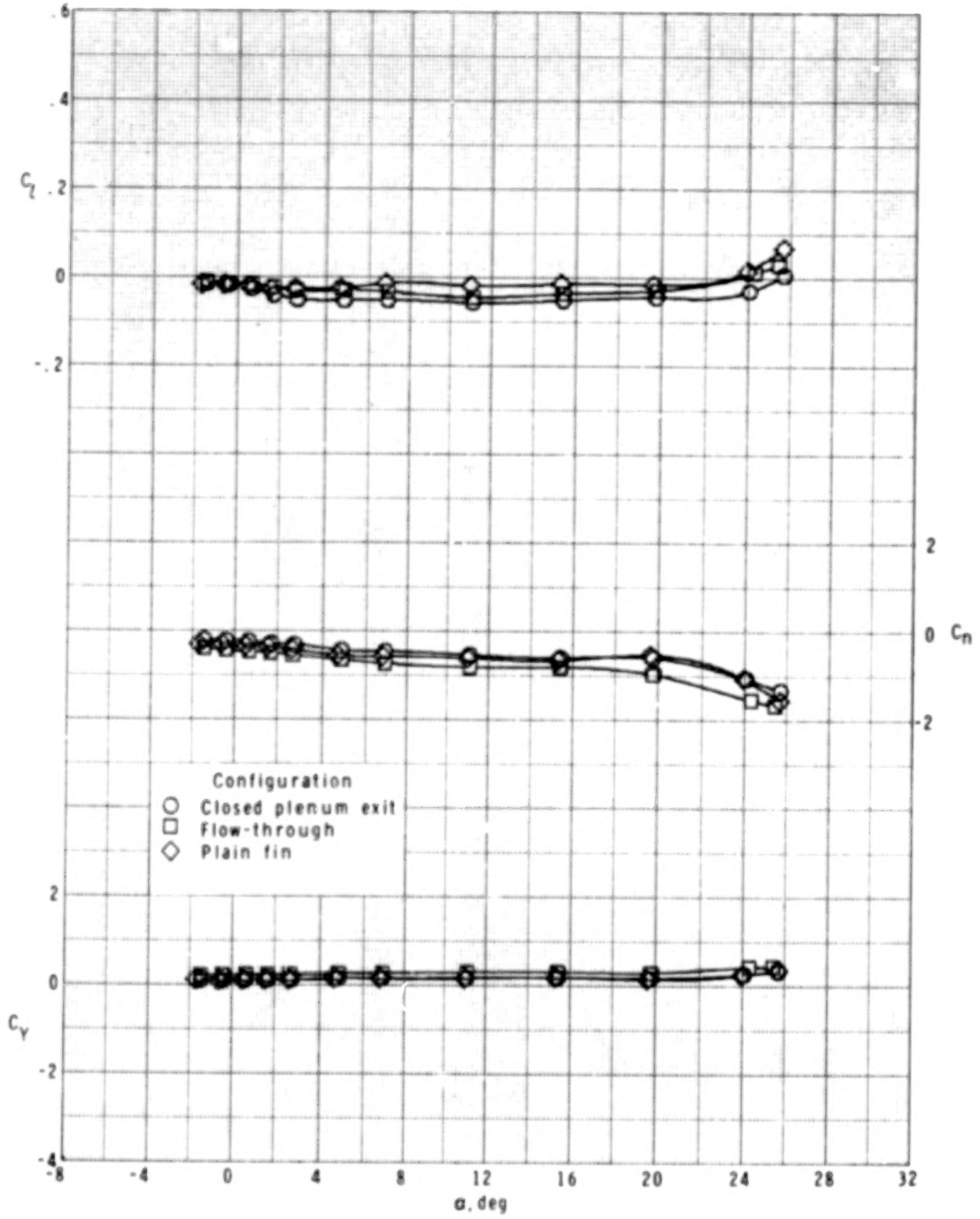

(b) $M_\infty = 2.16$.

Figure 12.- Continued.

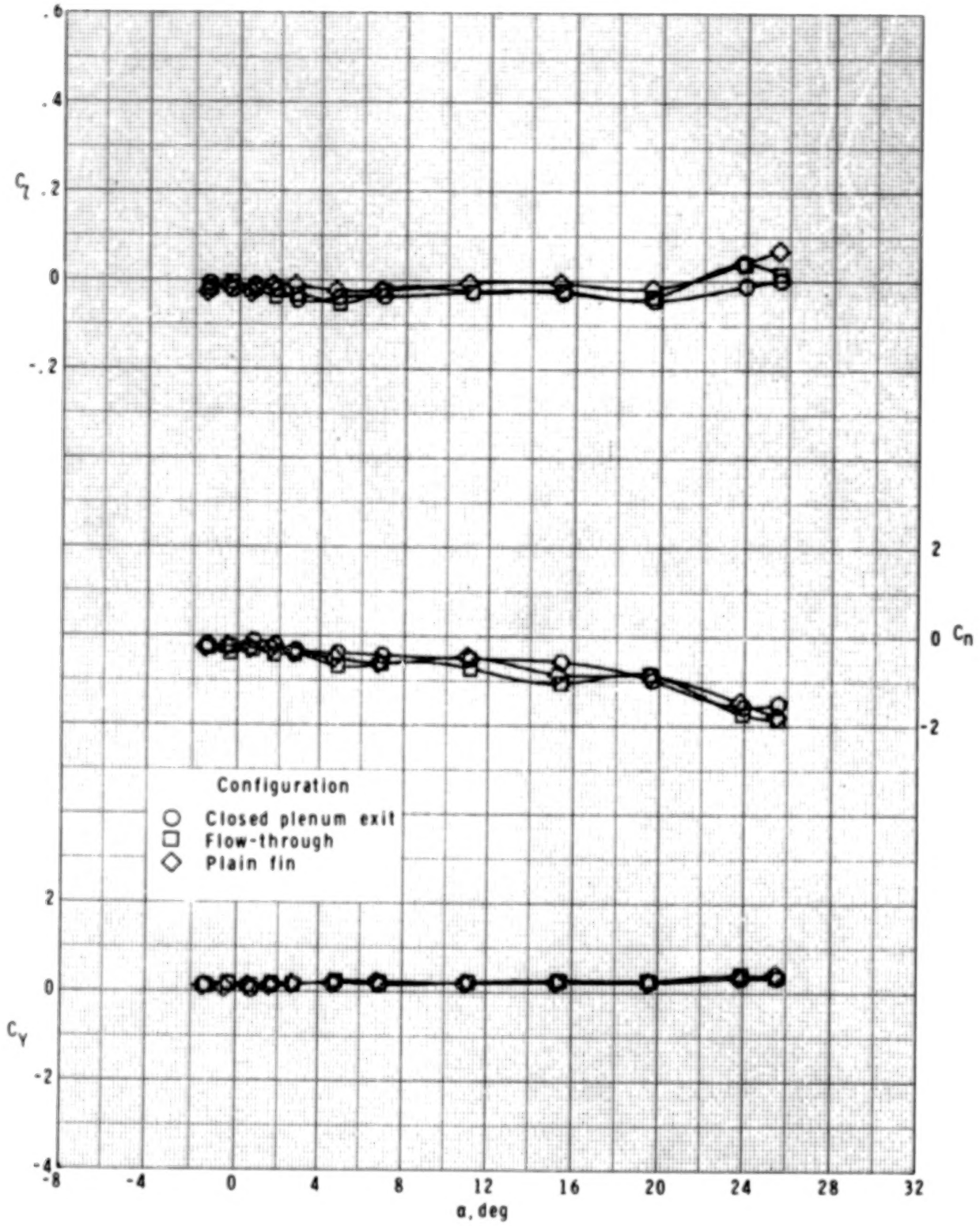

(c) $M_\infty = 2.40$.

Figure 12.- Continued.

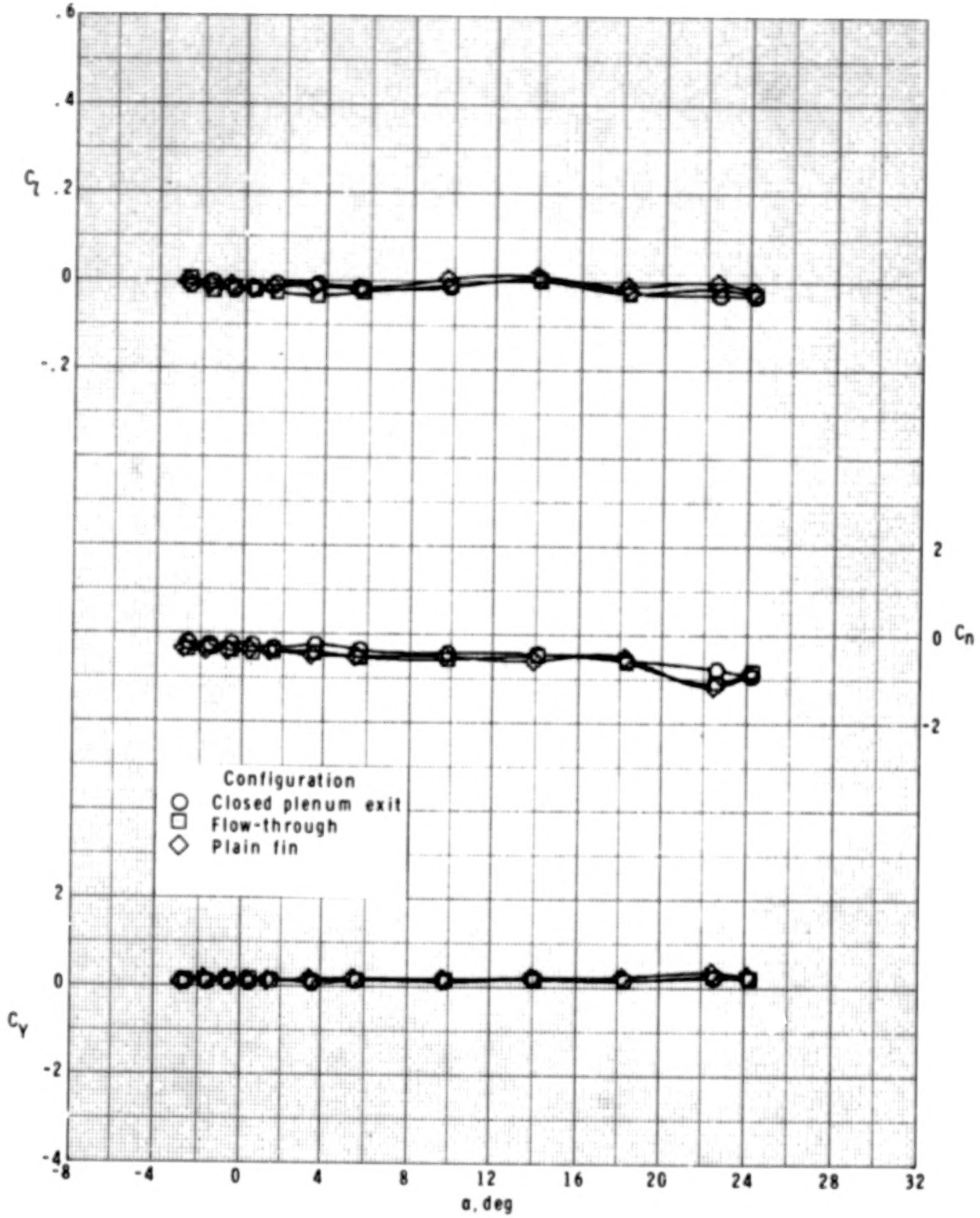

(d) $M_\infty = 2.86$.

Figure 12.- Concluded.

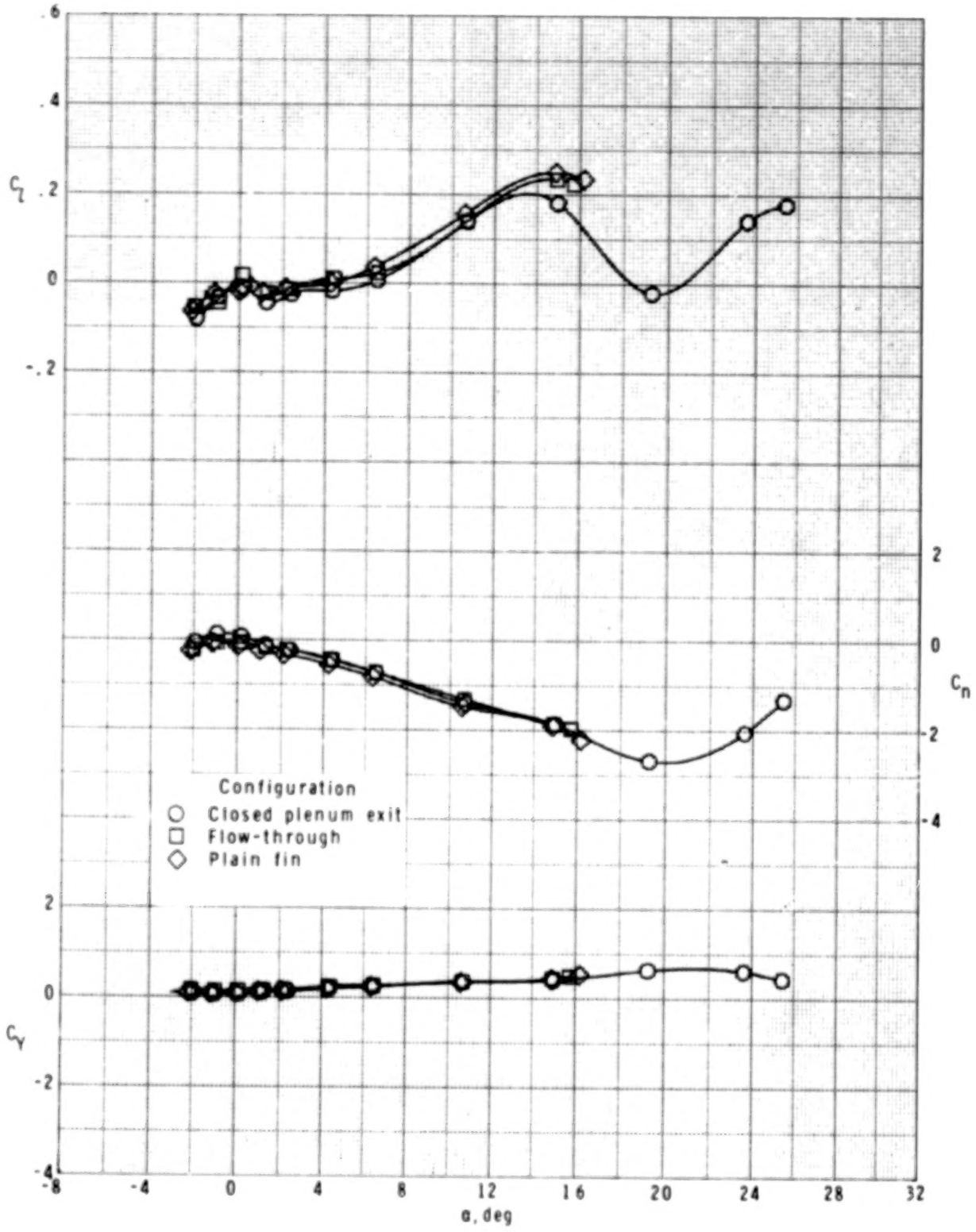

(a) M_∞ = 1.90.

Figure 13.- Effect of closed plenum exit and flow-through nacelle configurations on lateral aerodynamic characteristics of model. ϕ = 22.5°.

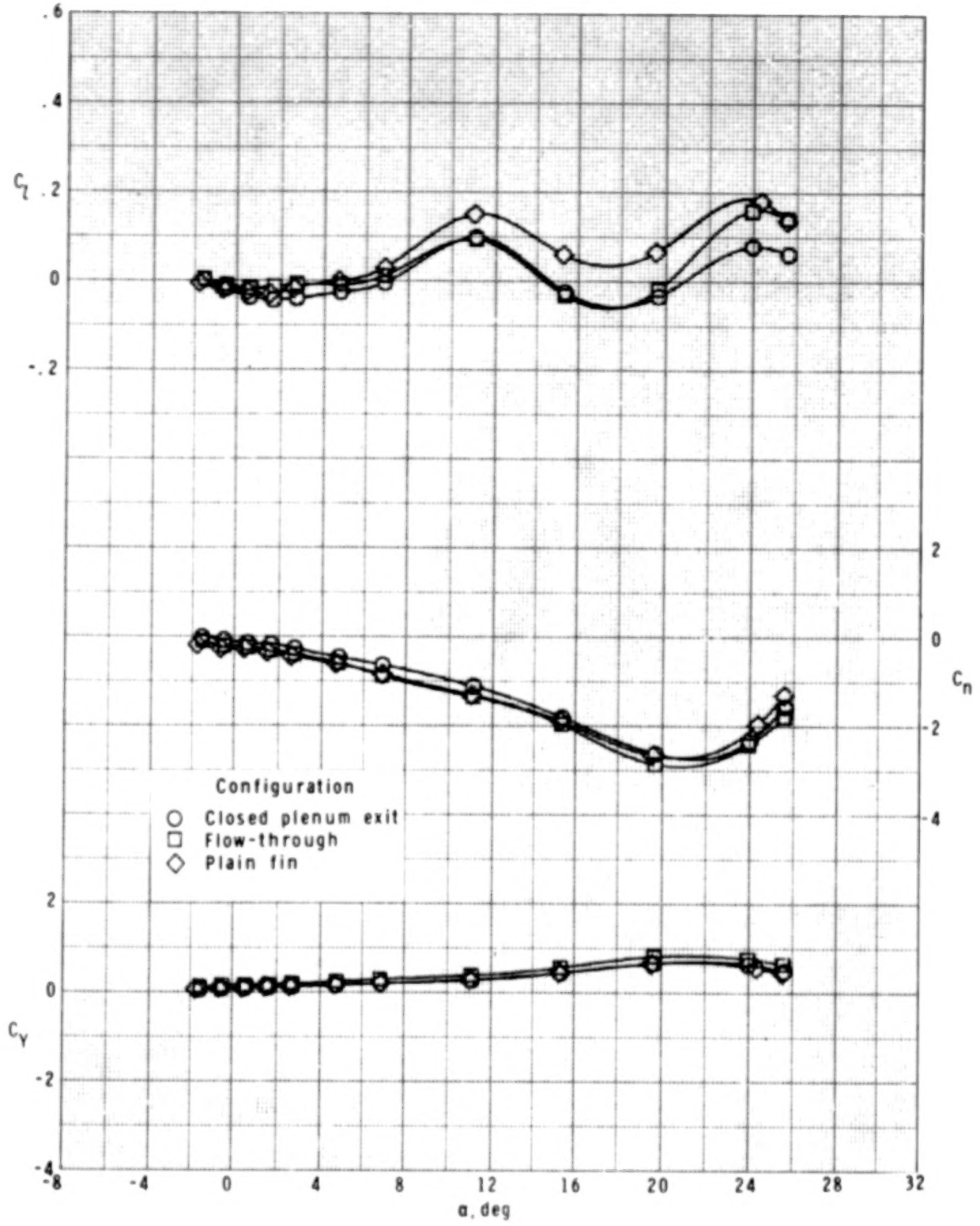

(b) $M_\infty = 2.16$.

Figure 13.- Continued.

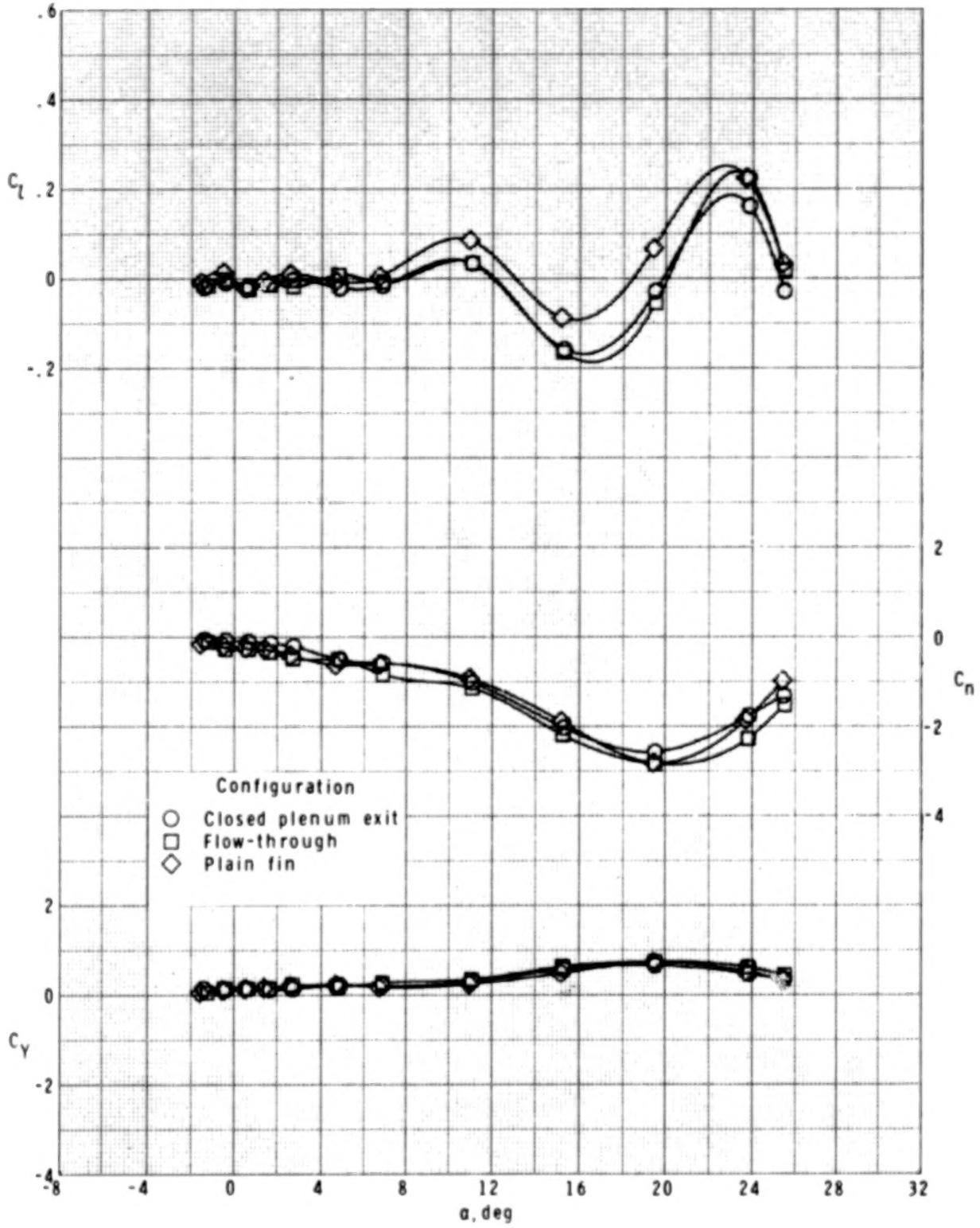

(c) $M_\infty = 2.40$.

Figure 13.- Continued.

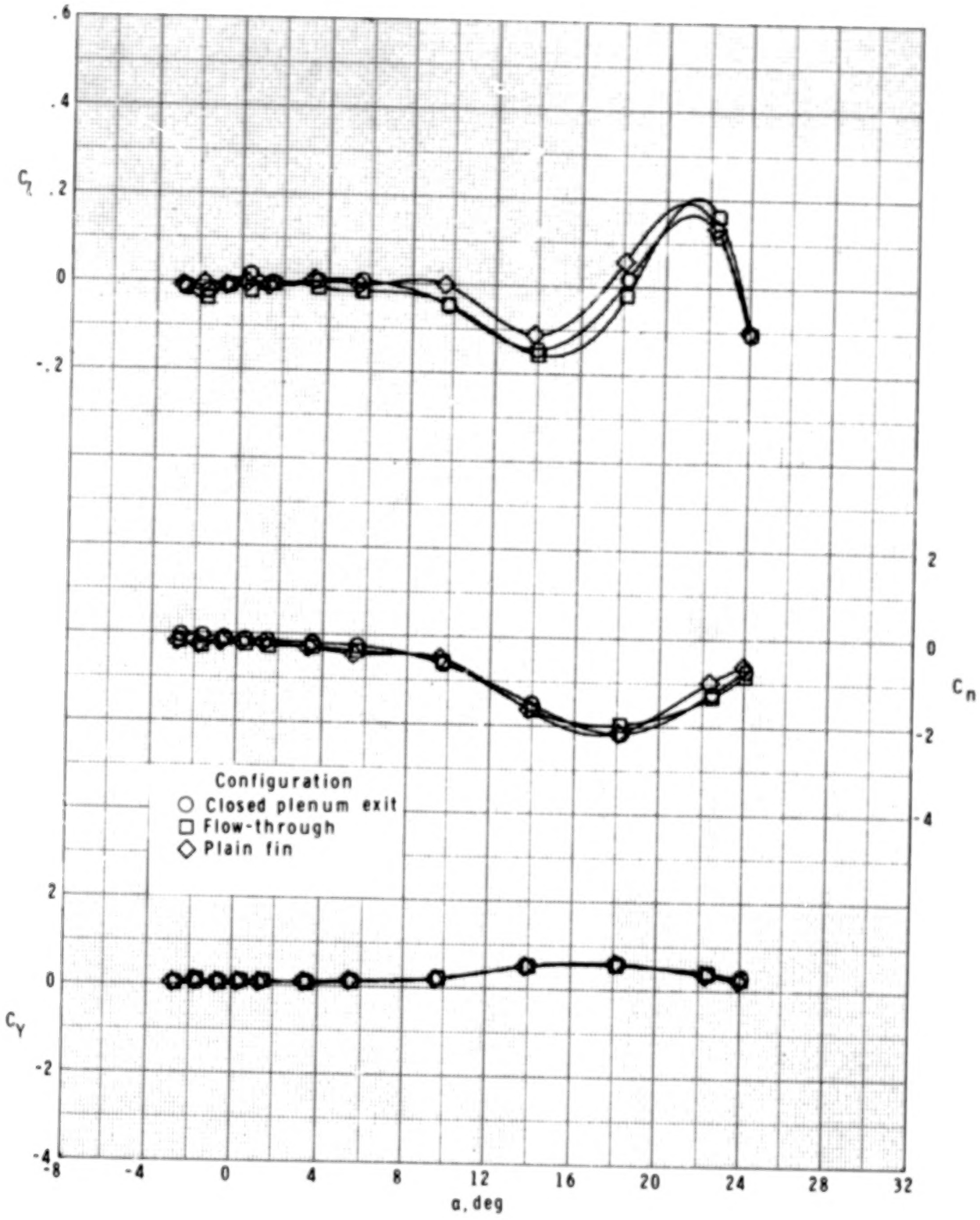

(d) $M_\infty = 2.86$.

Figure 13.- Concluded.

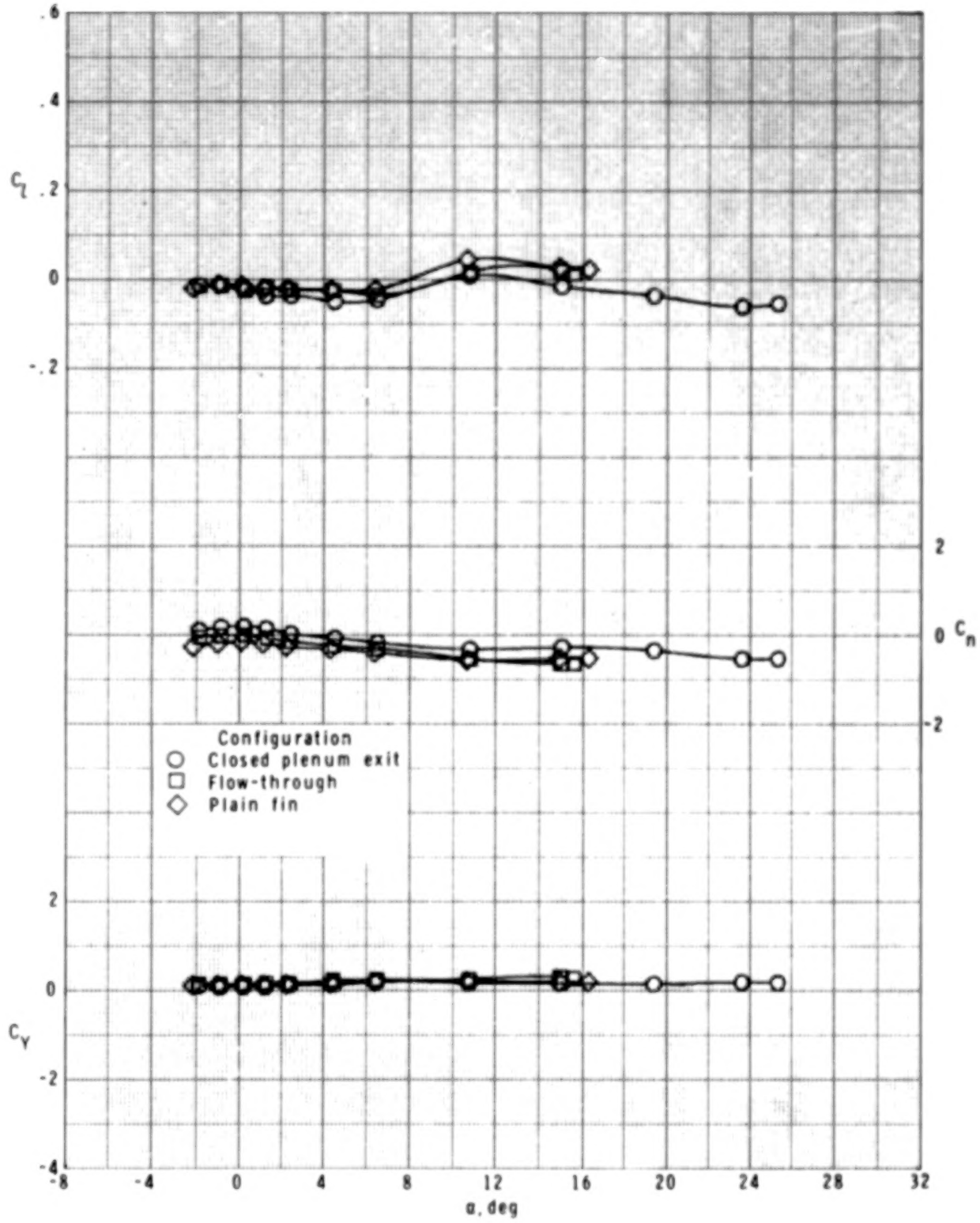

(a) $M_\infty = 1.90$.

Figure 14.- Effect of closed plenum exit and flow-through nacelle configurations on lateral aerodynamic characteristics of model. $\phi = 45^\circ$.

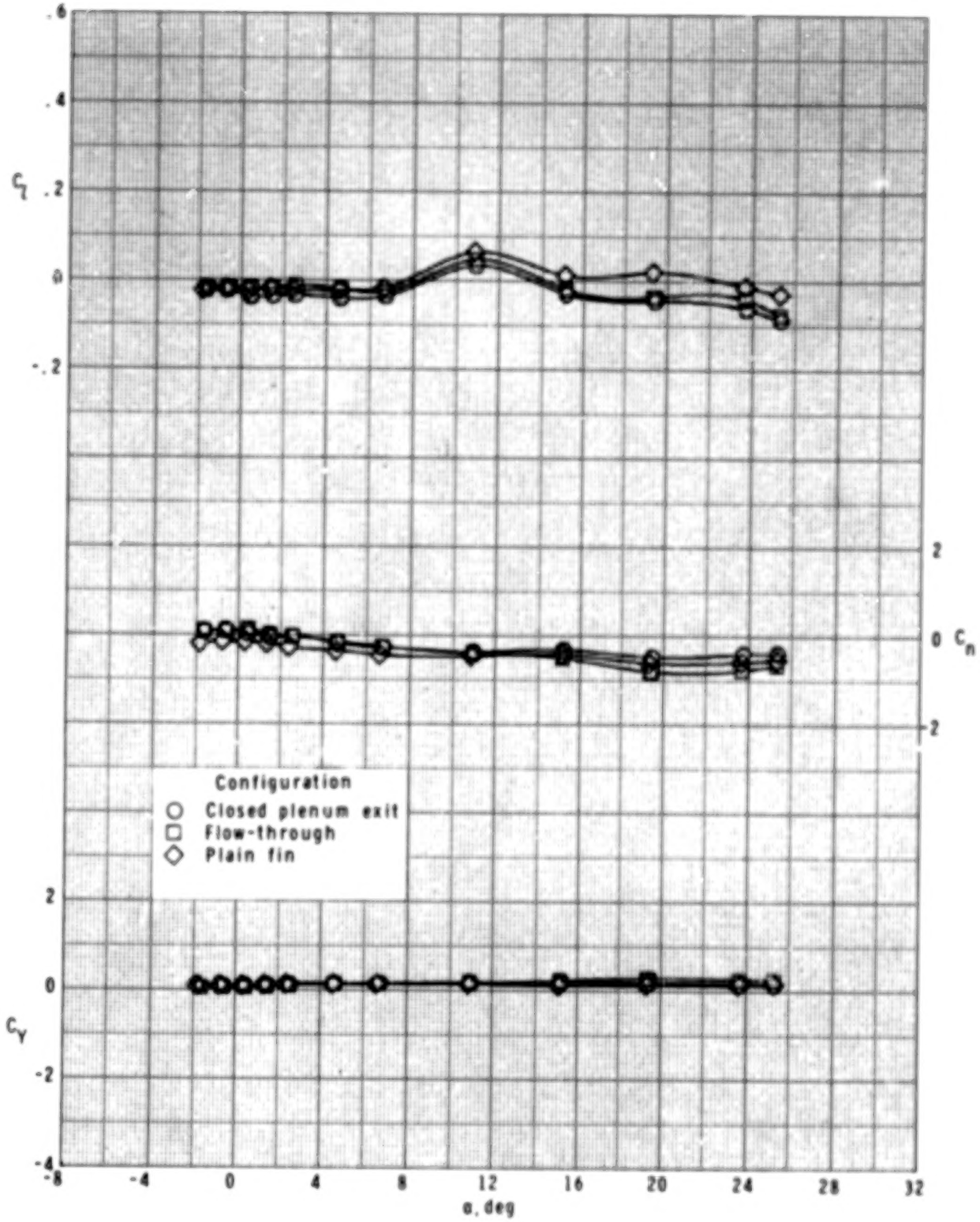

(b) $M_\infty = 2.16$.

Figure 14.- Continued.

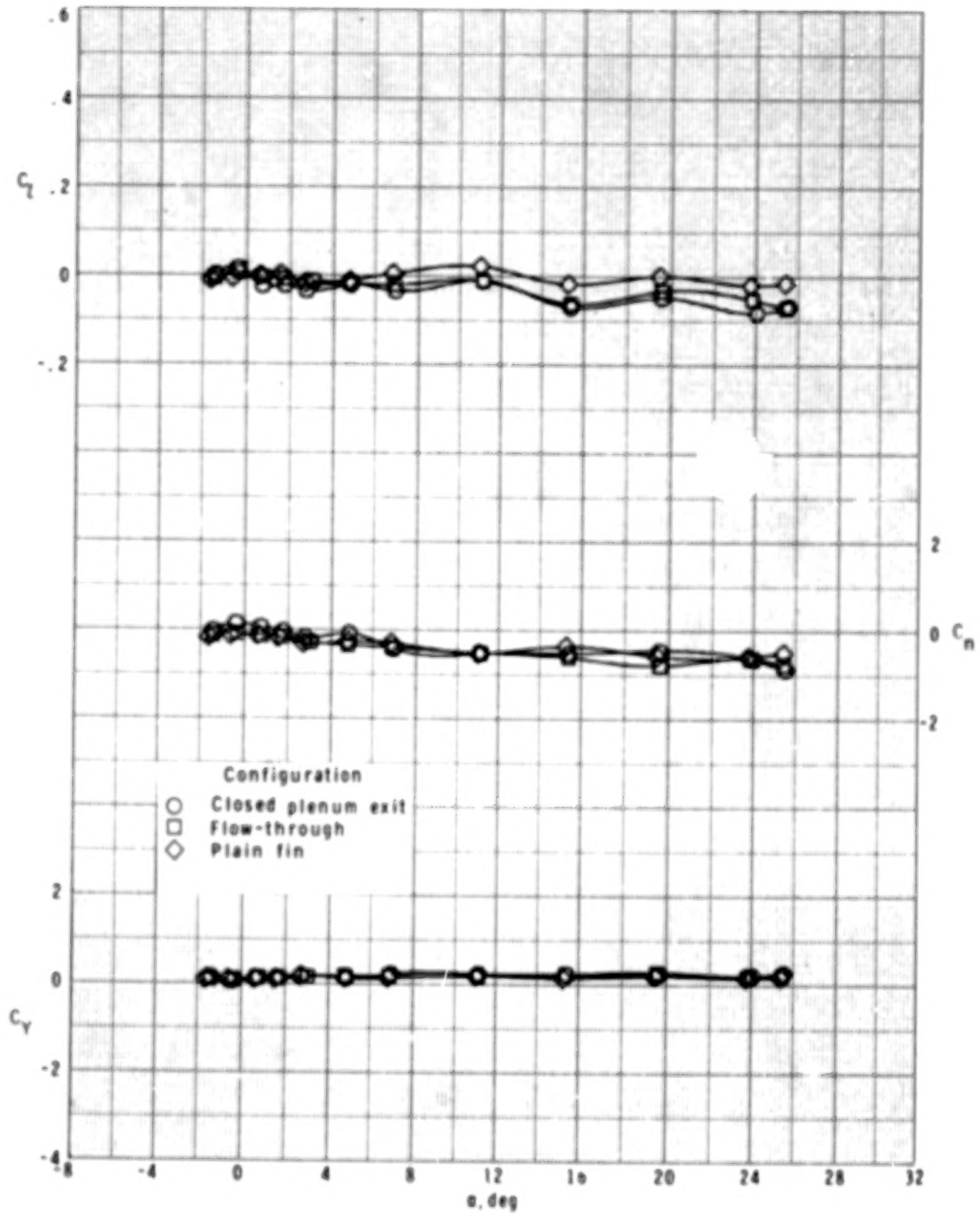

(c) $M_\infty = 2.40$.

Figure 14.- Continued.

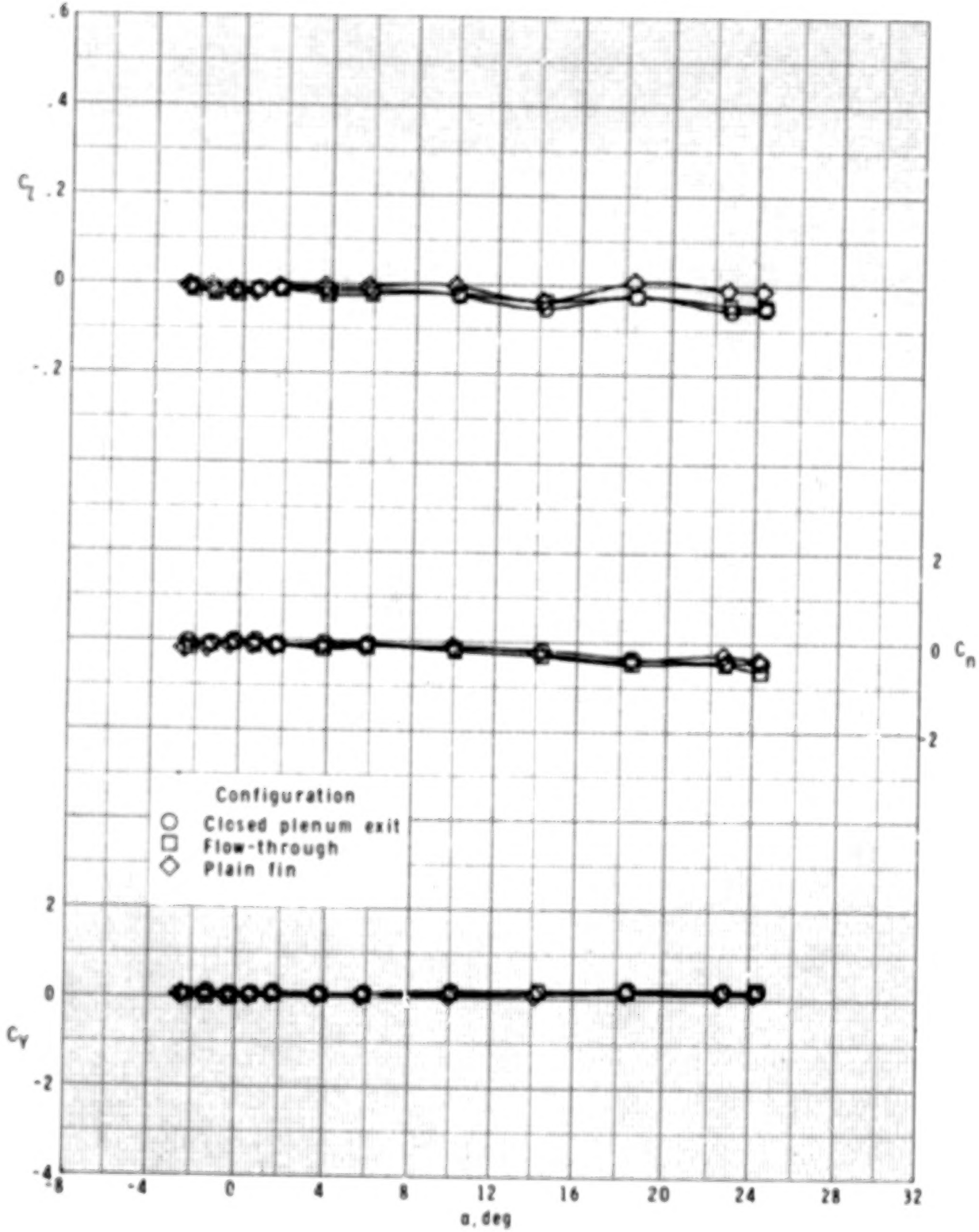

(d) $M_\infty = 2.86$.

Figure 14.- Concluded.

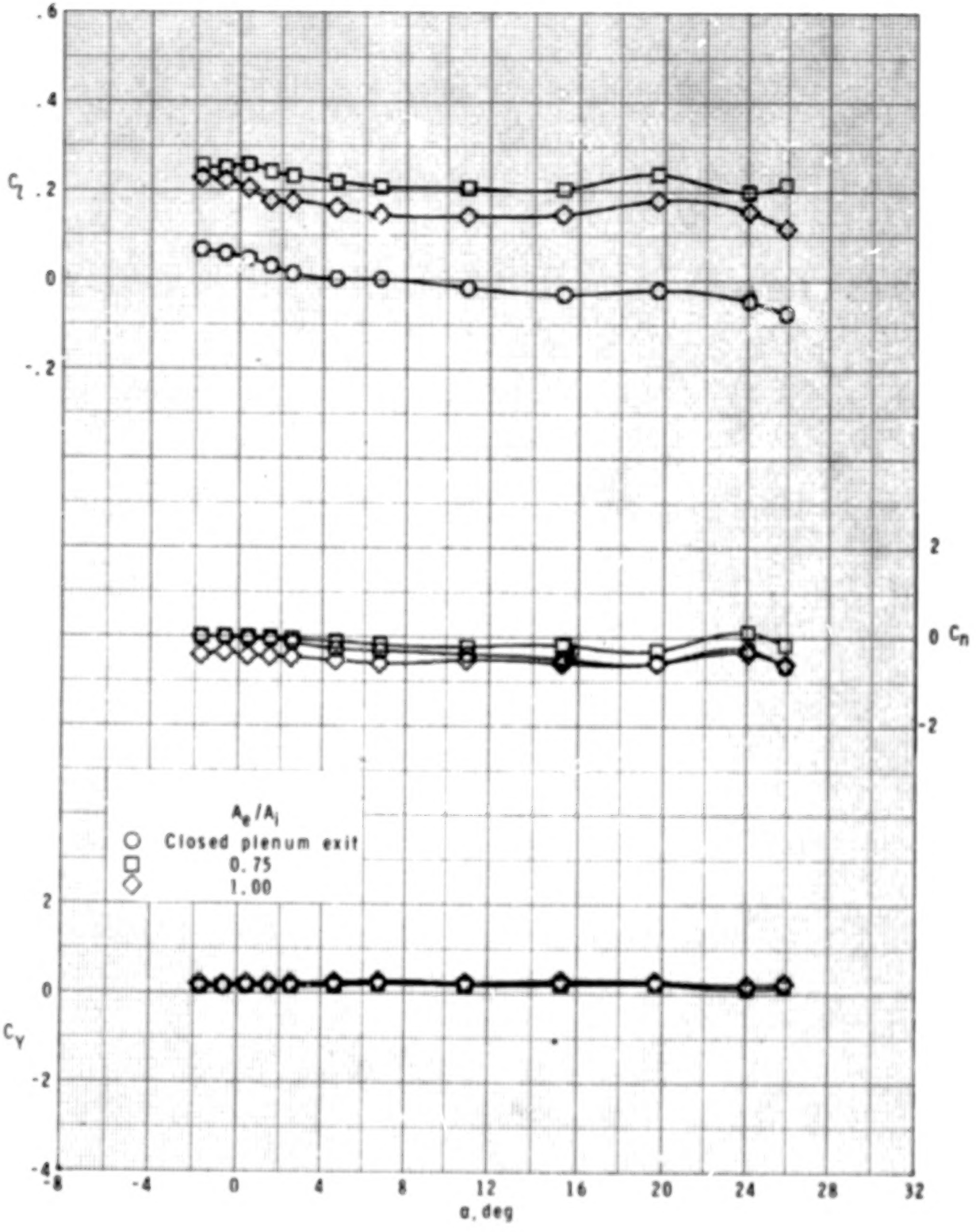

(a) $M_\infty = 1.90$.

Figure 15.- Effect of exit area to inlet area ratios for roll control on lateral aerodynamic characteristics of model with four ram-jet spoiler tail fins. $\phi = 0^\circ$.

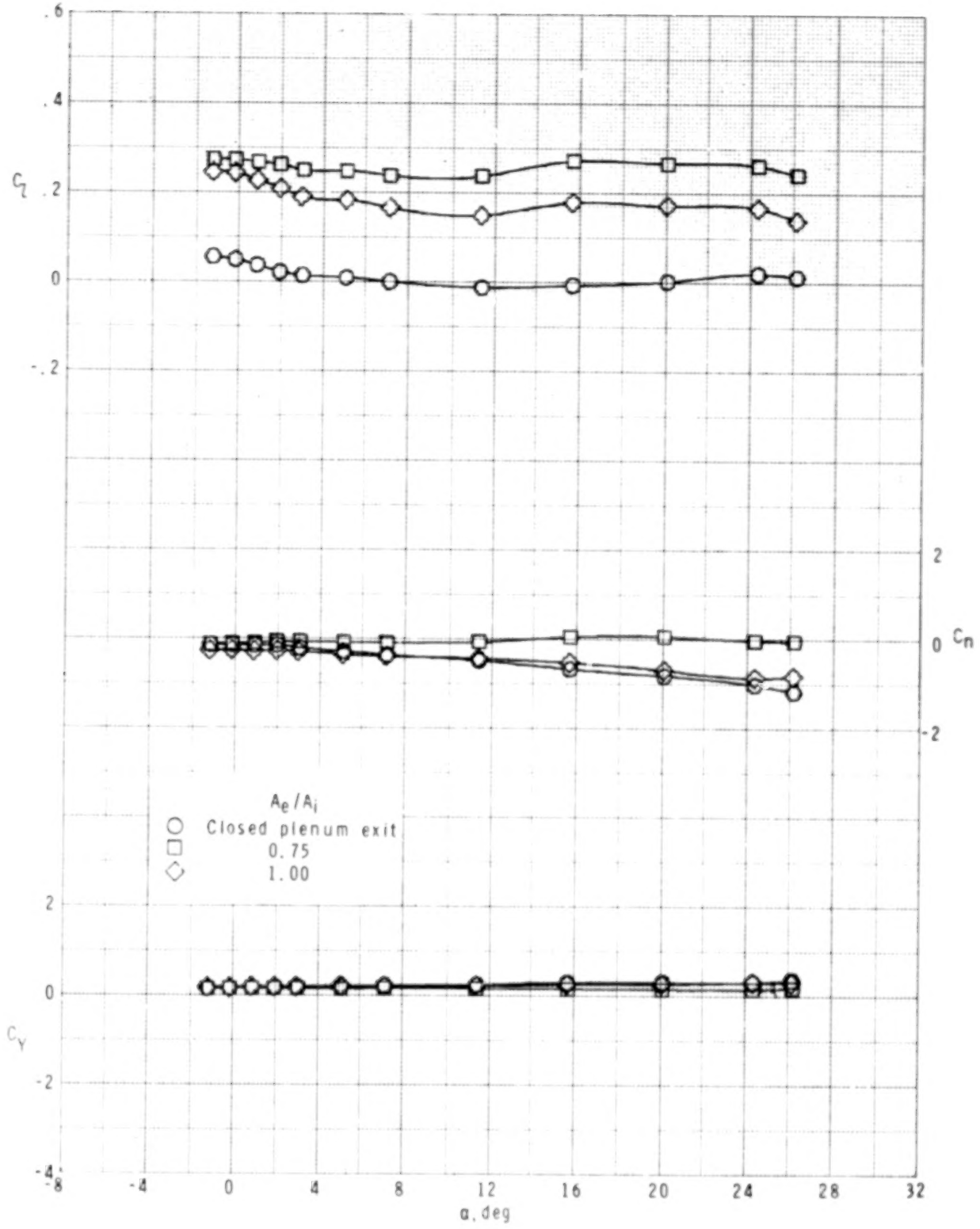

(b) $M_\infty = 2.16$.

Figure 15.- Continued.

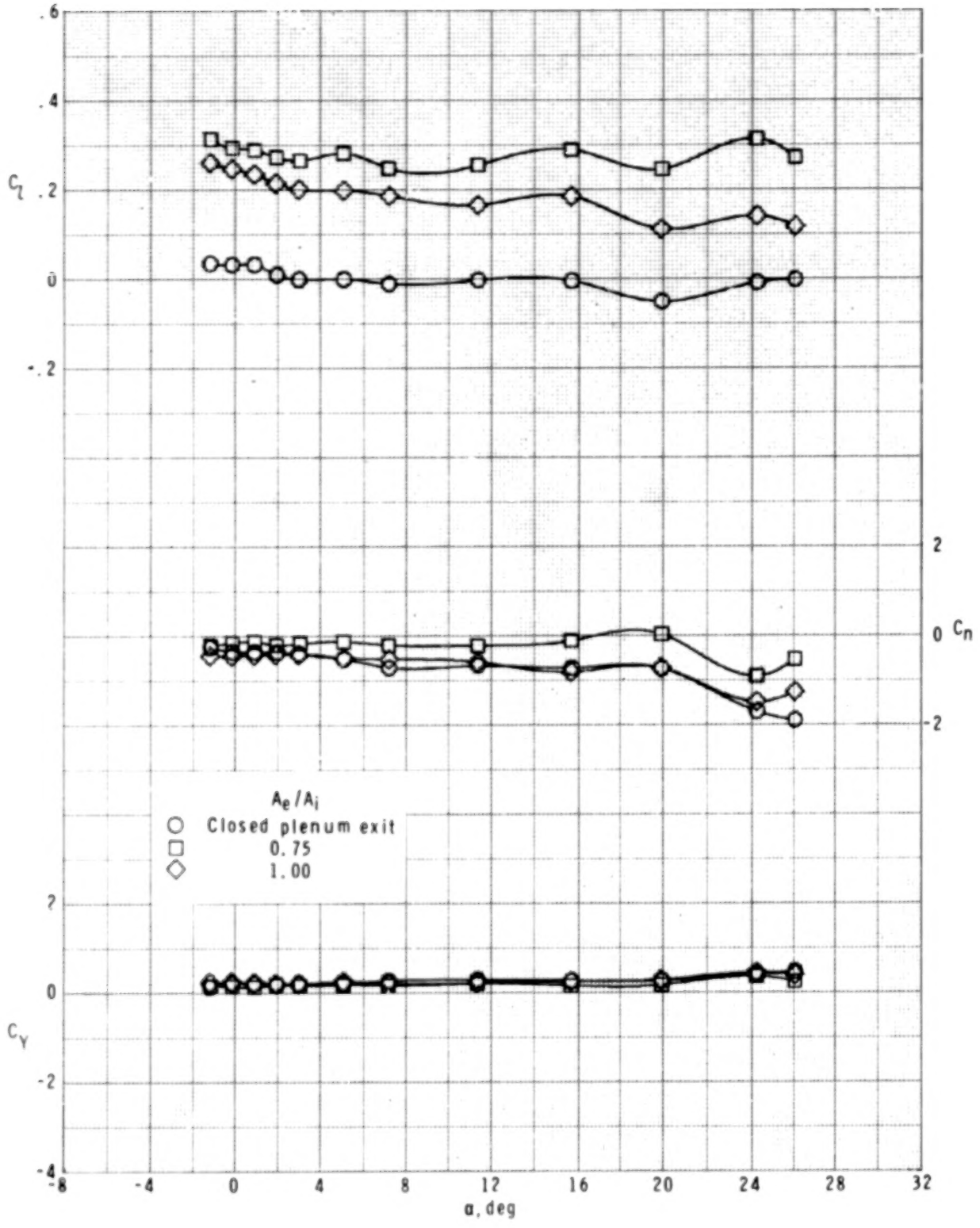

(c) $M_\infty = 2.40$.

Figure 15.- Continued.

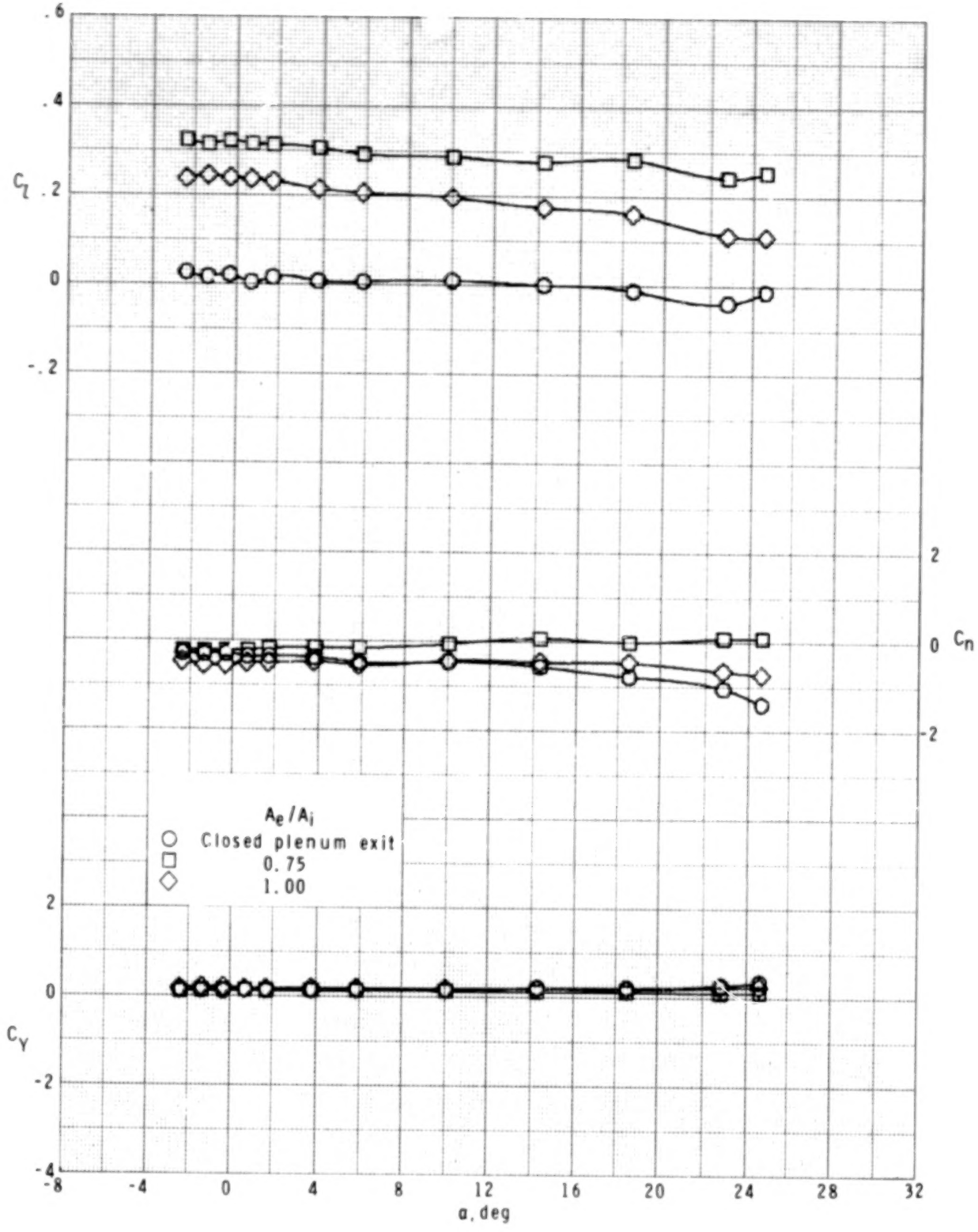

(d) $M_\infty = 2.86$.

Figure 15.- Concluded.

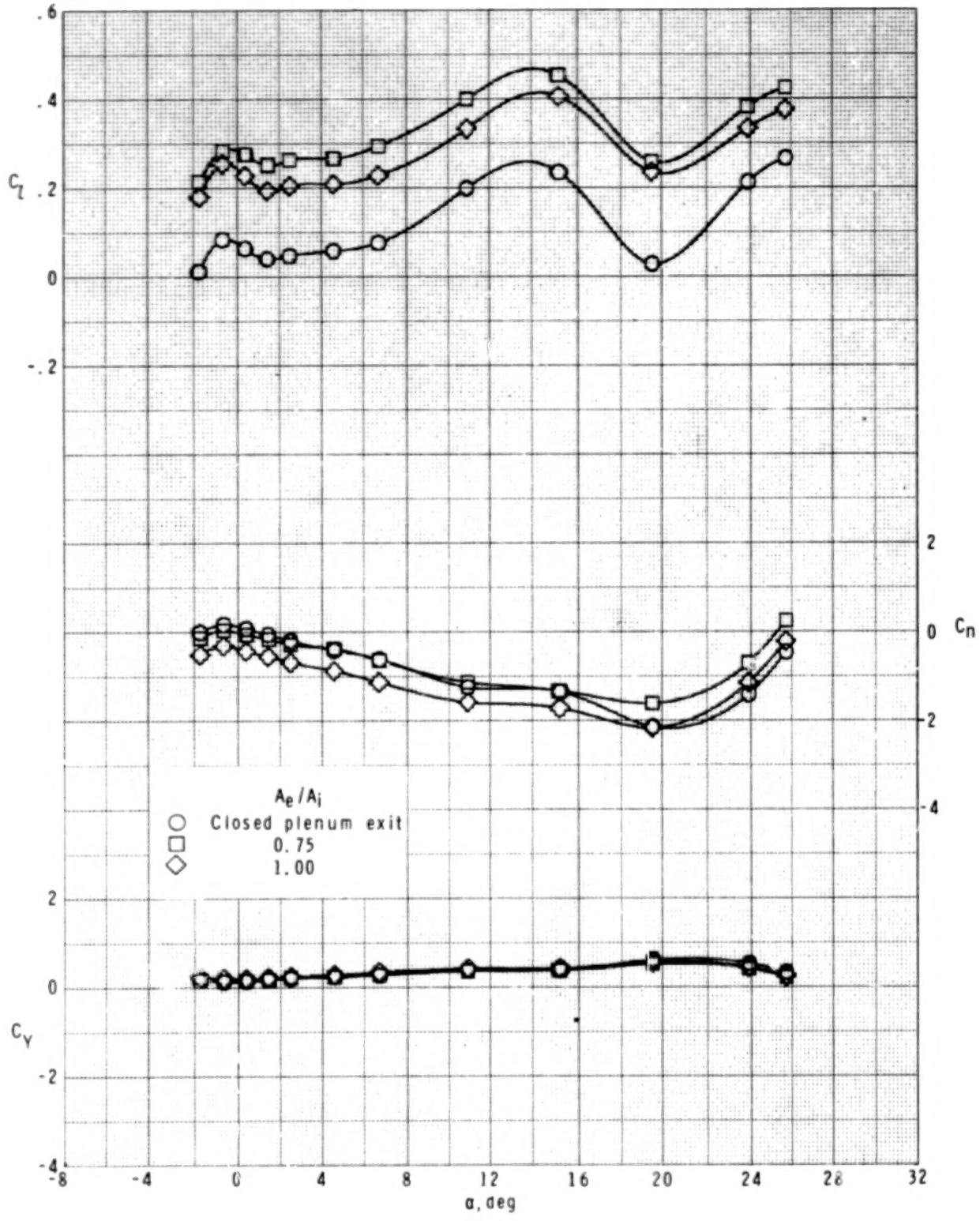

(a) $M_\infty = 1.90$.

Figure 16.- Effect of exit area to inlet area ratios for roll control on lateral aerodynamic characteristics of model with four ram-air-jet spoiler tail fins. $\phi = 22.5^o$.

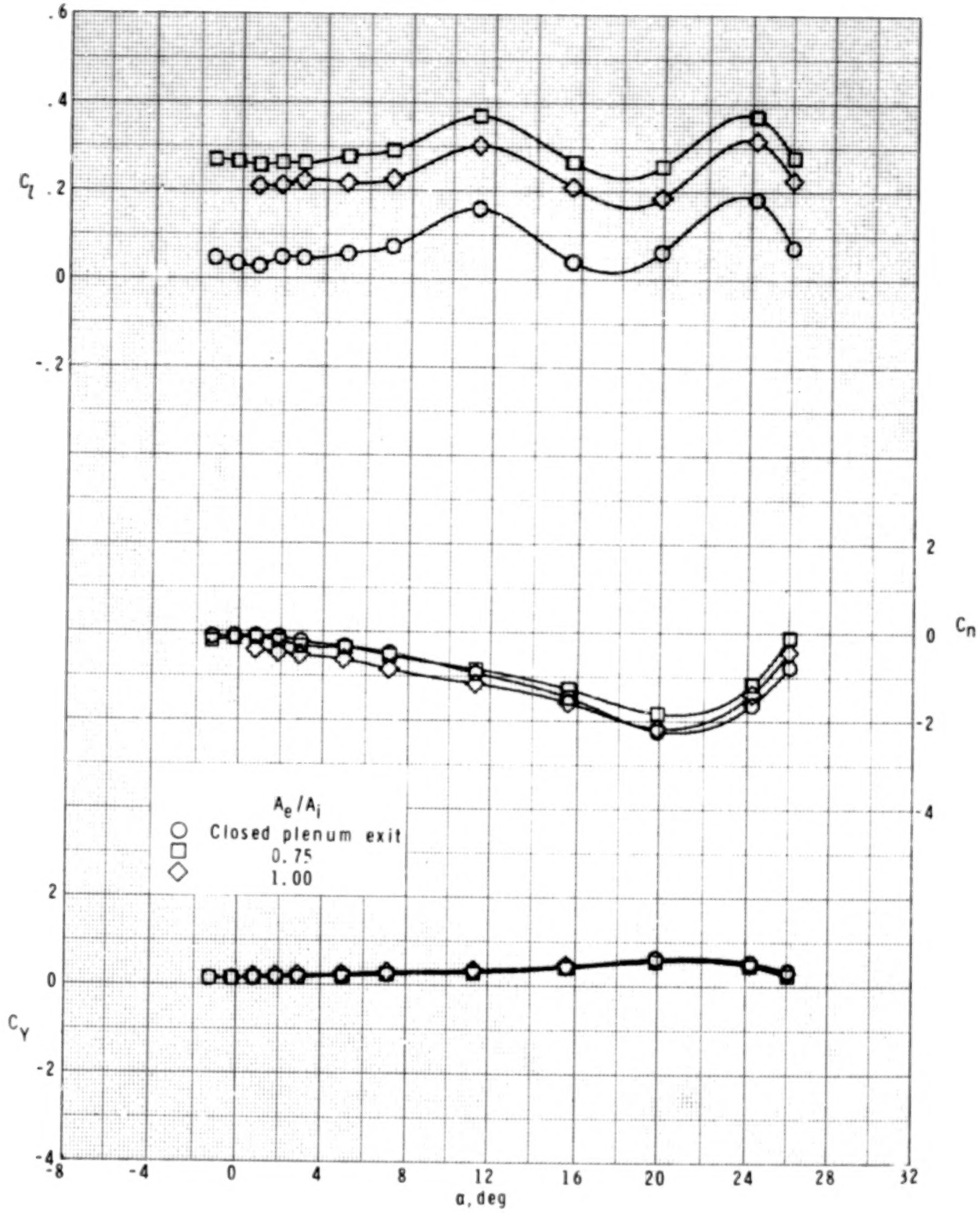

(b) $M_\infty = 2.16$.

Figure 16.- Continued.

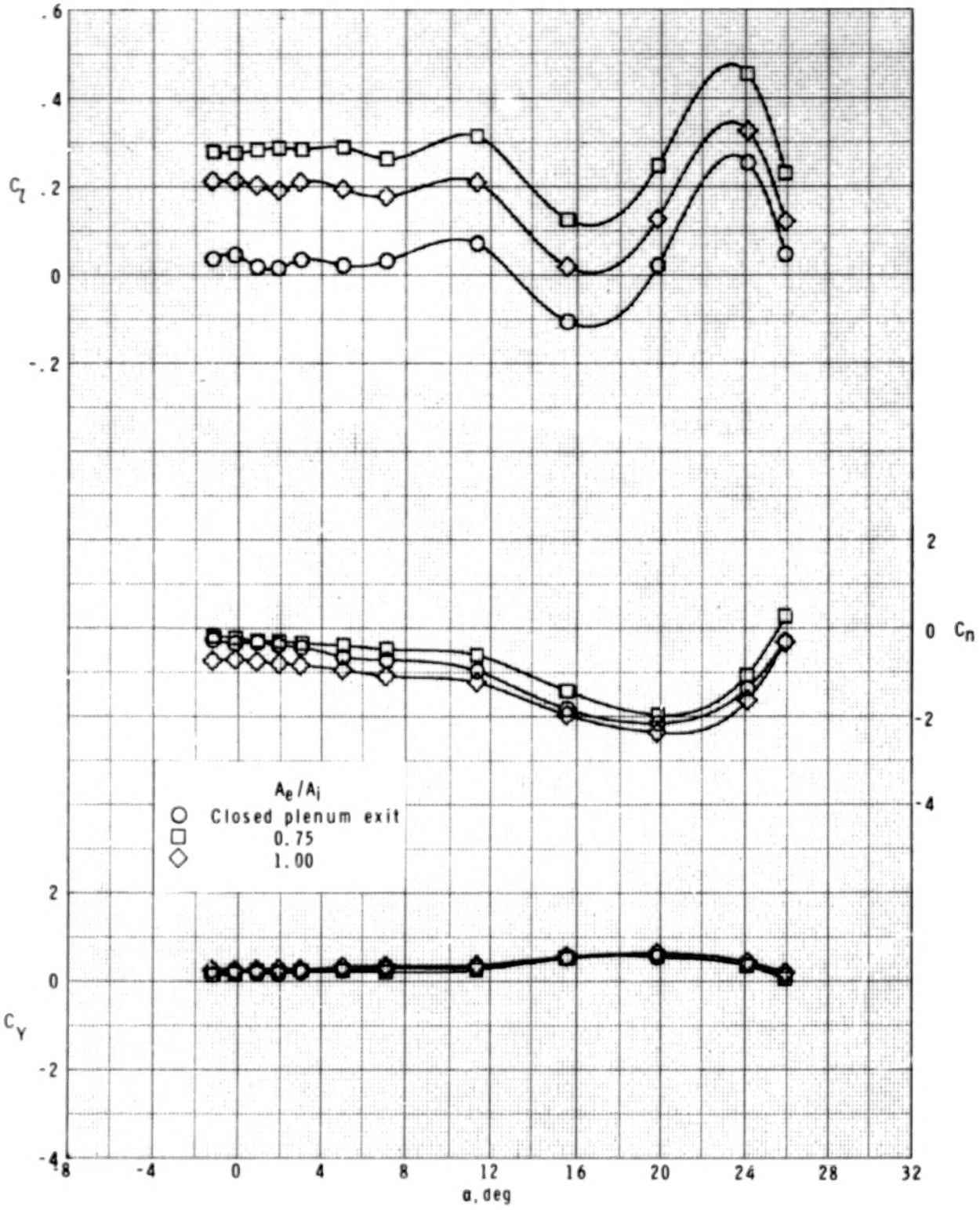

(c) $M_\infty = 2.40$.

Figure 16.- Continued.

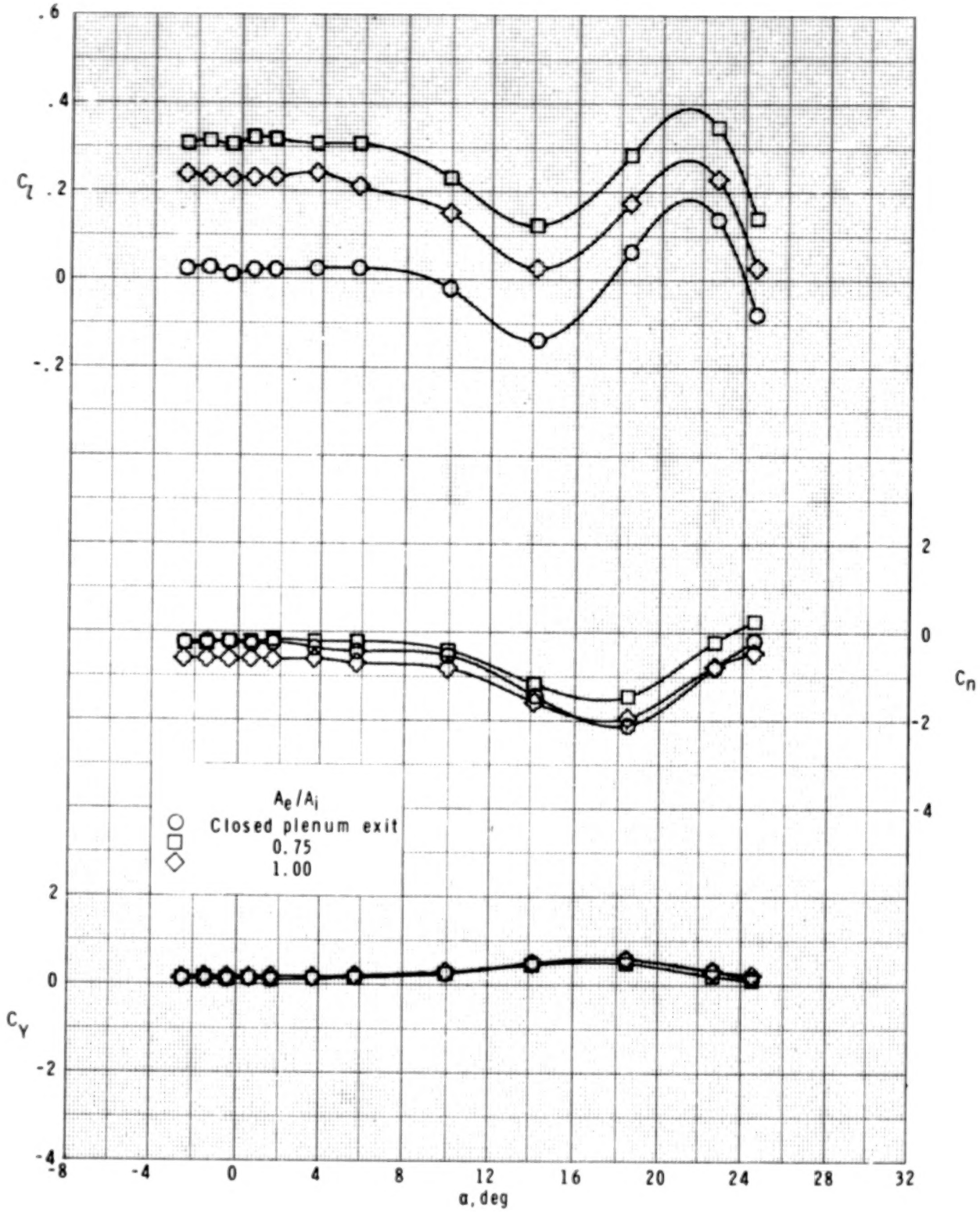

(d) $M_\infty = 2.86$.

Figure 16.- Concluded.

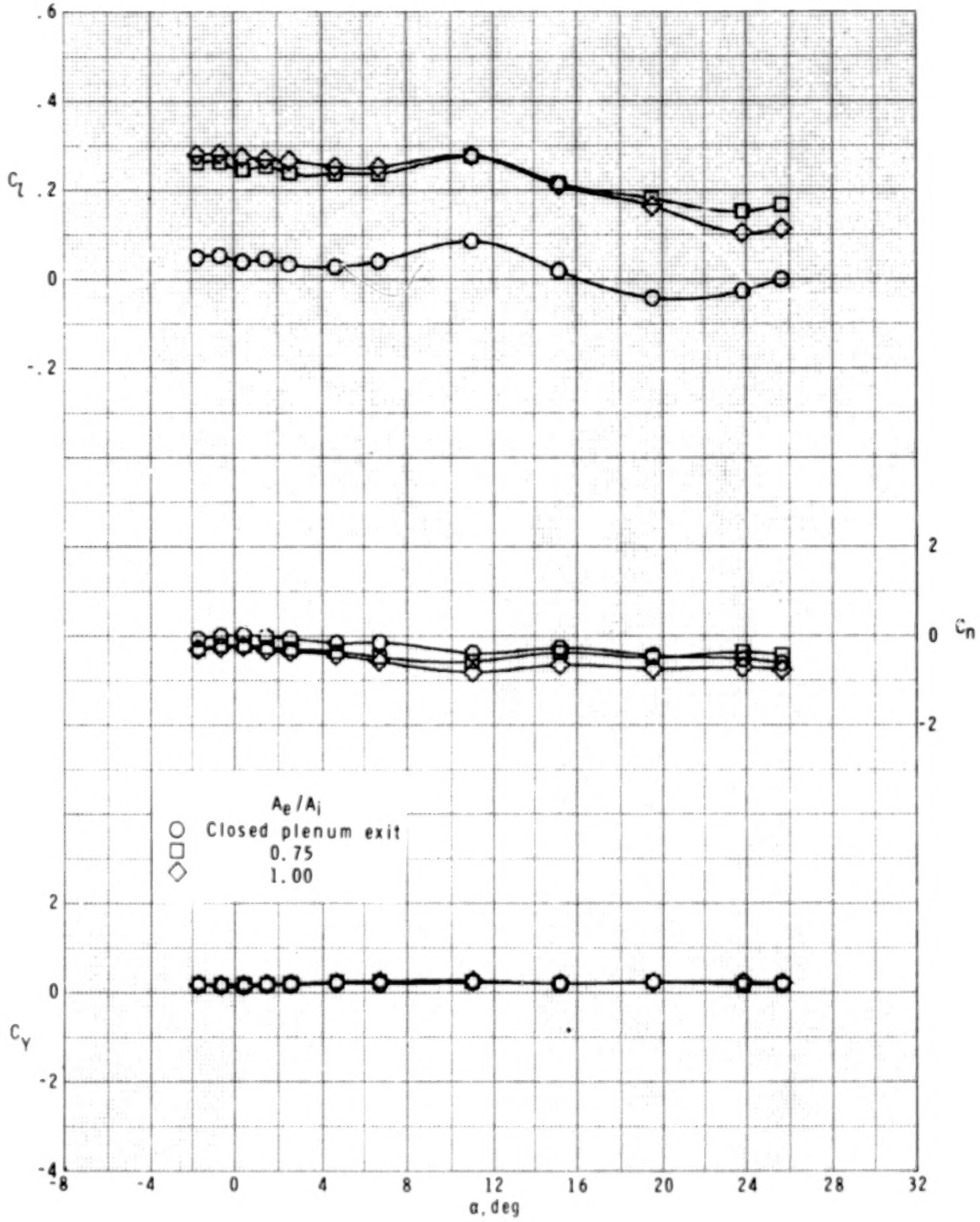

(a) $M_\infty = 1.90$.

Figure 17.- Effect of exit area to inlet area ratios for roll control on lateral aerodynamic characteristics of model with four ram-air-jet spoiler tail fins. $\phi = 45^\circ$.

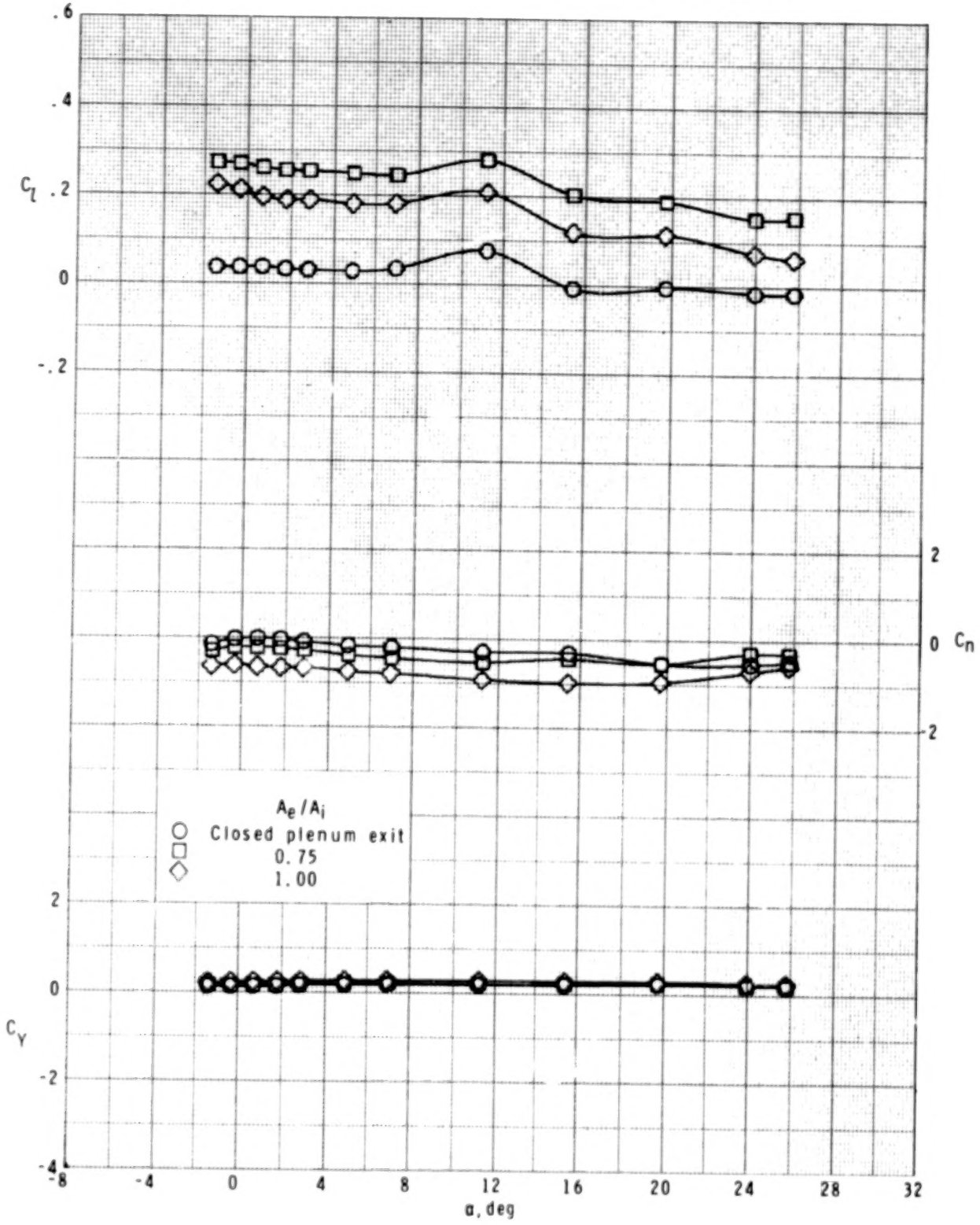

(b) $M_\infty = 2.16$.

Figure 17.- Continued.

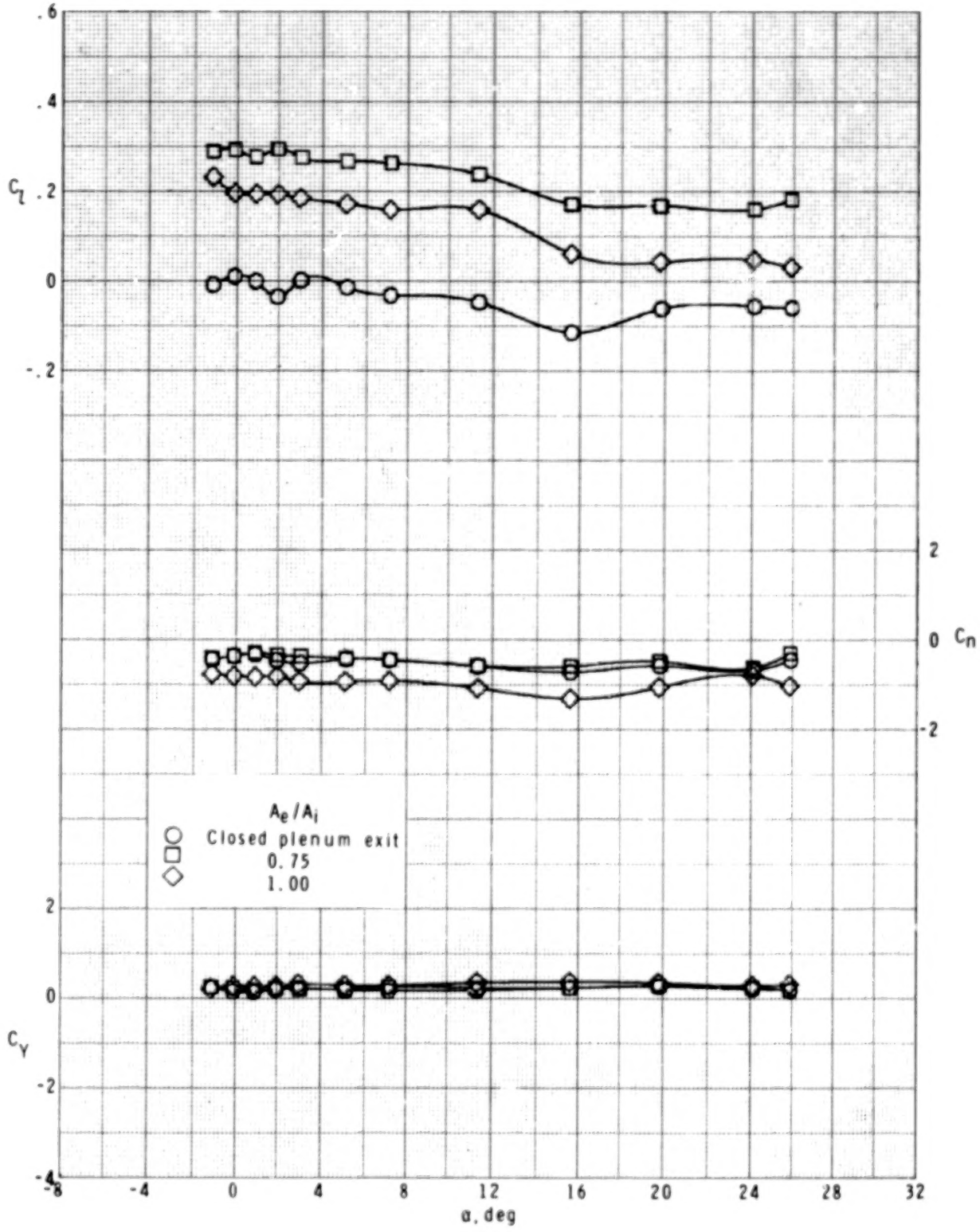

(c) $M_\infty = 2.40$.

Figure 17.- Continued.

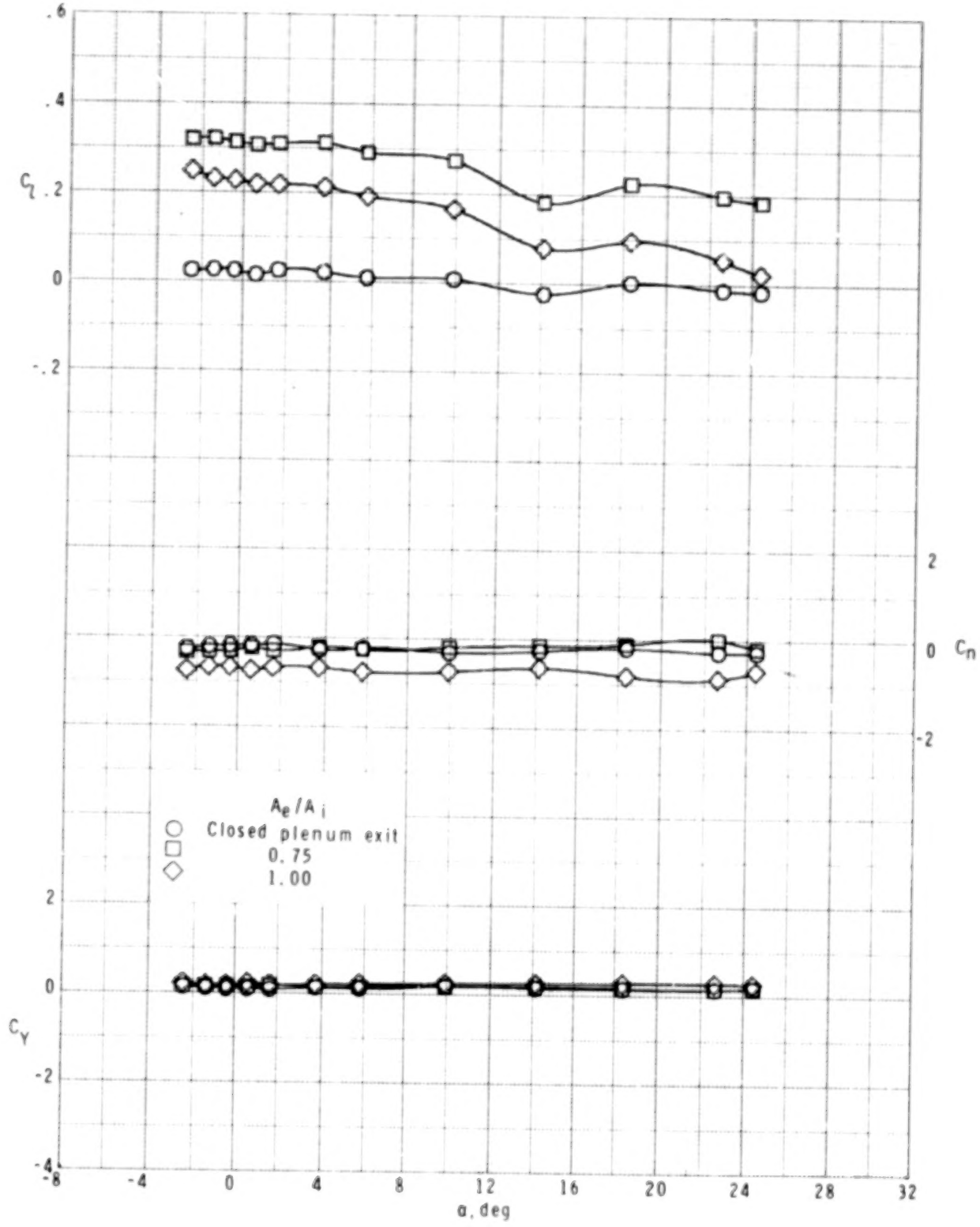

(d) $M_\infty = 2.86$.

Figure 17.- Concluded.

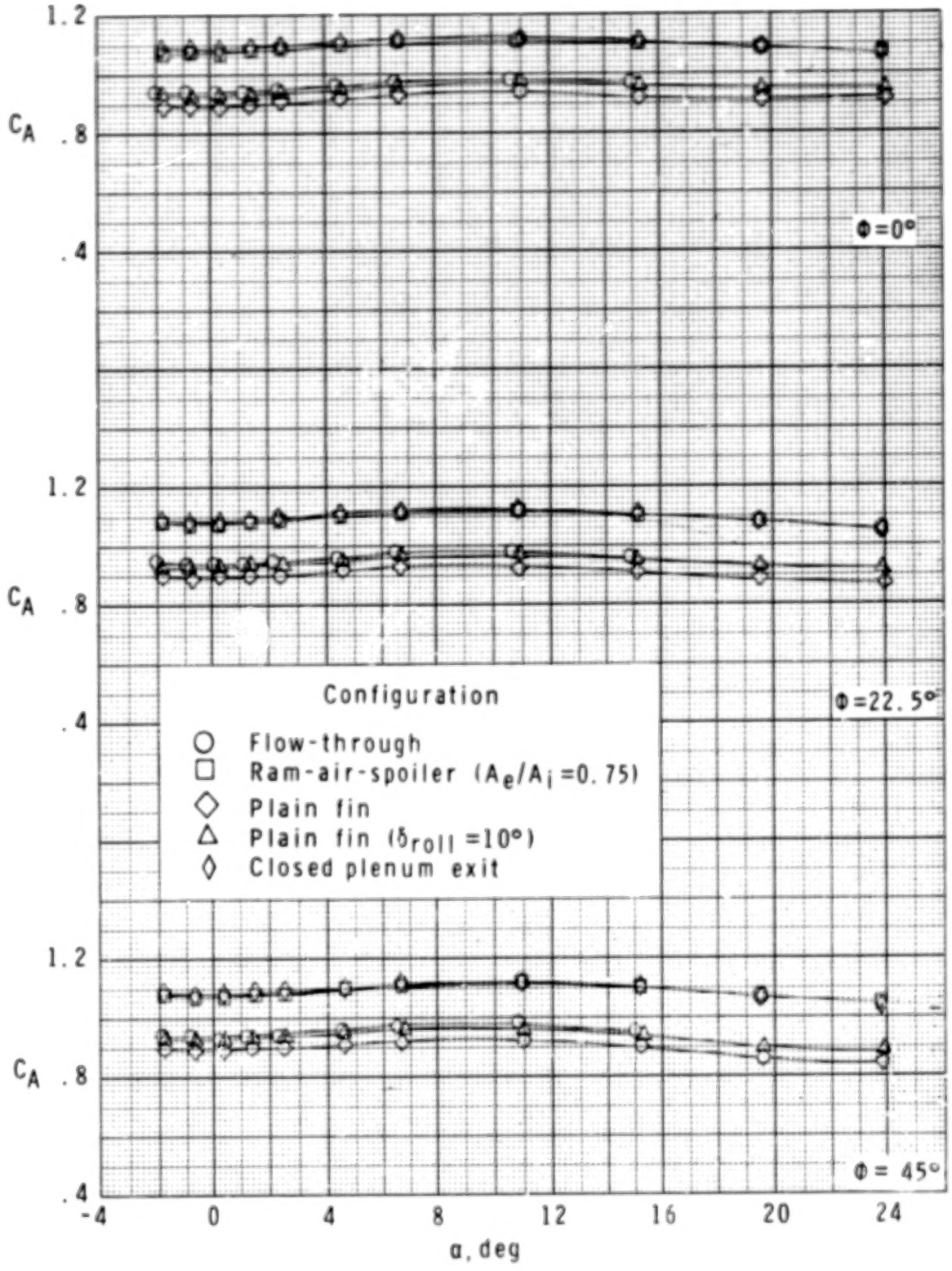

(a) M_∞ = 1.90.

Figure 18.- Summary comparison of total axial-force coefficient characteristics for each roll-control system operating and not operating.

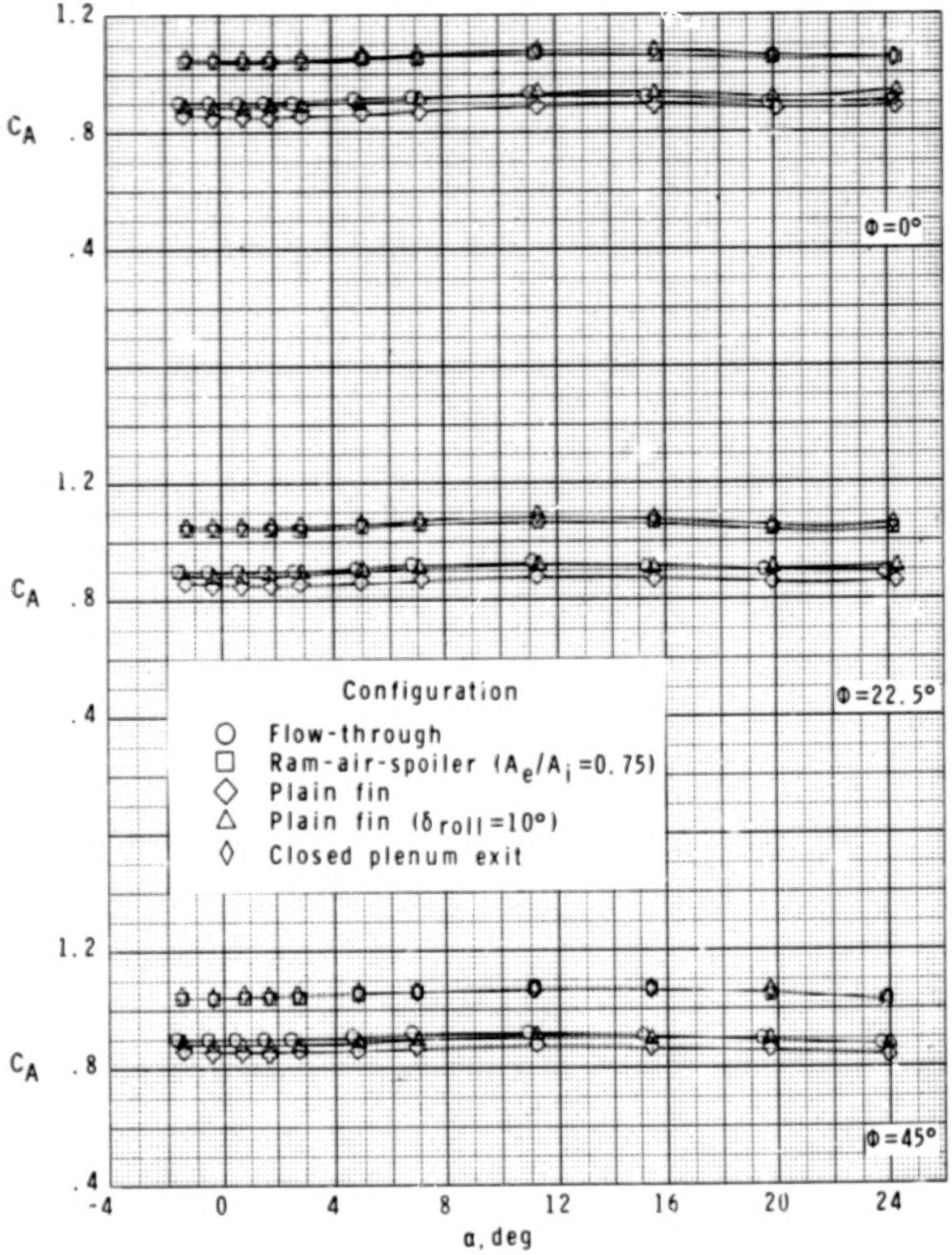

(b) M_∞ = 2.16.

Figure 18.- Continued.

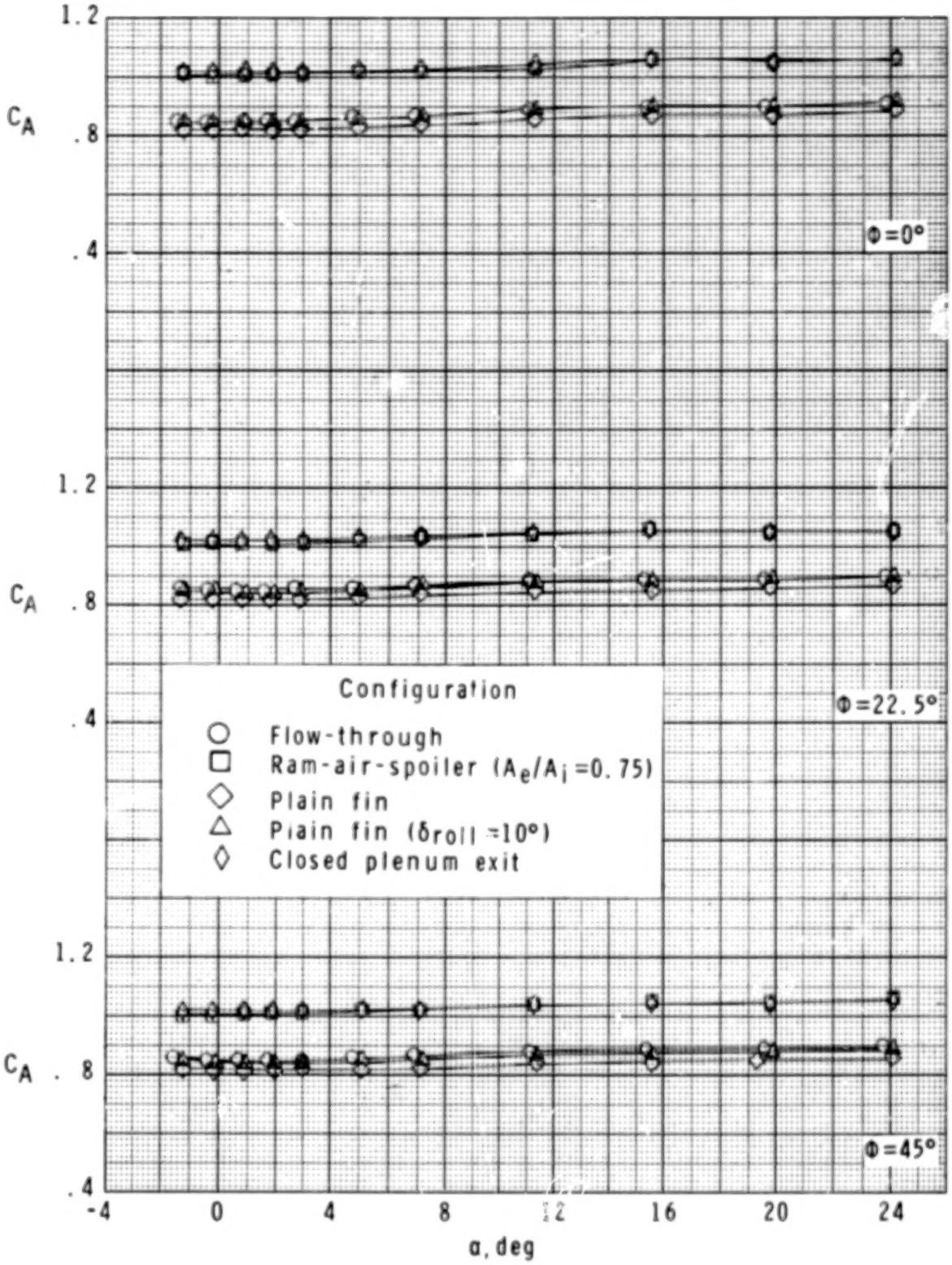

(c) M_∞ = 2.40.

Figure 18.- Continued.

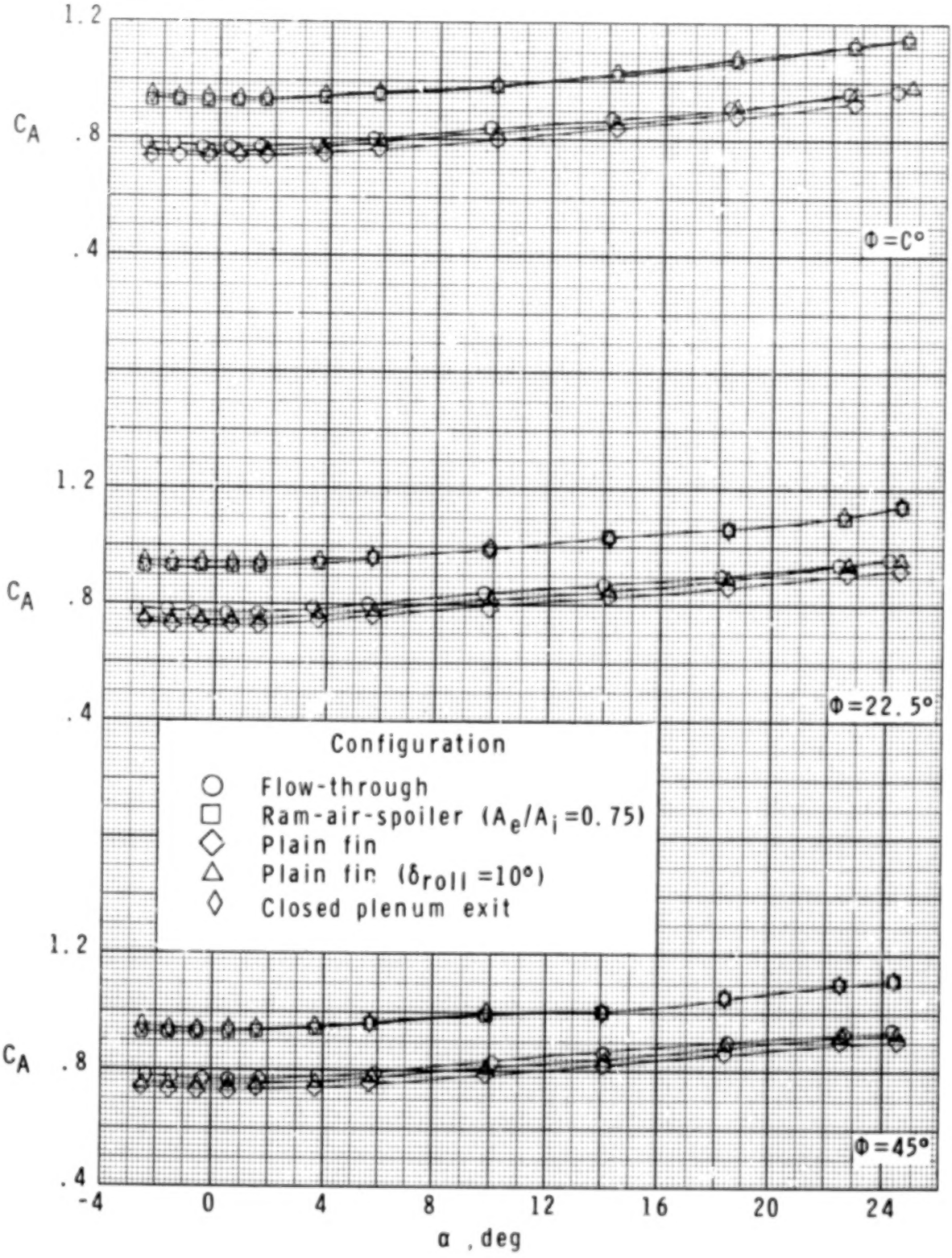

(d) M_∞ = 2.86.

Figure 18.- Concluded.

$M_\infty = 1.90$; $\alpha = 0.2^\circ$

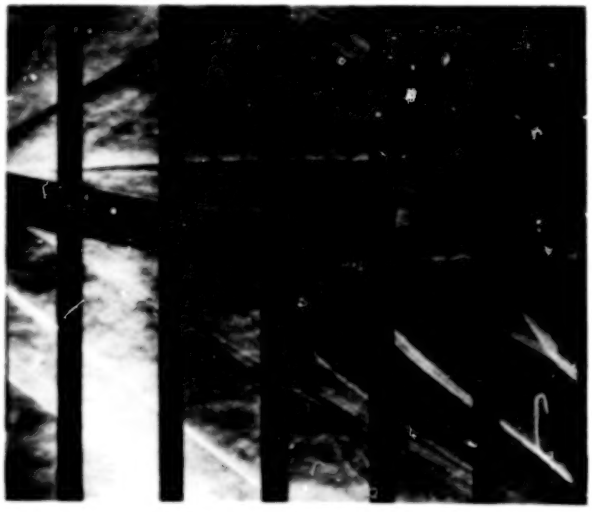

$M_\infty = 1.90$; $\alpha = 10.7^\circ$

L-78-2

$M_\infty = 1.90$; $\alpha = 19.4^\circ$.

(a) Closed plenum exit.

Figure 19.- Schlieren photographs of model.

$M_\infty = 2.86$; $\alpha = -0.6^\circ$

$M_\infty = 2.86$; $\alpha = 9.8^\circ$

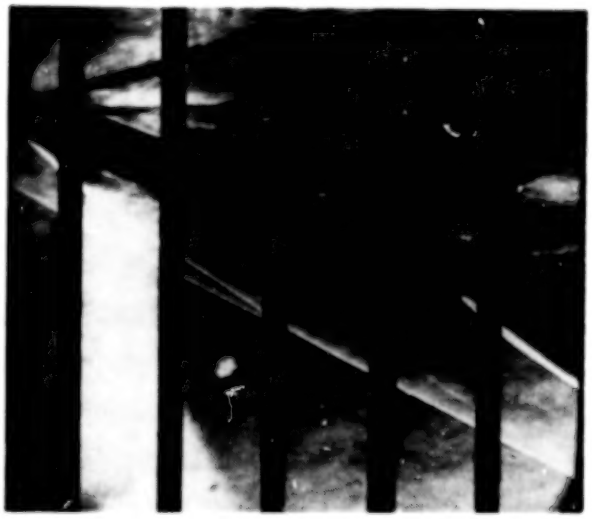

$M_\infty = 2.86$; $\alpha = 18.3^\circ$

L-78-3

$M_\infty = 2.86$; $\alpha = 24.2^\circ$

(a) Concluded.

Figure 19.- Continued.

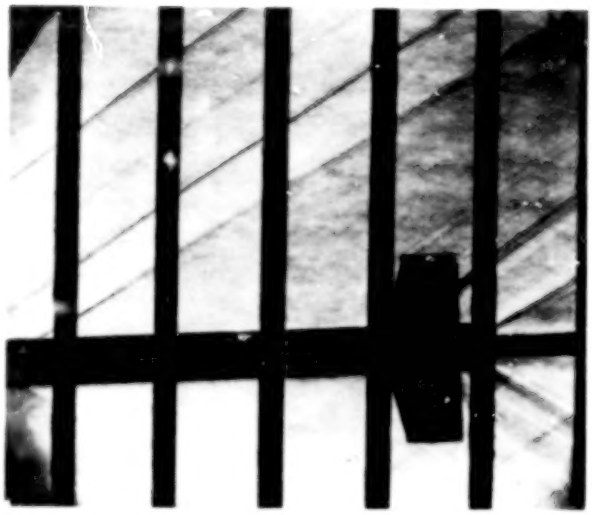

$M_\infty = 1.90$; $\alpha = -2.0^\circ$

$M_\infty = 1.90$; $\alpha = 10.7^\circ$

L-78-4

$M_\infty = 1.90$; $\alpha = 15.6^\circ$

(b) Flow-through nacelle.

Figure 19.- Continued.

$M_\infty = 2.86$; $\alpha = -0.6^\circ$

$M_\infty = 2.86$; $\alpha = 9.8^\circ$

$M_\infty = 2.86$; $\alpha = 18.3^\circ$

L-78-5

$M_\infty = 2.86$; $\alpha = 24.2^\circ$

(b) Concluded.

Figure 19.- Concluded.

1 Report No	2 Government Accession No	3 Recipient's Catalog No
4 Title and Subtitle		5 Report Date
		6 Performing Organization Code
7 Author(s)		8 Performing Organization Report No
		10 Work Unit No
9 Performing Organization Name and Address		11 Contract or Grant No
		13 Type of Report and Period Covered
12 Sponsoring Agency Name and Address		14 Sponsoring Agency Code
15 Supplementary Notes		
16 Abstract		
17 Key Words (Suggested by Author(s))	18 Distribution Statement	
19 Security Classif (of this report)	20 Security Classif (of this page)	21 No of Pages / 22 Price*

*For sale by the National Technical Information Service, Springfield, Virginia 22161

NASA-Langley, 1978